

Report

Report no. 10/25

Sustainable biofeedstock supply chains for advanced biofuels in Europe towards 2050





Sustainable biofeedstock supply chains for advanced biofuels in Europe towards 2050

This report was prepared by:

- R. Hoefnagels, S. Kwakernaak, F. van der Hilst, M. Junginger, Copernicus Institute of Sustainable Development, Utrecht University
- I. Vera, TNO Innovation for Life
- T. Neokosmidis, Concawe

Under the supervision of:

- T. Neokosmidis (Concawe Science Associate)
- A. Ramasary (Concawe Science Executive)

At the request of:

Concawe Special Task Force on Sustainable Bio-feedstock Availability (RT/STF-3)

Reproduction permitted with due acknowledgement

© Concawe Brussels November 2025



KEYWORDS

Biomass supply chains, biomass supply chain optimisation, biomass availability, lignocellulosic feedstocks, biofuel supply chain costs, biomass logistics, advanced biofuels, advanced biofuel techno-economics, refinery integration

INTERNET

This report is available as an Adobe pdf file on the Concawe website (www.concawe.eu).

NOTE

Considerable efforts have been made to assure the accuracy and reliability of the information contained in this publication. However, neither Concawe nor any company participating in Concawe can accept liability for any loss, damage or injury whatsoever resulting from the use of this information.

This report does not necessarily represent the views of any company participating in CONCAWE.



CONTENTS	Page
SUMMARY	XI
1. INTRODUCTION	1
1.1. BACKGROUND	1
1.2. OBJECTIVES AND SCOPE	2
2. SUPPLY CHAIN MODELLING STRUCTURE	4
2.1. INTRODUCTION TO THE SPATIALLY EXPLICIT SUPPLY	
OPTIMIZATION MODEL 2.2. OVERVIEW AND SELECTION OF BIOREFINING TECHNO	I OCIES
FOR ADVANCED BIOFUELS	5
2.3. OVERVIEW OF THE MODELLING APPROACH	7
	•
3. METHODOLOGY: CALCULATING AND MAPPING BIOMASS AVAILA	
POTENTIAL TOWARDS 2050	10
3.1. INTRODUCTION TO THE CONSIDERED BIOFEEDSTOCKS 3.2. AGRICULTURAL BIOMASS	S 10 11
3.2. AGRICULTURAL BIOMASS 3.2.1. Lignocellulosic energy crops biomass availability pot	
3.2.1. Agricultural residues biomass potential: cereal straw	
maize stover	13
3.2.3. Agricultural residues biomass potential: prunings	14
3.3. FOREST BIOMASS	15
3.3.1. Stemwood and primary forestry residues	15
3.3.2. Secondary forestry residues	17
3.4. BIOWASTES	18
4. METHODOLOGY: SUPPLY CHAIN CONFIGURATIONS AND CO-LOC	'ATION
OPTIONS	20
4.1. LOCATION AND INTEGRATION STRATEGIES	20
4.2. POSSIBLE LOCATIONS OF ADVANCED BIOFUEL PRODU	CTION IN
THE SUPPLY CHAIN MODEL	21
4.3. SUPPLY CHAIN CONFIGURATIONS	23
5. METHODOLOGY: SUPPLY CHAIN COST CALCULATIONS	25
5.1. GENERAL OUTLINE OF COST COMPONENTS IN SUPPLY	
5.2. BIOMASS COSTS AT ROADSIDE	25
5.2.1. Costs of agricultural biomass	26
5.2.2. Costs of forest biomass	26
5.3. TRANSPORT COST OF BIOMASS, BIOCRUDE AND BIOFU	
5.3.1. (Intermodal) transport cost	27
5.3.2. Transport network modelling	28
5.3.3. Transport cost parameters in BIT-UU 5.4. PROCESS TECHNO-ECONOMICS AND INTEGRATION EC	29
BENEFITS	32
5.4.1. Process Description: Gasification and Fischer-Tropsc	
synthesis (GFT)	32
5.4.2. Process Description: Hydrothermal liquefaction (HTL	_) and
upgrading	32
5.4.3. Levelized fuel production costs	33
5.4.4. Future cost reduction potential	34
5.4.5. Techno-economic data: Gasification and Fischer-Tro	ppsch 35
(GFT) 5.4.7. Techno-Economic Data: Decentralized Hydro-therma	
liquefaction (HTL)	38
5.4.8. Economies of scale	40



6.	ADVANCE	D BIOFUEL DEMAND INPUT IN THE MODEL	44
	6.1.	ADVANCED BIOFUEL DEMAND FOR TRANSPORT IN EU-27 + UK	44
	6.2. 6.3.	BIOMASS DEMAND FOR NON-ENERGY USES IN EU-27 + UK BIOMASS DEMAND FOR BIOENERGY (ELECTRICITY/HEAT) IN	46
	0.5.	EU-27 + UK	46
	6.4.	ADVANCED BIOFUEL AND COMPETING DEMAND LOCATIONS IN	
		THE SUPPLY CHAIN MODEL	47
7.	RESULTS:	BIOMASS AVAILABILITY AND COSTS MAPPING	49
	7.1.	AVAILABILITY, WATER STRESSES AND COSTS POTENTIAL OF AGRICULTURAL BIOMASS	49
	7.1.1.	Availability potential of agricultural biomass	49
	7.1.2.	Mapping (spatially explicit results) of biomass availability potential	52
	7.1.3.	Water balance (deficit) and impact on energy crop	-
		potentials	54
	7.1.3.1.	Water balance of lignocellulosic energy crops	54
	7.1.3.2.	Water balance of lignocellulosic energy crops spatially explicit results	55
	7.1.4.	Roadside cost of agricultural biomass	57
	7.2.	AVAILABILITY AND COSTS POTENTIAL OF FOREST BIOMASS	60
	7.2.1.	Availability potential of forest biomass	60
	7.2.2.	Mapping (spatially explicit results) of biomass supply and costs potential	62
	7.3.	AVAILABILITY AND COSTS POTENTIAL OF BIOMASS WASTE	64
	7.3.1.	Availability potential of biomass waste	64
	7.4.	BIOMASS FROM IMPORTS	66
	7.4.1.	Supply potential and price	66
	7.4.2.	Mapping (spatially explicit results) of biomass import	
	7.5	potential	67
	7.5.	TOTAL BIOMASS SUPPLY POTENTIAL	68
	7.5.1.	Total supply potential available to advanced biofuels and competing bioenergy demand	68
8.	OVERVIEV	V OF THE BASE AND ALTERNATIVE SCENARIOS	72
9.	RESULTS:	ADVANCED BIOFUEL SUPPLY CHAINS	74
	9.1.	COST-SUPPLY CURVES	74
	9.2.	BIOREFINING TECHNOLOGY MIX AND ADVANCED BIOFUEL	
		PRODUCTION COSTS	77
	9.2.1.	Conversion technologies selection	77
	9.2.2.	Advanced biofuel production costs	82
	9.3. 9.4.	GEOGRAPHICAL DISTRIBUTION OF BIOREFINERIES BIOMASS/BIOFUEL CONSUMPTION AND TRADE DYNAMICS	86 93
10.	CONCLUS		102
11.	ABBREVIA	TIONS	105
12.	REFERENC	CES	106



LIST OF FIGURES

Figure 1	The structure of the spatially explicit supply chain optimization model, adapted from Huang et al. (2019). Centralized: biomass pre-processing plus conversion and biofuel upgrading at one location. Decentralized: biomass pre-processing (e.g., biocrude production) and biofuel upgrading at different locations. Standalone: location without co-location benefits. Each
	biofuel blending location (at oil refineries) or competing demand (bioenergy for non-transport fuels) location (major cities NUTS-2) is connected to all possible supply locations in the EU-27 plus UK (NUTS-3 level), either via distributed or centralized conversion facilities, considering transport route-specific costs for biomass feedstock, biocrude and drop-in biofuel5
Figure 2	Distributed and centralized supply chains and scope of the model. Adapted from de Jong et al. (2017)
Figure 3	Overview of the modelling framework. The MILP model optimizes for the lowest cost of the entire supply chain system to meet the demand for advanced biofuels, and competing bioenergy uses (heat and electricity)9
Figure 4	Estimated relative distribution of prunings. Based on S2Biom (Dees et al. 2017)
Figure 5	Estimated spatial distribution of forest biomass availability in 2020 for all uses [in t ha ⁻¹ y ⁻¹] at (A) grid cell [10 km x 10 km], (Verkerk et al., 2019), and (B), proportion % of national forest biomass potentials at NUTS-3 level [% y ⁻¹]
Figure 6	Population per NUTS-3 region in the EU27+UK in 2021 (European Commission - Eurostat/GISCO, 2023)
Figure 7	Schematic visualization of possible degrees of integration with existing industries (de Jong et al. 2015)21
Figure 8	Overview of possible host locations for advanced biofuel production without integration benefits (A) and with integration benefits (B) considered in this study. The number of NUTS-3 regions had to be limited for the MILP model calculations.
Figure 9	Overview of the advanced biofuel supply chain configurations included in the analysis for the EU27 + UK. From left to right: centralized and distributed linear type and distributed hub-and-spoke (de Jong et al. 2017).
Figure 10	General outline of the biofeedstock supply chains with possible components and processes. The total cost of advanced biofuel production covers all costs from field side, pre-processing depot (only for the case of decentralized HTL biocrude production), final conversion in the biorefinery, and downstream distribution to blending terminals.
Figure 11	Stepwise cost structure of intermodal transport with road and maritime transport. Adapted from Rodrigue (2020). In most cases, biomass needs to be transported by truck to an intermodal terminal to provide access to rail or water transport.
Figure 12	Transport network topology of the EU used in the ArcGIS Model with links (or segments) of road, rail, inland waterways and short sea shipping. The included supply, demand, and terminal nodes that define the connections and access to these links are not shown for visual reasons29
Figure 13	EU average variable transport cost (in €2023/twb-km) per transport mode and transported freight (for both dry and wet bulk) for road, rail, inland waterways, and short sea transport. The uncertainty bars show the cost ranges between EU member states + UK for differences in labour cost, country-specific excise duties, VAT, and rail cargo tariffs used in the BIT-UU model. Details are provided in Annex C
Figure 14	EU fixed transport cost (in € ₂₀₂₃ /t _{wb}) per transport mode and transported freight (for both dry and wet bulk) for road, rail, inland waterways, and



	shortsea transport. Details are provided in Annex C. All countries were
	assumed to have similar fixed transport costs
Figure 15	Process configurations for the centralized and distributed HTL conversion
	systems in 2030 (de Jong et al. 2017). In 2050, the SMR and natural gas used
	for hydrogen production is assumed to be replaced by ex-situ green
	hydrogen supply
Figure 16	Impact of increasing learning rates (LR) on cost reduction for a factor of 10
rigare ro	and 100 cumulative capacity increase (Brown et al. 2020). The average LR
	of 5 and 10 was considered representative for GFT and HTL
Figure 17	
Figure 17	Capital cost estimates at three different levels (segment size) for
	Gasification and Fischer-Tropsch (GFT) and HTL Conversion plus upgrading
	(centralised (cs)) for greenfield locations in 2030. The other cases are
	provided in Annex B4
Figure 18	Projected advanced biofuel demand (excluding biomethane) in the
	transport sector for the EU-27 + UK for the scenarios of two studies: DI Fuels
	and S&P (EC, 2024; S&P, 2025)
Figure 19	Transport energy share per country within the EU-27 + UK. International
	maritime bunker fuel demand is included in the figures, which accounts for
	the high demand in certain smaller countries
Figure 20	Biomass demand for bioenergy calculated using the PRIMES model, as
50. 0 _0	reported in the DI Fuels study for the EU-27 (EC, 2024). The original results
	from the study have been adjusted to reflect the E/H demand based on
	lignocellulosic biomass considered in this study
Figure 21	
rigure 21	Demand locations for advanced biofuels (oil refineries) and electricity and
	heat (largest cities NUTS-2 regions). The same locations were assumed for
F: 22	both 2030 and 2050
Figure 22	Biomass availability potentials in the EU-27 + UK for the Low, Medium and
	High availability scenarios
Figure 23	Biomass potentials (for all markets) of lignocellulosic energy crops, cereal
	straw and maize stover for the high availability scenario in the EU-27 + UK.
	The Max-yield biomass potential represents the case based on which the
	lignocellulosic energy crop with the highest attainable yield is selected for
	each location. The individual energy crop bars represent the case when all
	the available marginal land is dedicated to a single crop
Figure 24	Spatial distribution of lignocellulosic energy crops (for the Max-yield case)
3	potential over time (t _{drv} /ha year) in the High availability scenario. The Max-
	yield case refers to the maximum yield biomass potential based on which
	the lignocellulosic energy crop with the highest attainable yield is selected
	for each location. The pixel size is enhanced for displaying purposes 52
Figure 25	Spatial distribution of cereal straw potential over time (t_{dry} /ha year) in the
rigure 23	High availability scenario. The pixel size is enhanced for displaying
Fig 27	purposes
Figure 26	Spatial distribution of maize stover potential over time (t _{dry} /ha year) in the
	High availability scenario. The pixel size is enhanced for displaying
	purposes
Figure 27	Water balance of lignocellulosic energy crops. The ranges indicate the
	spatial variability of water shortage due to the heterogeneity in biophysical
	conditions
Figure 28	Spatial distribution of lignocellulosic energy crops water balance over time
=	(mm/year). The pixel size is enhanced for displaying purposes 56
Figure 29	Spatial distribution of lignocellulosic energy crops water balance (mm/year)
	for 2030 (A) and for 2050 (C). Regional water stress for 2030 (B) and for
	2050 (D) (Kuzma et al., 2023). The pixel size is enhanced for displaying
	purposes
Figure 30	EU-27 + UK average costs of production and harvesting of lignocellulosic
i iguic 30	energy crops and collection of agricultural residues for the High availability
	and a second contraction of agricultural residues for the fright availability



	scenario (in €/t _{dry}). The ranges indicate the spatial variability of cost due to
Figure 31	the heterogeneity of yields
	purposes
Figure 32	Spatial distribution of cereal straw costs over time (€/t _{dry}). The pixel size is enhanced for displaying purposes
Figure 33	Spatial distribution of maize stover costs over time (€/t _{dry}). The pixel size is enhanced for displaying purposes
Figure 34	Availability potential of forest biomass available for all markets in 2030 and 2050 in million tonnes dry (Mt _{dry} /y) in the different availability scenarios61
Figure 35	Availability potential of forest biomass available for all markets in 2030 and 2050 (in Mtoe/y). Note that the potential in energy units deviates slightly from the ICL-Concawe study because it is calculated from feedstock-specific energy densities (Table 8) whereas ICL-Concawe assumed an average LHV of 2.5 t _{dry} /toe for all feedstock categories
Figure 36	Stemwood, primary forestry residues, and secondary forestry residues availability potentials for all markets at NUTS-3 level for 2030 in kilo tonnes dry material (kt _{dm} /y)
Figure 37	Stemwood, primary forestry residues, and secondary forestry residues availability potentials for all markets at NUTS-3 level for 2050 in kilo tonnes dry material (kt _{dm} /y)
Figure 38	Roadside cost of stemwood, primary and secondary forestry residues in € per tonne dry material (€/t _{dry}). Costs are assumed to remain constant between 2030 and 2050.
Figure 39	Availability potential of biowaste available for all markets in 2030 and 2050 in million tonnes dry (Mt_{dry}/y) in the different availability scenarios65
Figure 40	Availability potential of biowaste available for bioenergy in 2030 and 2050 in Mtoe/y for the different availability scenarios. Wood waste and paper cardboard waste is included in the supply chain model. Other waste (MSW, animal & mixed food waste, and vegetal waste) is assumed to be available for electricity/heat but not included in the model
Figure 41	Post-consumer wood waste and cardboard waste available for all markets at NUTS-3 level in 2030 and 2050
Figure 42	Solid biomass import potential to the EU-27 +UK 2020 - 2050 (Panoutsou & Maniatis, 2021)67
Figure 43	Development of industrial wood pellet spot prices between 2013 and 2024 (Gauthier, 2024)67
Figure 44	Distribution of pellet imports in 2030 and 2050 over ports in the EU-27 plus UK
Figure 45	Total domestic biomass availability potential for bioenergy in 2030 and 2050 for the different biomass availability scenarios in the EU-27 plus UK. The shaded columns are feedstock categories excluded from the supply chain model, with their availability values coming from the ICL-CONCAWE study.
Figure 46	Domestic roadside cost-supply curve of feedstock categories available to advanced biofuel production and competing uses in the EU-27 plus UK. Medium availability scenario, 2030
Figure 47	Domestic roadside cost-supply curve of feedstock categories available to advanced biofuel production and competing uses in the EU-27 plus UK. Medium availability scenario, 2050
Figure 48	Weighted average feedstock cost delivered to biocrude/biofuel plants in the Base and Alternative feedstock scenarios in the EU-27 + UK (in €/GJ biomass delivered). The error bars show the ranges between the minimum and



	maximum cost of feedstock delivered. LD: Low Demand, HD: High Demand.
- : 40	
Figure 49	Cost-supply curve of delivered feedstock (biomass roadside + transport
	costs) to meet the demand for advanced transport biofuels in the EU-27 + UK by 2030. Results are shown for the three biomass availability scenarios:
	Low, Medium (Med), and High
Figure 50	Cost-supply curves of delivered feedstock (biomass roadside + transport
rigure 30	costs) to meet the demand for advanced transport biofuels in the EU-27 +
	UK by 2050 for: A. Low advanced biofuel demand (37.6 Mtoe), B. High
	advanced biofuel demand (88.2 Mtoe). Results are shown for the three
	biomass availability scenarios: Low, Medium (Med), and High
Figure 51	Advanced biofuel/biocrude production per plant type (in Mtoe/y) in the
i igai c o i	Base scenarios for 2030 and 2050. The error bars show the ranges of the
	Alternative biomass availability scenarios (Low, High). LD: Low-Demand,
	HD: High-Demand, RP: Repurpose 81
Figure 52	Number of biocrude (HTL (ds)) and advanced biofuel plants (GFT, HTL (cs),
3	Upgrading) in the Base scenarios for 2030 and 2050. The error bars show the
	ranges of the Alternative biomass availability scenarios (Low, High) 81
Figure 53	Average biofuel production cost in the Base and Alternative scenarios. The
	error bars show the ranges between the minimum and maximum biofuel
	production costs calculated in the scenarios 82
Figure 54	Median, quartiles, and minimum/maximum ranges in supply chain cost of
	GFT in the Base and Alternative feedstock scenarios
Figure 55	Median, quartiles, and minimum/maximum ranges in supply chain cost of
	centralized and distributed HTL in the Base and Alternative feedstock
	scenarios 84
Figure 56	Breakdown of each pathway costs into the different components and
	average biofuel production cost per pathway/configuration. Base scenario,
	2030
Figure 57	Breakdown of each pathway costs into the different components and
	average biofuel production cost per pathway/configuration. Low-demand
Figure E0	Base scenario, 2050
Figure 58	Spatial distribution of modelled biocrude and biofuel plants required for advanced biofuels in the EU-27+UK. Base scenario, 2030
Figure 59	Distribution of biocrude and biofuel production per country in the EU-
rigure 39	27+UK. Base scenario, 2030
Figure 60	Spatial distribution of modelled biocrude and biofuel plants required for
rigure oo	advanced biofuels in the EU-27+UK. Low demand - Base scenario, 2050 90
Figure 61	Distribution of biocrude and biofuel production per country in the EU-
rigare or	27+UK. Low demand - Base scenario, 2050
Figure 62	Spatial distribution of modelled biocrude and biofuel plants required for
500 0_	advanced biofuels in the EU-27+UK. High demand - Base scenario, 2050 91
Figure 63	Distribution of biocrude and biofuel production per country in the EU-
	27+UK. High-demand Base scenario, 2050
Figure 64	Spatial distribution of modelled biocrude and biofuel plants required for
3	advanced biofuels in the EU-27+UK. Repurpose scenario, 2050 92
Figure 65	Distribution of biocrude and biofuel production per country in the EU-
	27+UK. Repurpose scenario, 2050 92
Figure 66	Biomass utilization as a fraction of the total domestic availability potential
	in the Base and Alternative scenarios in the EU-27 + UK 93
Figure 67	Biomass utilization for advanced biofuels (excluding electricity/heat) per
	feedstock type in the Base and Alternative feedstock scenarios in the EU-27
	+ UK
Figure 68	Inter- country (EU-27+UK) trade of biomass, biocrude, and biofuel trade in
	the Base scenarios. The % labels show the share of trade relative to the
	total demand of the respective flow (biomass, biocrude, biofuel) 95



Figure 69	Biomass trade flows among countries in the EU-27+UK of biomass used for biofuels (in ktoe biomass). Base scenario, 2030. Arrows point trade at
Figure 70	country level and not the exact location of supply or demand
Figure 71	exact location of supply or demand
Figure 72	Biomass trade flows among countries in the EU-27+UK of biomass used for biofuels (in ktoe biomass). Low-demand base scenario, 2050. Arrows point trade at country level and not the exact location of supply and demand98
Figure 73	Biomass trade flows among countries in the EU-27+UK of biomass used for biofuels (in ktoe biomass). High-demand base scenario, 2050. Arrows point trade at country level and not the exact location of supply and demand99
Figure 74	Biocrude trade among countries in the EU-27+UK from HTL (ds) to upgrading plants. Low-demand base scenario, 2050. Arrows point trade at country level and not the exact location of supply and demand99
Figure 75	Biocrude trade among countries in the EU-27+UK from HTL (ds) to upgrading plants. High-demand base scenario, 2050. Arrows point trade at country level and not the exact location of supply and demand
Figure 76	Drop-in biofuel trade among countries in the EU-27+UK from biofuel plants to blending terminals in refineries. Low-demand base scenario, 2050. Arrows point trade at country level and not the exact location of supply and
Figure 77	demand
LIST OF TABLES	
Table 1	A list of the RED III - Annex IX/Part A biofeedstocks considered in the biomass supply chain model
Table 2	Main assumptions for the availability scenarios of lignocellulosic energy crops.
Table 3	Main assumptions for availability scenarios of agricultural residues for 2030 and 2050.
Table 4	Main assumptions for stemwood and primary forest residues available for bioenergy in 2030 and 2050 (Panoutsou & Maniatis 2021)17
Table 5	Main assumptions for secondary forestry residues available for bioenergy in 2030 and 2050 (Panoutsou & Maniatis 2021)18
Table 6	Overview of the approach used to estimate the spatial distribution of secondary forestry residues in S2Biom, adapted from Dees et al. (2017)18
Table 7	Possible host locations of advanced biofuel production and their integration benefits
Table 8	Biomass feedstock, biocrude, and biofuel characteristics. A detailed table with individual feedstock sub-categories is provided in Annex A131
Table 9	Main input data for Gasification and Fischer-Tropsch (GFT) at reference scale in 2030: 164 MW fuel output (5.2 PJ/y or 124 ktoe/y), 428 MW (13.5 PJ/y or 323 ktoe/y) feedstock input. Details are provided in Annex B336
Table 10	Main input data Gasification and Fischer-Tropsch (GFT) at reference scale in 2050: 164 MW fuel output (5.2 PJ/y or 124 ktoe/y), 428 MW (13.5 PJ/y or 323 ktoe/y) feedstock input. Details are provided in Annex B336



Table 11	Main input data centralized HTL and upgrading at reference scale in 2030: 73 MW fuel output (2.3 PJ/y or 53 ktoe/y), 156 MW feedstock input (4.92
	PJ/y or 117 ktoe/y)
Table 12	Main input data centralized HTL and upgrading at reference scale in 2050: 73 MW fuel output (2.3 PJ/y or 53 ktoe/y), 112 MW feedstock input (3.5
	PJ/y or 84 ktoe/y). The SMR unit is replaced with ex-situ green hydrogen
T. I.I. 43	supply
Table 13	Main input data for decentralized HTL and upgrading at reference scale in 2030: 73 MW fuel output (2.3 PJ/y or 53 ktoe/y), 112 MW feedstock input
	(3.5 PJ/y or 84 ktoe/y)
Table 14	Main input data for decentralized HTL and upgrading at reference scale in 2050: 73 MW fuel output (2.3 PJ/y or 53 ktoe/y), 112 MW feedstock input
	(3.5 PJ/y or 84 ktoe/y). The SMR unit is replaced with ex-situ green
	hydrogen supply
Table 15	Scale factors and maximum scale of individual units for HTL (de Jong et al. 2017) and Gasification and Fischer-Tropsch (GFT) (Huang et al. 2019) 41
Table 16	Plant segment sizes for 1) Gasification and Fischer-Tropsch and 2) HTL
	conversion plus upgrading 41
Table 17	Average yield for each crop in the High availability scenario while
	considering all the potential locations suitable for each crop type in EU-27 +
	UK 51
Table 18	Total biomass availability potential (Mtoe) for bioenergy in 2030 and 2050 in
	the different biomass availability scenarios
Table 19	Overview of bioenergy supply and bioenergy demand, and main assumptions in the Base and Alternative scenarios



SUMMARY

Advanced biofuels, are expected to play a central role in the decarbonisation of the EU transport sector, especially in hard-to-abate segments such as aviation, maritime, and heavy-duty transport. Biomass availability, along with the costs tied to its distribution and conversion into fuels, have been identified as critical for the scalability and long-term viability of advanced biofuel deployment. Over the years, uncertainty has surrounded the most efficient supply chain strategy for biofeedstocks. While traditional thinking favours siting biorefineries near biomass sources to reduce logistics costs, an alternative approach argues for clustering production within existing industrial sites, such as oil refineries, to benefit from integration synergies. Although several studies (e.g., ICL-Concawe 2021) have estimated Europe's biomass availability for 2030 and 2050, few have examined the economic side of biomass supply. Publicly available cost assessments remain scarce and are typically narrow in scope, often focusing on individual countries or regions.

This study addresses this gap by providing a detailed, cost-optimised assessment of biomass supply chains needed to meet advanced biofuel demand across the EU-27 + UK by 2030 and 2050. It focuses on key lignocellulosic biofeedstocks listed under Annex IX of RED III, including agricultural residues, energy crops, forest biomass, and post-consumer wood, with availability estimated at high spatial granularity through a dedicated crop model and literature sources. These data, combined with detailed cost elements for biomass production, transport, and conversion, are inputs in a mixed-integer linear programming model that determines the most cost-efficient biomass supply chain routes and configurations for Europe (see Figure S1).

The modelling incorporates Europe's transport network (trucks, rail, inland waterways, and shipping) and evaluates two representative biorefining pathways: Gasification and Fischer-Tropsch (GFT), suitable only for centralised configurations due to its high capital costs, and Hydrothermal Liquefaction (HTL), which can operate in both centralised and decentralised setups. The set advanced biofuel demand at both EU and national level is consistent with EU legislation projections.

1. Biofeedstock availability 2. Biorefinery siting options 4 Regional availability analysis for EU-27+UK (greenfield) 3. Possible supply chain configurations (retrofitting 4. Transport Network Direct transport 1. Centralised Jion Transport network in Europe included in ArcGIS model (road, Biomass rail, inland n waterways, shipping) Liquefaction 6. Bioenergy Demand 5. Cost Components Electricity, heat and advanced transport biofuel demand at country level for EU-27 +UK Biomass production Transport MILP optimisation model Optimising advanced biofuel **€**₂₀₂₃ supply chains considering competing bioenergy demand Conversion technologies (GFT, HTL)

Figure S1 Structure of biomass supply chain optimisation modelling

The supply chain optimisation was run across different scenarios reflecting different possible developments by 2050, including three biomass availability cases (capturing varying improvements in agroforestry practices), one advanced biofuel



demand case for 2030, and two demand cases for 2050. This approach enabled testing supply chain structure and resilience under diverse mobilisation pressures.

Centralised vs. Decentralised systems:

Large-scale, centralised GFT plants integrated with industrial assets are generally more cost-effective (especially in refineries) when biomass availability is sufficient. However, under high-demand or low-availability conditions, decentralised biocrude-producing HTL systems become more efficient, enabling the use of dispersed or remote biomass. Ultimately, optimal system choice depends on biofuel demand, local resource availability, and geographic factors such as inland vs. port access.

Geographic patterns and trade:

Geography is decisive for the optimal supply chain configuration and technology. For example, Western European countries with limited biomass availability like the UK, Belgium, and the Netherlands, emerge as key hubs for importing and upgrading biocrude due to their strong port and refinery networks. In contrast, biomass-rich regions such as Scandinavia and the Iberian Peninsula consistently emerge as biocrude producers for export. Large, centrally located countries like Germany and France require a mixed approach, investing in both centralised and decentralised supply systems. As biomass availability tightens relative to demand, cross-border trade intensifies, with liquid intermediates like biocrude and drop-in fuels preferred over solid biomass due to superior energy density and transport economics.

Biomass demand vs. biomass availability:

Europe's domestic biomass is sufficient to meet demand across scenarios in both 2030 and 2050. However, by 2050, the biomass availability-to-demand ratio tightens considerably in scenarios of high demand and/or low availability. This strains the supply chain, requiring deployment of costlier decentralised HTL plants across Europe to tap into scattered resources. To meet future biofuel targets, improvements in biomass management and innovations, especially in using marginal lands for energy crops, are essential.

Advanced biofuel supply chain costs:

In 2030, the average supply chain cost difference across scenarios is small, with process technology costs varying by less than 10%. This means that optimal technology selection is sensitive to input assumptions, and in practice, short-term deployment will likely favour the most commercially mature option.

By 2050, the cost landscape shifts considerably as learning effects drive down process technology costs. GFT benefits most from these reductions, emerging as the preferred option in scenarios with relatively high biomass availability to demand ratios (> 1.5), where centralised systems are more efficient. However, when this ratio declines, decentralised HTL becomes necessary, driving up cost variability as these systems are more widely distributed across Europe to effectively tap into remote biomass resources.

Infrastructure needs:

Looking ahead, Europe faces an infrastructure challenge: by 2050, depending on the biofuel demand and availability scenario, between 92 and 265 biocrude and biofuel plants will need to be built, a big jump from today's near-zero baseline. A large portion of biomass supply needs to come from energy crops grown on marginal land, which are not yet produced commercially. These findings underscore the urgent need for coordinated investment to develop a robust EU biofuel infrastructure, but also to advance the cultivation and commercialisation of energy crop systems.



1. INTRODUCTION

1.1. BACKGROUND

The transition towards a climate-neutral economy by 2050, as aimed for by the European Union (EU), requires structural and urgent changes of all sectors of the economy. Among these, transport is proven to be one of the more difficult sectors to decarbonize. While electrification will be a key element for the transition of road transport, low carbon liquid fuels will continue to play a significant role in difficult to decarbonise sectors such as heavy-duty transport, aviation and shipping for the foreseeable future. The production of renewable carbon-based fuels needs to ramp up urgently. Although stand-alone electrofuels (e-fuels) are expected to become increasingly important on the longer term towards 2050 (Brynolf et al., 2022), advanced biofuels are considered the most feasible and sustainable option to scale-up production in the next decade.

The high production cost of advanced biofuels is one of the most prominent barriers to their market deployment. Today, advanced biofuels cannot compete directly with fossil fuels, and neither with conventional biofuels currently available on the market. However, according to IEA Bioenergy (Brown et al., 2020), the capital and operating costs of advanced biorefineries can be significantly reduced with a large-scale market roll-out as a result of technological learning and economies of scale. As a result of these reductions, feedstock supply costs are expected to become even more prominent in the total production cost. Next to cost, also environmental considerations are becoming increasingly important with the need to comply with stringent sustainability criteria, such as the minimum requirements for greenhouse gas (GHG) savings of the Renewable Energy Directive (RED III) (EU, 2023). The availability of reliable, sustainable, and cost-effective feedstock supply chains is, therefore, essential for a successful market roll-out of advanced biofuels.

A range of biomass resources are potentially available. A study commissioned by Concawe (Panoutsou & Maniatis, 2021), hereafter to as the ICL-CONCAWE study, provides detailed insights into the potential availability of biomass in the EU-27 plus UK towards 2050, on a country level. It covers most biomass types that are listed as suitable feedstock for advanced biofuel production in Annex IX (part A and B) of the RED II. Three different availability scenarios (low, medium, and high) were employed in the study to show the impact of different levels of ambition to mobilize biomass and sustainability constraints. In addition, EU imports were analysed, though at lower level of detail. The study calculated that between 126 - 262 Mtoe for 2030 and between 101 - 252 Mtoe for 2050 of biomass could be available to produce advanced and waste-based biofuels in the EU, including imports. If converted into advanced and waste-based biofuels, after deduction of the biomass required for other uses as per Impact Assessment of the European Commission (EC, 2020), total production could be 46 - 97 Mtoe for 2030 and 71 - 176 Mtoe for 2050. Although the ICL-Concawe study provides detailed insights into the future amount of biomass that could be made available under technical and sustainability constraints, any feedstock supply costs and economic criteria were not considered.

The dispersed, erratic, and heterogeneous nature of many biomass feedstocks, which are often remote from locations of fuel demand, results in a mismatch with the scale and feedstock requirements of advanced biorefineries. This creates logistical challenges that cannot be identified when biomass supply is presented at country level, as in previous studies. For this reason, this study employs a spatially explicit approach, with the geographic locations of biomass supply presented at least on a regional level, and preferably on a local level. In addition, a



representation of all logistical activities and associated assets to move biomass from the production site to biorefinery is included. These cover handling, storage, preprocessing, transportation, infrastructure, and associated costs. Furthermore, downstream logistical processes are also becoming increasingly important in determining facility locations, in particular for new markets, including sustainable aviation fuels. The ICL-CONCAWE study (Panoutsou & Maniatis, 2021) highlights that the realization of the biomass potential availability depends on enormous efforts in terms of supporting mechanisms, feedstock production, and infrastructure (logistics, processing industry etc.).

1.2. OBJECTIVES AND SCOPE

The aim of this report is to provide a geospatial explicit assessment of the optimal cost of biomass feedstock supply chains for advanced biofuels in the EU-27 plus UK¹ for 2030 and 2050. The project focuses on the primary solid lignocellulosic biofeedstocks listed in Annex IX-Part A of the Renewable Energy Directive (RED), namely primary agricultural residues and lignocellulosic energy crops, forestry biomass such as low grade stemwood and forestry residues and woody biowaste.

The research was organized around the following five sub-objectives, employing various methodologies and modelling tools:

- Spatially explicit mapping of domestic biomass availability potentials and costs at roadside in the EU-27 + UK until 2050 at regional level: For agricultural biomass (lignocellulosic crops grown on marginal lands and primary residues), bioenergy potentials and costs were calculated and mapped on a 1 km² resolution basis using a spatial explicit model². Forest biomass and biowastes were mapped based on up-to-date studies that have quantified their spatial distribution and costs in Europe at NUTS-3 level. Three biomass availability scenarios were considered, Low, Medium, and High, each reflecting different assumptions on future land use, biomass yield improvements, and technological progress. Biomass potentials were calculated on an annual basis, and seasonality impacts on productivity were not modelled.
- Spatially explicit mapping of existing biorefinery locations and identifying
 key hotspots where future biorefineries may develop: The research combined
 a literature review of future scenario projections and supply chain modelling
 studies for advanced biofuels combined with expert interviews to identify the
 most important criteria for supply chain strategies and potential hot spots for
 advanced biofuel production. These include, amongst others, options for colocation and agglomeration (clustering), as well as access to infrastructure.
- Developing spatially explicit transport routes that link supply and demand locations: The analysis integrated actual transport infrastructure (road, rail, waterways, sea) and key logistical hubs (for example, ports, inland terminals, biofuel plants and oil refineries), capable of hosting advanced biofuels production. An existing spatially explicit biomass intermodal (road, rail, inland waterways, sea) transport network model³ was used to calculate the lowest-cost transport routes between different biomass supply locations and demand

2

¹ Countries such as Norway and Switzerland were not included in the analysis, as the data and information available in the literature, including that used in the ICL-Concawe study, primarily focus on the 27 European Union member states plus the UK, which was formerly an EU member.

² The model builds on work for the European Union's Horizon 2020 project ADVANCEFUEL, published by Vera et al (2021).

³ The GIS-based biomass intermodal transport model BIT-UU is, amongst others, applied in Hoefnagels et al. (2014) and Lamers et al. (2015).



- nodes in the EU-27 + UK. These demand nodes are represented by existing oil refineries for biofuels and major cities for bio-electricity and heat.
- Calculation and assessment of the economically optimal biomass supply chain network for advanced biofuels in the EU-27 + UK by 2030 and 2050: A mixed-integer linear programming (MILP) model was used to calculate the minimum cost for biomass mobilisation, conversion and advanced biofuel distribution in the EU-27 + UK. The model covers feedstock availability, intra EU-transport and logistics, conversion processes and the distribution of the finished transport fuels to national demand nodes. This comprehensive framework enables the evaluation of trade-offs between economies of scale and feedstock supply logistics, as well as the merits of centralized versus decentralized supply chain strategies.

⁴ The modelling framework was, amongst others, applied for a case study in Sweden, see in de Jong et al. (2017).



2. SUPPLY CHAIN MODELLING STRUCTURE

2.1. INTRODUCTION TO THE SPATIALLY EXPLICIT SUPPLY CHAIN OPTIMIZATION MODEL

The advanced biofuel supply chains in this study are optimised with a mixed-integer linear programming (MILP) model. MILP mathematical optimization models combine linear programming (LP) with integer constraints. The combination of binary (integer) and continuous decisions in MILP allows for detailed modelling of bioenergy supply chains, accounting for facility location, feedstock selection, and supply chain options for a large variety of possible supply chain configurations. The main drawback of MILP is its significantly higher computational requirements compared to continuous linear programming.

While mathematical optimization models, including MILP, to a certain extent, are commonly used in bioenergy supply chain studies, so far, these studies have typically been limited to regional or national case studies with minimal integration of transport infrastructure (Korpinen et al., 2023). The optimization model used for this study is adapted from two existing MILP models that were applied to case studies of advanced biofuel production in Sweden and Brazil. Both models used GAMS as a modelling system and Cplex as a solver:

- The spatially explicit supply chain configuration model was developed by de Jong et al. (2017) to evaluate the impact and interconnections of four cost-reduction strategies of advanced biofuel production in Sweden,
- The Bioenergy and Land Optimization Spatially Explicit Model (BLOEM) was developed by Tagomori et al. (2022) (Tagomori et al., 2023) to evaluate bioenergy pathways and carbon storage in Brazil.

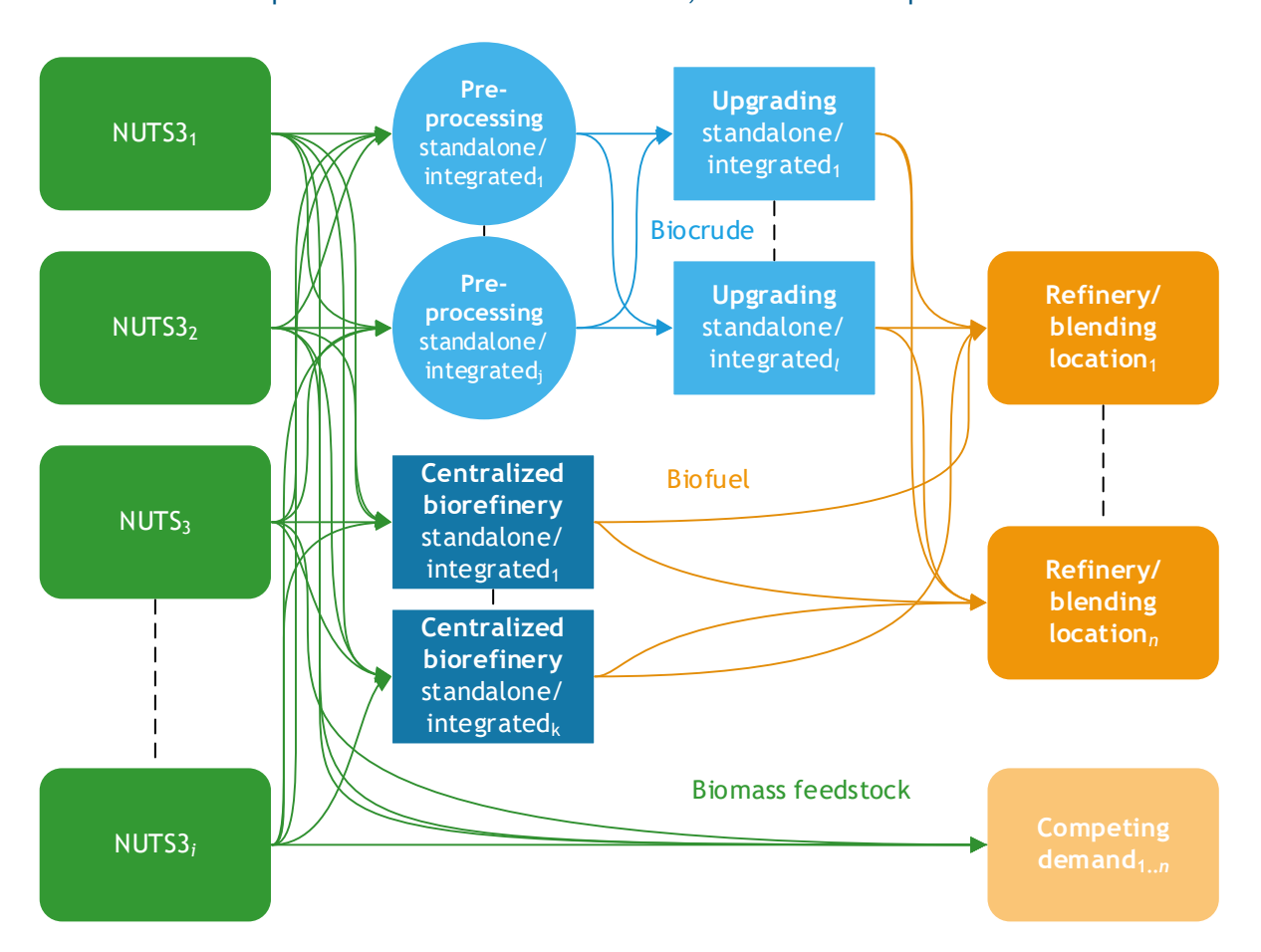
The MILP model itself does not include geographic locations and the transport network infrastructure connecting these locations. To address this, the model was combined with a Geographic Information Systems (GIS) based Biomass Intermodal Transport network model (BIT-UU) that calculates the least-cost route between each possible origin (e.g., biomass production site) and destination in the model (see Figure 1).

With this approach, advanced biofuel supply chains can be calculated and evaluated while taking into account regional dynamics and potential trade interactions between EU countries in meeting their projected demand for advanced biofuels in 2030 and 2050. The model incorporates biomass availability at NUTS-3 level, the costs of transporting biomass to conversion facilities, its processing at biorefineries, and the subsequent transport of drop-in biofuels to blending terminals. It also captures the influence of competing biomass demand from the electricity and heat sector, which affects supply chain dynamics (see Figure 1). Moreover, the model identifies the economically optimal biofuel production pathways, including the choice between decentralised and centralised configurations, as well as co-location strategies, which are further explained in Chapter 4.



Figure 1

The structure of the spatially explicit supply chain optimization model, adapted from Huang et al. (2019). Centralized: biomass pre-processing plus conversion and biofuel upgrading at one location. Decentralized: biomass pre-processing (e.g., biocrude production) and biofuel upgrading at different locations. Standalone: location without co-location benefits. Each biofuel blending location (at oil refineries) or competing demand (bioenergy for non-transport fuels) location (major cities NUTS-2) is connected to all possible supply locations in the EU-27 plus UK (NUTS-3 level), either via distributed or centralized conversion facilities, considering transport route-specific costs for biomass feedstock, biocrude and drop-in biofuel.



2.2. OVERVIEW AND SELECTION OF BIOREFINING TECHNOLOGIES FOR ADVANCED BIOFUELS

The potential technological pathways for producing advanced biofuels from lignocellulosic biomass along with their corresponding Technology Readiness Levels (TRL), as given by Motola et al. (2024) and Bardon et al. (2025), are summarised. Some pathways rely on biochemical processes, such as fermentation to alcohols, while others are based on thermochemical conversion. Since the primary goal of this study is to evaluate supply chain potentials for transport fuels (such as SAF and renewable diesel) towards 2050, processes targeting alcohol production are excluded, due to model size constraints and the expectation that their role in the transport sector will be limited, given their lower energy density, blending restrictions, and the availability of more suitable drop-in fuel alternatives.



The processes for the conversion of lignocellulosic bio mass to bio-oils/biofuels and their respective TRLs are:

- Alcohol fermentation: TRL 7-8
- Gasification followed by Fischer-Tropsch (GFT) synthesis: TRL 6-8
- Fast pyrolysis (without bio-oil upgrading⁵): TRL 8-9
- Hydrothermal liquefaction (HTL) (without biocrude upgrading): TRL 5-6
- Biomethanol synthesis: TRL 8
- Alcohol-to-Jet (ATJ): TRL 6-7

Each technology has distinct advantages and drawbacks. For instance, GFT is capital-intensive but highly versatile, capable of processing diverse feedstocks and producing high-quality drop-in fuels (Brown et al., 2020). Most recently announced advanced biofuel projects are based on GFT, such as the BioTfuel® / BioTJet⁶ in France.

Pyrolysis and HTL are similar in that both produce intermediate biocrude. However, both technologies face challenges regarding scalability, primarily due to limited heat-transfer efficiencies in large reactors (Bridgwater, 2018; Castello et al., 2018). While fast pyrolysis is already advanced in terms of technological readiness, HTL is an emerging technology with significant potential, particularly suitable for biomass with significant water content. HTL produces a higher quality biocrude, characterized by better stability and lower oxygen content, making storage and transport easier (Yáñez et al., 2021). At a conceptual process level, the cost differences between pyrolysis and HTL are not significant (Karimi et al., 2025). Nevertheless, ongoing technological progress, particularly in the lower-TRL HTL technology, may further refine our understanding of these processes' performance and economics, potentially revealing both opportunities and challenges.

Alcohol-to-Jet (ATJ) is an emerging route with potential for sustainable aviation fuel (SAF) production, although it is currently considered costly, especially at large scale, compared to other thermochemical processes (Chireshe et al., 2025; Dyk, 2024).

This study does not aim to perform an in-depth technological evaluation or forecast future advancements for these processes. Instead, the goal is to select representative technologies to illustrate their impacts on supply chain costs. Given that both centralized and decentralized supply chain configurations are analyzed, GFT and HTL were selected as representative technologies. GFT, despite high capital expenses, benefits significantly from economies of scale and is thus suitable for centralized supply chains. Conversely, HTL is characterized by lower capital requirements and smaller reactor systems, making it adaptable to both centralized and decentralized configurations.

It is important to emphasize that not all processes are currently efficient in handling every biomass feedstock. For instance, thermochemical processes face efficiency and operational challenges when processing agricultural biomass, primarily due to high chlorine and ash content, whereas biochemical processes typically show better suitability (Lammens et al., 2016). However, as the objective of this study is not a detailed technical analysis, and ongoing research aims to overcome these

⁵ Upgrading bio-oil is not yet at the same TRL, as challenges remain in achieving drop-in fuel specifications.

⁶ https://www.ifpenergiesnouvelles.com/article/biotfuelr-project-entry-industrialization-and-commercialization-phase



feedstock-related constraints, it is assumed here that both GFT and HTL can effectively process all lignocellulosic biofeedstocks.

2.3. OVERVIEW OF THE MODELLING APPROACH

An overview diagram illustrating the different supply chain steps and configurations, including the mobilized biomass feedstocks, transport modes, and conversion processes considered in this study, is provided in Figure 2. Further details on the assumptions for each step of the supply chain are discussed in the following chapters of this report.

The approach used in this study consists of five large datasets that are combined as input to the MILP optimization model (see Figure 3). These data sets are categorized into techno-economic data covering biomass production, transport and conversion to biofuels, spatially explicit biomass availability, spatially explicit locations for advanced biofuel production, logistic transport network data, and projections of future bioenergy demand for both transport and electricity and heat applications. This means that the model also incorporates supply chain optimisation for competing bioenergy uses, focusing on electricity and heat production from solid biomass, to better understand their influence on optimal biofuel supply chains. The data categories and modelling steps are explained in more detail in the next chapters.



Figure 2 Distributed and centralized supply chains and scope of the model. Adapted from de Jong et al. (2017).

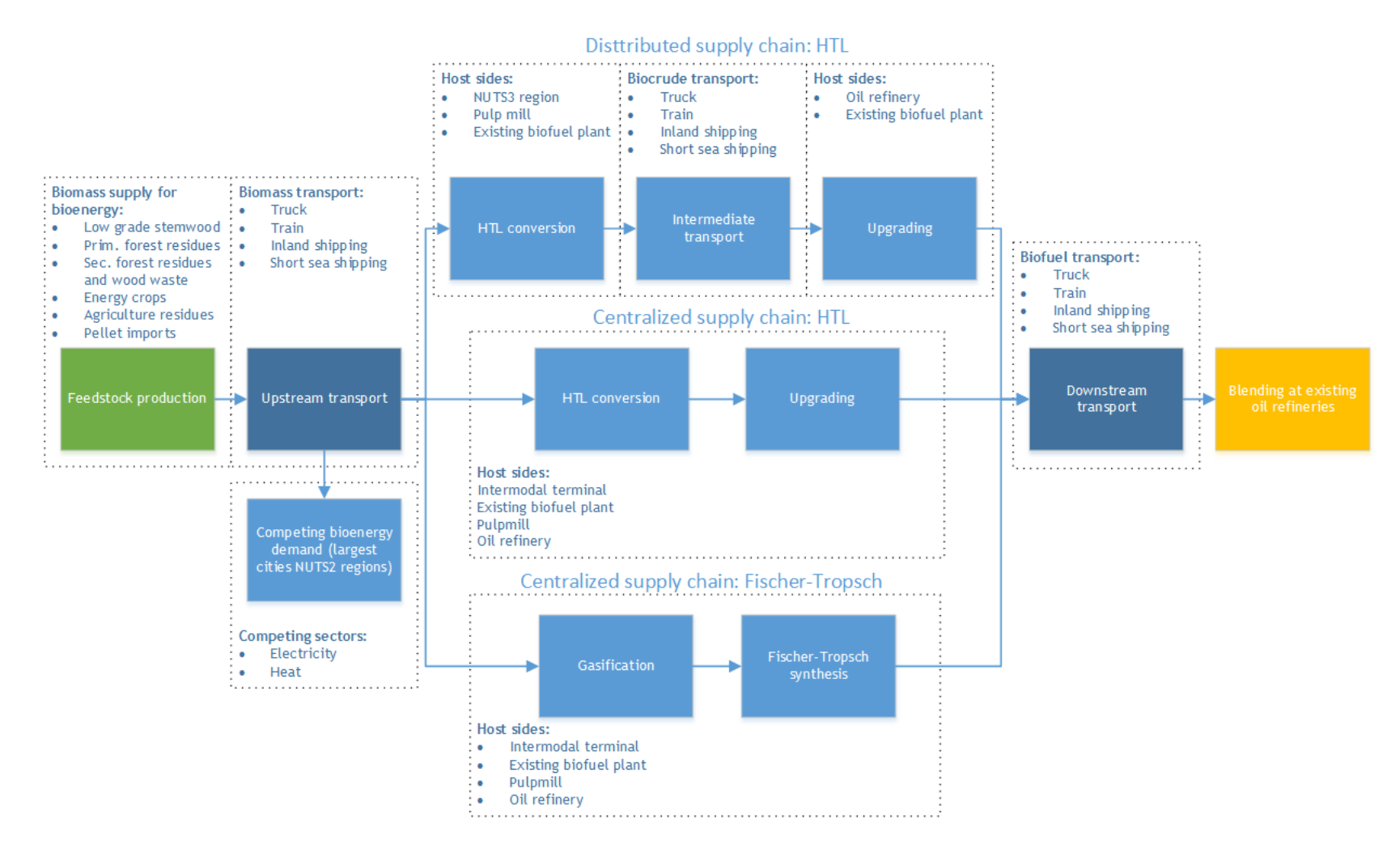
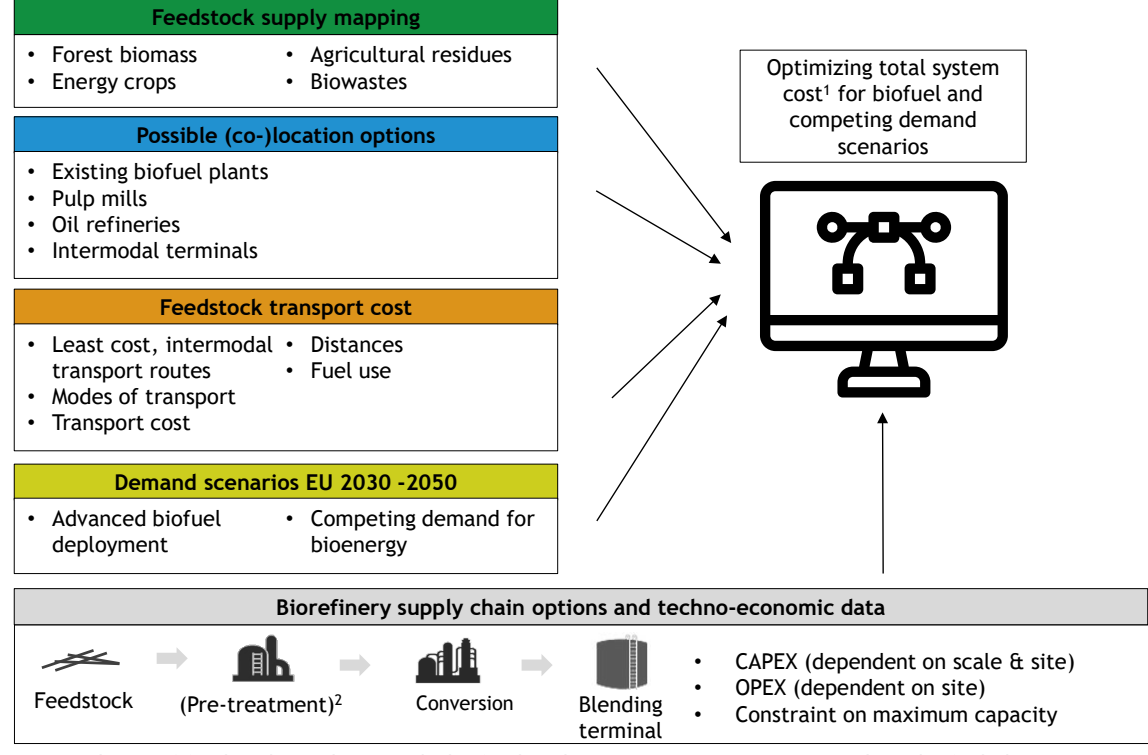




Figure 3 Overview of the modelling framework. The MILP model optimizes for the lowest cost of the entire supply chain system to meet the demand for advanced biofuels, and competing bioenergy uses (heat and electricity).



- 1) Total cost of feedstock supply at roadside, feedstock transport (to preprocessing plant, biofuel plant or competing demand location), centralized or distributed conversion, and transport of biocrude and biofuels.
- 2) Pretreatment only applies to HTL biocrude production in distributed supply chains.



3. METHODOLOGY: CALCULATING AND MAPPING BIOMASS AVAILABILITY POTENTIAL TOWARDS 2050

3.1. INTRODUCTION TO THE CONSIDERED BIOFEEDSTOCKS

The eligible biofeedstocks for advanced biofuel production in the EU, most of them lignocellulosic in nature, are defined in Annex IX - Part A of the Renewable Energy Directive (RED III). These feedstocks are not subject to a usage cap, making them central to EU strategies for sustainable transport decarbonisation.

As defined in the scope, liquid or high in water content biofeedstocks such as manure, sewage sludge and algae biomass were excluded, as these are typically processed close to their point of generation due to technical and regulatory constraints on transportation. Secondary agricultural residues, including olive pomace, fruit pits, and peels, were also excluded due to their diverse nature, scattered availability, and predominant use in other applications, like composting.

Additionally, although municipal solid waste (MSW) represents the largest stream within the broader biowaste category, it was excluded from supply chain modelling because of its heterogeneous composition, low energy density, and the need for specialized logistics and pre-processing infrastructure. Similarly, animal, mixed food waste and vegetal waste were considered outside the scope, given their relatively small volumes and their prioritisation for alternative uses like composting. Finally, other biofeedstocks of low volume, such as palm oil mill effluent and empty palm fruit bunches, tall oil pitch, crude glycerine, bagasse, grape marcs and wine lees, nut shells, husks, were not considered. These materials lack consistent availability data in public literature. Moreover, including them would substantially increase the complexity of the modelling exercise while their limited availability suggests they would have only a modest impact on the overall structure of an optimal EU supply chain network.

It is also important to note that a few feedstocks were newly added to Annex IX during the course of this study, such as intermediate crops, non-food/feed crops cultivated on severely degraded land, raw methanol from kraft pulping, and fusel oils. These were not considered in the analysis due to the current lack of scientific tools and methodologies for reliably estimating their availability.

As with other biomass availability studies, such as ICL-Concawe (2021), this analysis estimates feedstock potentials for 2030 and 2050 under three availability scenarios, Low, Medium, and High, to capture uncertainties in future supply. The Low scenario assumes current agricultural and forestry practices, while Medium and High scenarios incorporate progressive improvements in productivity and mobilisation. More details are given in the following sections.



Table 1 A list of the RED III - Annex IX/Part A biofeedstocks considered in the biomass supply chain model.

Biofeedstocks in Annex IX - RED III	
Algae/bacteria	
Algae if cultivated on land in ponds or photobioreactors	X
Cyanobacteria (1)	X
Agricultural biomass	
Straw	✓
Maize stover	√
Animal manure	X
Oilseed crop residues	√
Agricultural prunings	√
Lignocellulosic (energy) crops in marginal lands	/
Non-food and feed crops on severely degraded lands (only for aviation sector) (1)	X
Secondary agricultural residues from agro-industries	X
Palm oil mill effluent and empty palm fruit bunches; Tall oil pitch; Crude glycerine; Bagasse; Grape marcs and wine lees; Nut shells; Husks;	X
Intermediate crops such as catch and cover crops (only for aviation sector) (1)	X
Forestry biomass	
Primary and secondary forestry residues	√
Low-grade stemwood such as fuelwood	/
Biowaste	
Municipal solid waste	X
Animal and mixed food waste, vegetal waste	X
Sewage sludge	X
Post-consumer wood	√
Paper cardboard	√
Raw methanol from kraft pulping (1)	X
Fusel oils from alcoholic distillation (1)	X

(1): Biofeedstocks added in the recently amended Annex IX in March, 2024

3.2. AGRICULTURAL BIOMASS

In this report, agricultural biomass refers to primary agricultural residues and lignocellulosic energy crops. A multiple-step approach was applied to determine and map (on a 1 km² basis) the availability of agricultural biomass (for all competing uses) for 2030, 2040, and 2050. The section covering land availability for agricultural biomass is presented in Annex A1. Cereal straw and maize stover are estimated and mapped since they are Europe's most relevant agricultural residue feedstock types (Dees, Datta, et al., 2017; García-Condado et al., 2019). The main cereal crops produced in Europe (wheat, rye, barley, oats, triticale and sorghum) are considered for cereal straw (Eurostat, 2024). Other agricultural residues, including prunings and oil seed crop residues, are based on existing biomass resource assessment data from EU S2Biom (Dees, Datta, et al., 2017). For lignocellulosic energy crops, the most representative crop types for Europe are selected (Perpiña Castillo et al., 2015). These feedstocks include perennial grasses and short-rotation coppice. From perennial grasses, miscanthus, switchgrass, reed canary grass (RCG) and giant reed are considered; for short rotation coppice, willow, poplar and eucalyptus are considered. Results are presented on a dry tonne/(ha-year) basis. Note that this mapping assessment builds upon the work on



the detailed supply maps of lignocellulosic energy crops cultivated on marginal land in the EU-27+UK under land-based sustainability criteria of RED II/III (European Commission, 2018; Vera et al., 2021).

3.2.1. Lignocellulosic energy crops biomass availability potentials

The steps to estimate biomass potentials for lignocellulosic energy crops are summarized in the following three points, and a detailed explanation of the methods is presented in Annex A1.

- 1. The maximum amount of biomass (crop-specific) that can be produced annually, given the water use efficiency of biomass production in relation to water loss from evapotranspiration¹ is estimated. Irrigation practices were not considered, and biomass availability estimates are therefore based exclusively on rainfed conditions. The maximum amount of biomass is defined as the gross biomass potential. To estimate the gross biomass potential for each crop, daily evapotranspiration rates are assessed spatially explicitly for the reference years. The climatic parameters used to estimate daily evapotranspiration rates align with the RCP 2.6 scenario. This scenario reflects the pathway required to keep the average global temperature rise below 2 °C (in alignment with the Paris Agreement, however, the current temperature forecasts indicate a significant deviation from this pathway).
- 2. Crop and location-specific suitability parameters, such as soil texture, frost-free days, and precipitation are applied to the crop-specific gross biomass potential to reflect the effect of distinct biophysical conditions on crop growth.
- 3. Finally, harvest indices (the crop ratio between yield and total biomass) are applied to obtain biomass potentials for lignocellulosic energy crops.

This approach builds upon the methods presented in (Dees, Datta, et al., 2017; Ramirez-Almeyda et al., 2017). It has been consistently applied in literature and EU model frameworks such as the JRC-EU-TIMES model and S2Biom.

Regarding water efficiency, although precipitation was included in the model, in practice, not all rainfall is effectively available to crops, a phenomenon known as effective precipitation. For effective precipitation, equations were used to generate high-level water balance estimates. However, given their phenological characteristics, crops can reach only 90% of the gross biomass potential even under no water-limiting conditions (Ramirez-Almeyda et al., 2017). Three availability scenarios for lignocellulosic energy crops are considered for this study and presented in Table 2. The availability scenario assumptions are aligned with (Baranzelli et al., 2014; Lavalle et al., 2016; Ruiz et al., 2015). Balanced fertilization is considered².

12

¹ It is the combined loss of water in the form of evaporation from the soil surface and transpiration from the plant

² The input rate of fertiliser is directly proportional to the amount removed by harvesting the crop. An additional 33% is accounted for by potential losses from mineral uptake and terrain conditions. Annex A1 provides the mineral content of each crop.



Table 2 Main assumptions for the availability scenarios of lignocellulosic energy crops.

Parameter	Low Scenario	Medium Scenario	High Scenario
Share of potentially available marginal land (Meeting RED II/III sustainability criteria and suitably parameters for lignocellulosic energy crop production)	50%	75%	100%
Annual yield increases over time for lignocellulosic energy crop (Reflecting productivity increases from improved crop management practices)	0.5%	0.75%	1%

3.2.2. Agricultural residues biomass potential: cereal straw and maize stover

Agricultural residue biomass availability potentials are assessed considering the available agricultural land for each point in time. Agricultural residues are directly correlated to crop-specific yields. Therefore, spatially explicit yields were estimated for wheat, rye, barley, oats, triticale, sorghum, and maize. These crops are selected as they represent the largest majority of EU cereal production (European Commission, 2023). A detailed explanation of methods to estimate agricultural residue biomass potentials is presented in Annex A1.

The current country-specific shares of utilized agricultural area dedicated to each cereal crop were used to map (spatially explicitly) potential yields for wheat, rye, barley, oats, oats, triticale, sorghum, and maize. These shares were applied given that the land use/cover projections lack the distinction between uses for agricultural land. In addition, the shares of utilized agricultural land for cereals have remained relatively constant over the past 15 years (European Commission, 2023). Therefore, it is assumed that the shares of these cereal crops within the total utilized agricultural land projections remain constant over time. It is acknowledged, however, that rapid policy shifts could potentially impact these shares in the future. Currently utilized agricultural areas dedicated to wheat, rye, barley, oats, triticale, sorghum and maize were retrieved from Eurostat (Eurostat, 2024). To avoid overestimating the areas dedicated to each of these crops, the areas with the highest crop suitability were selected until specific shares of the utilized agricultural area dedicated to each crop were met (at a country level). This assumption is made to reflect the importance of cereal crops compared to other agricultural land-use commodities in the EU (European Commission, 2023).

Future cereal yields were estimated for each location using the current and historic average yields in the EU, agroclimatic yields, and agroecological suitability maps under the 2.6 RCP scenario. The suitability maps were employed to derive a location-specific score index to adjust EU average yields to local characteristics. Subsequently, the residues-to-yield ratio was applied to obtain overall residue potentials. Three availability scenarios for agricultural residues are considered for this study as presented in Annex A1, which are based on Eurostat (2024), Schils et al. (2018), and Tian et al. (2021). Note that results are presented for cereal straw, which includes residues from wheat, rye, barley, oats, triticale, and sorghum, as well as for maize stover.



Table 3 Main assumptions for availability scenarios of agricultural residues for 2030 and 2050.

Parameter	Low Scenario	Medium Scenario	High Scenario		
	30% of the cereals yield difference ¹ is covered by 2050	60% of the cereals yield difference ¹ is covered by 2050	90% of the cereals yield difference ¹ is covered by 2050		
Annual yield increases	Explanation: This assumption is based on the principle that crop yields can increase to the agroclimatic attainable yield. The larger the gap between the attainable and the actual yield, the more room for yield improvement. This trend is evident from historical yield data reported by Eurostat. Countries with a larger yield gap (e.g., Romania) showed a higher yield increase over the last years compared to countries such as Germany, which have already invested more in agricultural improvements, and have yields that are closer to the maximum, resulting in smaller increases.				
for cereal crops (Reflecting productivity increases	To adhere this principle and capture past trends in how EU countries (based on their current yield status) will progress towards closing the gap, the following classification was applied:				
from improved crop management practices)	• EU countries with a yield gap ≥ 30%: A higher yield increase is assumed within the first 15 years (2025-2040) than for the last decade of the evaluated horizon (up to 2050). This is in alignment with the fast progress currently observed in these countries. More specifically, 75% of the yield gap closure decided per scenario is assumed to be achieved in the first 15 years (up to 2040). In the last 10 years (up to 2050), the annual yield increase is lower, assuming the remaining 25% is covered.				
	• EU countries with a yield gap < 30%: It is assumed that the yield increases linearly until it reaches the set yield gap closure % per scenario. This assumption is applied as countries with a smaller yield gap are expected to increase their yields at a lower and close-to-constant pace. This assumption is applied to all crop types.				
Removal rate (%) of agricultural residues	40%	45%	50%		

¹⁾ Cereals yield difference = agroclimatic attainable yield in 2050 - yield in 2025

3.2.3. Agricultural residues biomass potential: prunings

Prunings and cuttings from fruit trees, vineyards, olive groves, and nut orchards represent another source of lignocellulosic biomass. These residues are commonly produced during orchard management practices aimed at enhancing productivity, disease control, and mechanization efficiency (Pari et al., 2017).

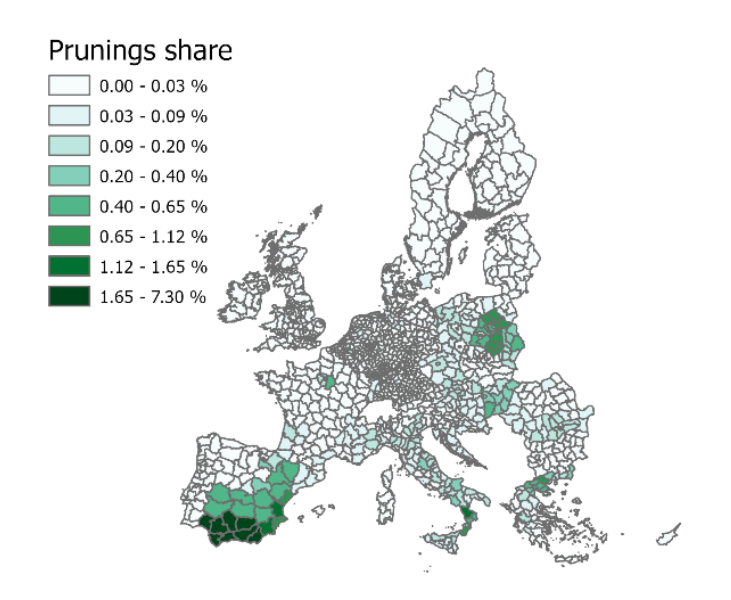
A large proportion of these residues remains underutilized, often being incorporated into the soil or simply left to decompose in the field. While this practice contributes positively to soil health and carbon sequestration, a significant share could still be sustainably mobilized for bioenergy and bio-based uses. In terms of resource potential, the ICL-CONCAWE study (Panoutsou & Maniatis, 2021) estimates that by



2030, the total quantity of agricultural prunings will reach between 10 and 12 Mt (dry), corresponding to approximately 4 to 5 Mtoe. By 2050, this figure is projected to increase by 20%, reaching between 12 and 15 Mt (dry) (5 to 6 Mtoe), in line with the gradual intensification of perennial crop production and improvements in biomass collection.

To map the potential of prunings for all markets and bioenergy, the availability data from the ICL-CONCAWE study (Panoutsou & Maniatis, 2021) were used. The spatial distribution at the NUTS-3 level was based on the estimated distribution of prunings in 2030 from the S2Biom project (Dees et al. 2017) shown in Figure 4Error! Reference source not found. The same distribution shares were also applied to 2050.

Figure 4 Estimated relative distribution of prunings. Based on S2Biom (Dees et al. 2017).



3.3. FOREST BIOMASS

3.3.1. Stemwood and primary forestry residues

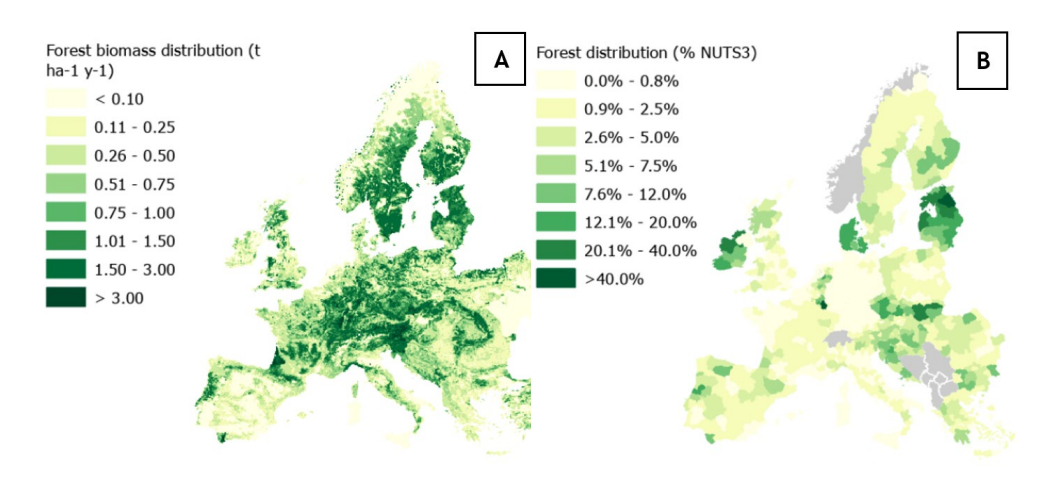
To map the potential of stemwood³ and primary forestry residues for all markets and bioenergy markets, the country-level availability data for all markets (materials, energy) from the ICL-CONCAWE study (Panoutsou & Maniatis, 2021) were used. Stemwood used for energy purposes is generally of lower quality than stemwood used for materials and is often referred to as low-grade stemwood. To scale the resource estimates of stemwood and primary forestry residues from the ICL-CONCAWE study from a national level to NUTS-3 level, scaling factors were applied. These scaling factors were derived from an estimate of the spatial distribution of forest biomass availability in Europe in 2020 by Verkerk et al. (2019) as shown in Figure 5 (A). Based on the forestry biomass distribution, the proportion of national forest biomass potential was calculated at NUTS-3 level (B). The spatial distribution within countries is based on the existing distribution of tree species in

³ Stemwood is defined by Camia et al. (2021) as "the wood of the stem(s) of a tree, i.e. the above ground main growing shoot(s). Stemwood includes wood in main axes and in major branches where there is at least X m of 'straight' length to Y cm top diameter." In Camia et al. (2021), it is the "over bark biomass of the stem from 15 cm height (thus excluding the stump) up to a minimum top diameter of 9 cm.".



Europe and are assumed to remain constant over time to 2050. Although factors, including climate change and human interventions, could have an impact in the future, the distribution of forests is not expected to change significantly in Europe in the period before 2050 (Material Economics, 2021).

Estimated spatial distribution of forest biomass availability in 2020 for all uses [in t ha⁻¹ y⁻¹] at (A) grid cell [10 km x 10 km], (Verkerk et al., 2019), and (B), proportion % of national forest biomass potentials at NUTS-3 level [% y⁻¹]⁴.



Stemwood is already extensively utilized by wood processing industries. Industrial grade stemwood is excluded later from this analysis because it is primarily directed to material markets rather than being used as fuel, for example in wood stoves for residential heating. Nevertheless, stemwood currently represents approximately 65% of today's primary wood used for energy (Camia et al., 2021), although it is generally prioritized for material uses over energy production (Camia et al., 2021)., in line with cascading use principles.

Furthermore, part of the stemwood available for bioenergy is currently used as fuelwood. Fuelwood is typically a lower quality stemwood directly used for combustion. Although it is expected that fuelwood consumption for residential heating will decline in the future, it is important to note that it cannot be entirely mobilized for other markets as a significant portion is sourced from private and informal sources (Camia et al., 2021). The shares of low-grade stemwood available for bioenergy are provided in Table 4.

16

 $^{^4}$ The supply potential of forest biomass for bioenergy (transport, E&H) was calculated by multiplying the national potential with these shares per NUTS-3 region



Table 4 Main assumptions for stemwood and primary forest residues available for bioenergy in 2030 and 2050 (Panoutsou & Maniatis 2021).

Parameter	Low Scenario	Medium Scenario	High Scenario
Stemwood availability share for energy purposes (Current stemwood share for energy = 45%)	25%	30%	50%
Primary forestry residues availability share for energy purposes	40%	50%	60%

It should be noted that in reality utilization rates of forest residues are region specific. Verkerk et al. (2019) identified that existing wood uses in some forest-rich regions, including south Sweden and southwestern France, are already at high levels. As a result, the unused potential of primary forest biomass is therefore limited in these regions while other regions, including central Portugal and regions in central Europe, still have more underutilized forest biomass available.

3.3.2. Secondary forestry residues

Secondary forestry residues are by-products or residue streams from wood processing industries, including sawmills, pulp and paper production, and other wood processing industries. The potential is, therefore, directly linked to the development of these industries. The following different types of secondary residues are considered:

- Sawmill by-products and sawdust from sawmills
- Other forestry industry by-products (for example, residues from wood-based panels production)
- Black liquor

The estimated availability potentials of secondary forestry residues in the ICL-CONCAWE study (Panoutsou & Maniatis, 2021) are based on existing EU projects, including S2Biom and Biomass Policies⁵. To map the spatial distribution of secondary forest residues at NUTS-3 level, results of the EU S2Biom project Base scenario⁶ were used (Dees et al. 2017). The approach to calculate the spatial distribution of secondary forestry residues at NUTS-3 level used in S2Biom is summarized in Table 6. The main assumptions for the Low, Medium and High availability scenarios consider the availability of secondary forestry residues for bioenergy, and are consistent with the ICL-CONCAWE study (see Table 5).

⁵ EU Intelligent Energy Europe (IEE) - Biomass Policies.

⁶ The S2Biom base potential considers currently applied sustainability practices (Dees et al. 2017).



Table 5Main assumptions for secondary forestry residues available for
bioenergy in 2030 and 2050 (Panoutsou & Maniatis 2021).

Parameter	Low Scenario	Medium Scenario	High Scenario
Secondary forestry residues and post-consumer wood availability share for bioenergy	55%	60%	65%

Table 6 Overview of the approach used to estimate the spatial distribution of secondary forestry residues in S2Biom, adapted from Dees et al. (2017).

Category	Approach
Sawmill residues	Spatial distribution of forest biomass availability
Residues from industries producing semi-finished wood-based panels	National level to NUTS-2: Employees of the wood industry sector retrieved from EUROSTAT. NUTS-2 to NUTS-3: land area.
Residues from further wood processing	National level to NUTS-2: employees per sector "Construction", "Furniture", "Packaging", "Other" retrieved from EUROSTAT applied to residues from the respective sectors. NUTS-2 to NUTS-3: land area.
Secondary residues from pulp and paper industries	Number of pulp and paper mills per NUTS-3 area

3.4. BIOWASTES

Current and future waste potentials at country level were taken from the ICL-CONCAWE study (Panoutsou & Maniatis, 2021), which used a statistical method to determine the availability potentials in each country based on Eurostat and national waste generation and waste treatment data. Biowaste contains several categories, such as municipal solid waste (MSW), vegetal waste, animal & mixed food waste, paper cardboard, and post-consumer wood waste (PCW). Municipal solid waste (MSW) is the largest waste source but is also a challenging feedstock for biofuel production due to its heterogeneous content, low energy density, contaminants, and high moisture content. Although many biowaste categories are suitable for conversion to biofuels, they require dedicated logistic and pre-processing steps, such as waste separation and cleaning, which were beyond the scope of this study. We used the S2Biom Bio2Match tool (Lammens et al., 2016) to select biowaste feedstock categories suitable for biofuel conversion without complex pre-processing requirements. These include:

- Post-consumer wood waste (PCW): suitable for biofuels;
- Paper cardboard: suitable for biofuels.



As outline before, the following categories were excluded from biofuel production for the reasons explained above:

- Animal & mixed food waste;
- Vegetal waste;
- Municipal solid waste (MSW);
- Other organic waste, including sewage sludge.

The potential availability of post-consumer wood waste (PCW) and paper cardboard distribution was calculated at NUTS-3 level based on current population data. Due to a lack of data on future changes in population densities, the spatial distribution within countries was assumed to remain constant over time. The distribution was calculated with the following equation, adapted from (Hamelin et al. 2016):

$$BMW_i = MSW_{c(i)} * POP_i$$

Where:

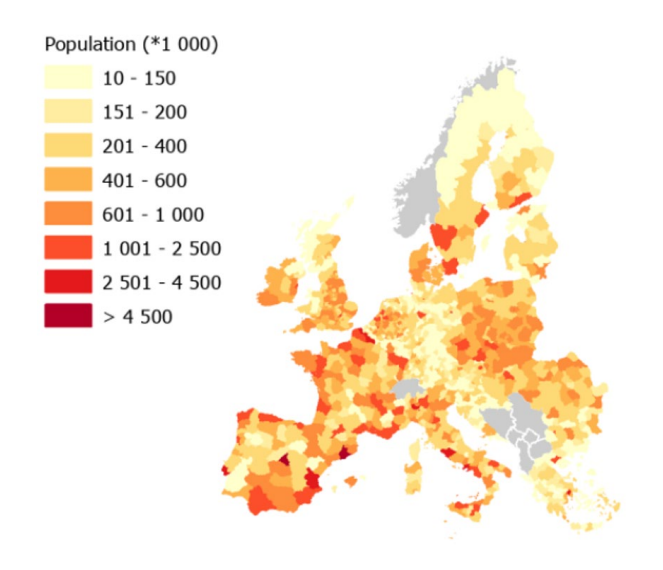
BMW_i: Biowaste potential for NUTS-3 area i (t y⁻¹; dry weight)

 $MSW_{c(i)}$: Biowaste potential per capita of the country where the NUTS-3 area i belongs (t person⁻¹ y⁻¹). The potential per country is derived from the ICL-CONCAWE study (Panoutsou & Maniatis, 2021).

POP_i: Population of NUTS-3 area i (person) (see Figure 6)

i: NUTS-3 area.

Figure 6 Population per NUTS-3 region in the EU27+UK in 2021 (European Commission - Eurostat/GISCO, 2023).





4. METHODOLOGY: SUPPLY CHAIN CONFIGURATIONS AND CO-LOCATION OPTIONS

Current advanced biofuel production facilities are still in early stages of commercialization. Nevertheless, locational choices of these existing plants provide insights into how the market might develop. Firms and production plants tend to be located in clusters to benefit from interactions and economic activities in the same region. These advantages are called agglomeration economies (Rodrigue, 2020). For biorefineries, key aspects of agglomeration economies include, amongst others, shared infrastructure, supply chain efficiencies, labour market pooling, and market access. Research on biofuel production is limited, but studies in the USA showed that rail and other infrastructure access, population density, and proximity to blending terminals are key location factors of first-generation ethanol and biodiesel plants (Fortenbery et al., 2013; Haddad et al., 2009). In fact, biodiesel plants were more attracted to output markets than feedstock supply. Our assessment of advanced biofuel production plants resulted in similar findings: 17 out of 19 existing plants⁷ in Europe that process lignocellulosic biomass and produce biofuels or intermediates are located in industrial areas to benefit from agglomeration economies with strategic access to infrastructure. A more detailed assessment is provided in Annex E and in Rothenburger (2023).

4.1. LOCATION AND INTEGRATION STRATEGIES

There are four types of integration strategies between industrial processes defined by de Jong et al. (2015):

- 1. **Greenfield:** Building a new, stand-alone facility at a new site. In most cases, greenfield locations are also strategically chosen in clusters with other economic activities to benefit from agglomeration economies, such as access to logistic infrastructure.
- 2. **Co-locating:** Placing a new, separate facility next to an existing one to share resources (e.g., feedstock, utilities) without altering the original production line.
- 3. **Retro-fitting:** Modifying an existing facility's production line to produce an additional output by utilizing by-products or unused components.
- 4. **Repurposing:** Converting an existing, inactive facility to produce a completely different output than it originally did.

Options 2,3 and 4 are examples of co-production strategies that provide integration benefits. The possible integration benefits depend on the degree of integration on the host side and options for integration, as depicted in Figure 7. Repurposing of existing plants is not included in the main cases of the supply chain simulations because it requires a detailed analysis considering the equipment's lifetime, current use, and future status, which is beyond the scope of this project focusing on feedstock supply chains. However, an approximate assessment of cost reductions achievable through repurposing will be explored through an additional scenario.

Key insights from expert interviews (Annex E) showed the following preference in terms of integration strategy (1st is best).

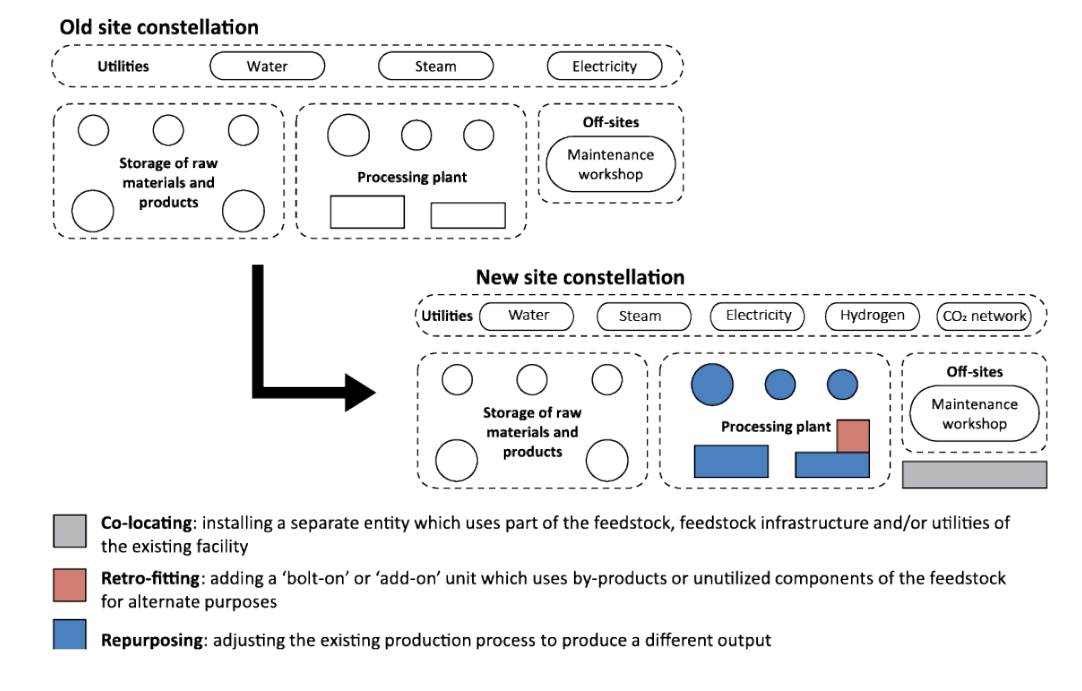
⁷ Note that many advanced biofuel plants are demo plants or first-of-a-kind commercial plants. For that reason, they are often located near R&D facilities, for example, research institutes.



- 1. Retrofitting
- 2. Co-location
- 3. Repurposing
- 4. Greenfield

Among the important criteria identified by experts for selecting these locations include the availability of sufficient space at the host site and reliable access to essential utilities, particularly hydrogen.

Figure 7 Schematic visualization of possible degrees of integration with existing industries (de Jong et al. 2015).



4.2. POSSIBLE LOCATIONS OF ADVANCED BIOFUEL PRODUCTION IN THE SUPPLY CHAIN MODEL

In this study, we used the insights on locational choices to select 1239 possible host sites for biofuel production. Because of modelling constraints, a pre-selection of possible host locations for pre-processing and biofuel production was made. Although more locations could be relevant, the problem size (model complexity) is constrained by the MILP model. The computational time and memory requirements increase exponentially with the number of variables added. The host locations for advanced biofuel production used in the supply chain modelling are summarized in Table 7 and Figure 8.

Greenfield facilities can be located either directly within biomass-producing regions (detailed at the NUTS-3 level) or at intermodal terminal sites. Intermodal terminals do not directly provide benefits of co-production, but they do provide access to high-capacity transport corridors for both upstream feedstock supply and downstream biofuel distribution. These benefits are addressed in transport network modelling as production at these sites reduces the need for shifts between modes of transportation and direct access to low-cost transport networks (rail, inland waterways, sea).

21



Co-location options with the biofuel facility installed as a separate entity at the host site, are assumed for existing biofuel plants, and kraft pulp and paper mills. These locations offer advantageous infrastructure, such as biomass handling capabilities at pulp mills and biofuel plants.

Retrofitting options are assumed to be available only at existing oil refineries. Given that this study focuses on thermochemical biofuel production routes, oil refineries generally offer superior integration possibilities for fuel upgrading processes compared to existing biofuel plants (primarily ethanol producers) and pulp and paper mills. However, the technical and spatial feasibility of retrofitting each individual refinery, such as scale, available land, or unit compatibility, was not assessed within the scope of this study. As such, all existing refining sites are treated equally and considered eligible for retrofitting, regardless of their actual site-specific constraints.

Table 7 Possible host locations of advanced biofuel production and their integration benefits.

Location/host side	Integration benefits	Other benefits	Nodes/host sides	Data source
Oil refineries ¹	Retrofitting	Access to utilities (natural gas, electricity) and fossil fuel infrastructure	84	ESRI (2024) and S&P (2025)
Kraft pulp and paper mills	Co-location	Access to utilities (natural gas, electricity) and solid fuel infrastructure	67	CEPI (2015)
Existing biofuel plants ²	Co-location	Access to utilities (natural gas, electricity) and infrastructure	121	Bio+ project: bioplusportalen.se (2024)
Intermodal terminals ³	Greenfield	Access to intermodal transport infrastructure	467	ETISPlus (2010)
NUTS-3 regions ⁴	Greenfield	Access to local biomass	500	
Total			1239	

^{1 84} refineries that were in operation in 2024 are included based on the updated refinery map by S&P (2025).

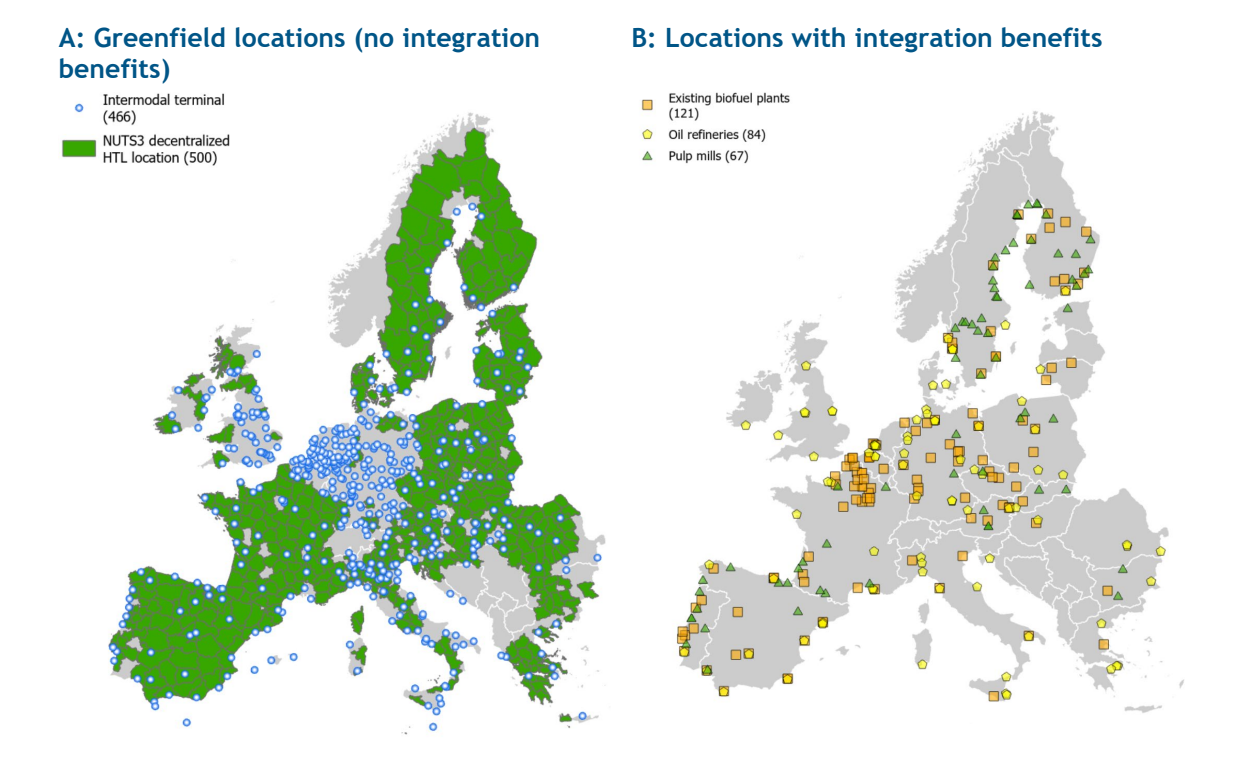
² The limited integration of co-location with biofuel plants is primarily due to the fact that most existing facilities focus on the production of first-generation biofuels, such as food-based ethanol. These plants offer only a few synergies in terms of equipment and infrastructure compatibility with the thermochemical processes considered in this study.

³ The database includes over 1,000 intermodal terminals. Some terminals are located in the same cluster. These have been aggregated to 467 original host locations to reduce computational requirements in the MILP model.

⁴ Only applicable to distributed HTL (biocrude) production. A selection of 500 (out of 1223) supply regions was made based on the highest biomass availability potential. This simplification was needed for the computational feasibility of the MILP model.



Overview of possible host locations for advanced biofuel production without integration benefits (A) and with integration benefits (B) considered in this study. The number of NUTS-3 regions had to be limited for the MILP model calculations.

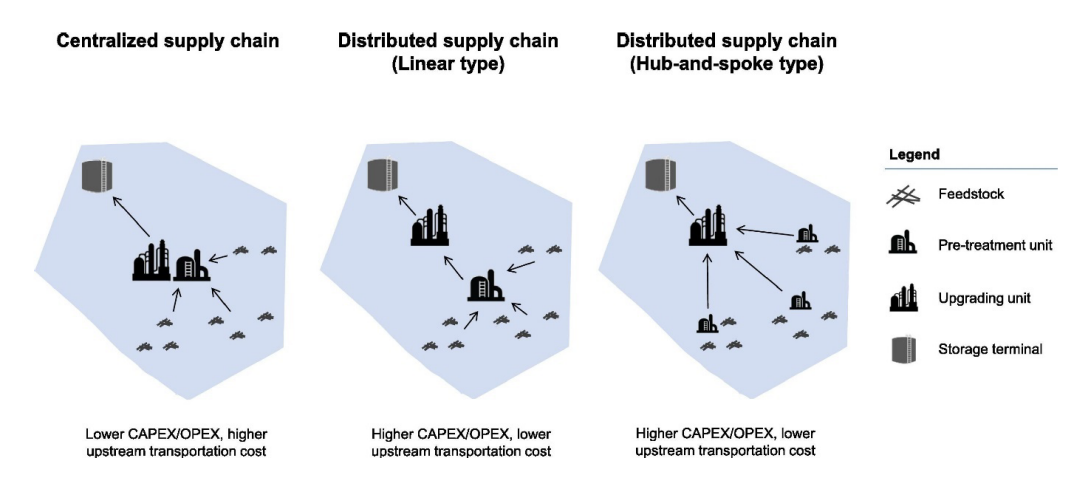


4.3. SUPPLY CHAIN CONFIGURATIONS

As shown in Figure 9, three different configurations are selected for analysis; a centralized and two distributed supply chains (de Jong et al 2017). For the centralized supply chain configuration, the process of converting the biofeedstock into biofuel as its main product is concentrated in a single location. Whereas for the two distributed supply chains, the conversion of biomass to a biofuel is decoupled from the upgrading unit in the production routes, transporting a solid or liquid intermediate (such as biocrude) to the upgrading unit. For the linear type, only one pre-processing unit is required, whereas for the hub-and-spoke-type supply chain, multiple pre-processing units with smaller capacity are located at strategic feedstock supply locations.



Overview of the advanced biofuel supply chain configurations included in the analysis for the EU27 + UK. From left to right: centralized and distributed linear type and distributed huband-spoke (de Jong et al. 2017).



Based on the factors influencing the locations of biofuel plants today, possible locations of centralized and decentralized supply chains of advanced biofuel production were selected:

- Centralized (cs) conversion can only occur in existing industrial areas or at the site of an incubator facility to benefit from co-production. Biofuel production requires access to infrastructure, blending terminals or markets, utilities, and energy for large-scale operation. Consequently, greenfield centralized conversion plants are strategically placed at intermodal terminals, while facilities benefiting from integration through co-location or retrofitting are located respectively at existing biofuel plants, pulp and paper mills, and refineries (Figure 7).
- **Distributed (ds) conversion** occurs in feedstock supply regions (greenfield) with pre-processing (conversion to intermediate) of low-energy-density biomass upstream in the supply chains, but also at biofuel plants and existing pulp mills with co-location benefits (Figure 8). Final upgrading from these intermediates into transport fuels is conducted at oil refineries using retrofitting strategies (Figure 7).



5. METHODOLOGY: SUPPLY CHAIN COST CALCULATIONS

5.1. GENERAL OUTLINE OF COST COMPONENTS IN SUPPLY CHAINS

The general supply chain of advanced biofuels follows a series of operations occurring at different locations, starting from the field or forest to the conversion to liquid transport fuels in a biorefinery and ending with the downstream distribution to blending terminals. These operations vary per feedstock type, design of the supply chain, and type of biorefinery (Hoefnagels, Searcy et al. 2014). In a traditional, centralized supply chain, the biorefinery is situated relatively close to feedstock supply sources to avoid long-distance transport of raw biomass. It often involves basic pre-processing with mobile equipment at the field side or forest, such as baling and chipping before transport by truck to the biorefinery.

As biorefinery scale increases, traditional centralized systems face economic challenges in transporting biomass feedstocks over longer distances. Furthermore, relying on a single biomass feedstock source increases economic risks due to seasonal and regional variations in availability, affecting feedstock costs (Searcy et al., 2016). Decentralized pre-processing facilities with more advanced techniques, including size reduction, drying, densification (pelletization), or liquefaction options (such as pyrolysis, hydrothermal liquefaction (HTL)) and intermodal transportation, are strategies that could address these challenges. In this study, distributed pre-processing at depot locations is limited to liquefaction by HTL. Pellets are only considered for extra-EU imports of solid biomass but are not modelled in detail. The addition of pelletization or torrefaction would increase the model complexity substantially, while for intra-EU trade of solid biomass, the economic benefits of pelletization are limited due to its additional cost (Fritsche et al., 2019).

Figure 10

General outline of the biofeedstock supply chains with possible components and processes. The total cost of advanced biofuel production covers all costs from field side, pre-processing depot (only for the case of decentralized HTL biocrude production), final conversion in the biorefinery, and downstream distribution to blending terminals.



Each supply chain cost component is discussed in the following sections. All supply chain costs are presented in euros and adjusted to the reference year 2023 based on inflation indices.

5.2. BIOMASS COSTS AT ROADSIDE

The roadside costs for biomass refer to the cost-price at which biomass is made available at a roadside location after cultivation, harvesting and collection but before transportation to a processing facility. These costs include harvesting,



collection, and processing expenses at the field or roadside. Typical processing steps that take place before transportation are baling and chipping.

5.2.1. Costs of agricultural biomass

Production costs for lignocellulosic energy crops and agricultural residues are assessed on a $\[mathbb{e}/\]$ basis. Cost estimates are available for all biomass potential scenarios in the Annex. However, in this report, maps only show the High biomass availability potential scenario. A detailed explanation of methods to estimate costs is presented in Annex A1.

For lignocellulosic energy crops, costs include:

- The machinery costs of agricultural activities (including machinery inputs and labour costs associated with the time dedicated to each activity)
- Land rent
- Pesticides and fertilizer costs

For agricultural residues, costs are based on:

- The activities related to residues collection (including machinery inputs and labour costs)
- The costs of the additional fertilization required to compensate for the nutrient loss when removing the residues.

The costs are estimated for 2023 as the reference year and kept constant for 2030, 2040 and 2050, given that there can be significant uncertainties on future changes in prices for parameters related to agricultural activities such as fossil energy/inputs, labour, machinery and land rent (Dees, Datta, et al., 2017). In addition, future prices are also driven by uncertain market and social forces that are challenging to consider. For lignocellulosic energy crops, no irrigation costs were included, as the crop yields were calculated and their selection was optimised based on the available precipitation. Irrigation practices involve high costs, therefore irrigation is not prioritised for lignocellulosic crops, where resilience to water stress and the delivery of biomass at low and competitive costs are key considerations.

5.2.2. Costs of forest biomass

The costs of stemwood and primary forestry residues are derived from the EU S2Biom project database. The general workflow for these cost calculations is provided in Annex A1. A detailed explanation of the calculation method is provided by Dees et al. 2017.

The S2Biom project assumed that all secondary forestry residues are available at zero cost at the mill or production side with all cost allocated to the main product output of the respective wood industry. However, sawmill residues and other secondary forestry residues are valuable outputs that are either used internally, for example, as a boiler fuel, or used to produce wood pellets, etc. Instead of production costs, actual market price data was used for secondary forest residues. These were based on market price data of sawmill residues and wood product manufacturing residues used in pellet production as reported in Fritsche et al. (2019).



5.3. TRANSPORT COST OF BIOMASS, BIOCRUDE AND BIOFUEL

5.3.1. (Intermodal) transport cost

Transport costs are composed of two main cost components:

- Variable costs that are proportional to the distance. These include fuel cost, labour, maintenance, etc. (in €/t-km)⁸. Note that future developments in transport fleet, related investments, and performance characteristics were not considered in this study.
- **Fixed costs** that do not vary by distance. These include loading, unloading, and intermediate transhipment costs at terminal facilities (in €/t). Note that future developments and investment in new infrastructure, including terminal facilities, were not considered in this study.

Each mode of transport has different cost functions. Road transport has relatively low fixed cost, but high variable cost. Maritime transport has the highest fixed cost and lowest variable cost. The cost functions of rail and inland waterways are between those of road and maritime transport. A general rule of thumb is that for short distances, road transport is the cheapest and most flexible option, while for longer distances (typically above 500 - 700 km), rail and inland waterways become more attractive. Finally, maritime transport becomes more profitable for distances >1500 km (Rodrigue, 2020). In this study, the mode(s) of transportation are selected based on least-cost route calculations with transport network modelling as explained in Section 5.3.2.

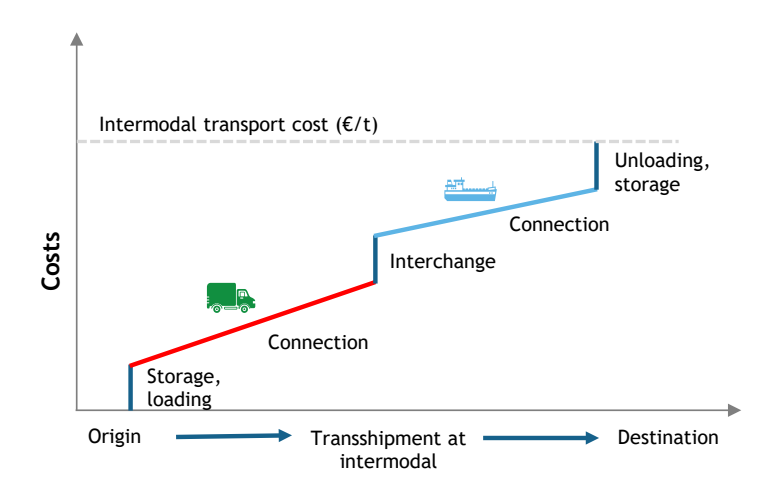
Direct access to rail or maritime transport infrastructure is not available for most feedstock supply locations, but pre-processing depot locations and biorefinery locations can be strategically chosen to benefit from direct access to rail, inland waterways, or sea transport infrastructure, for example, at an intermodal terminal location. Furthermore, cost reductions can be achieved for longer distances through combined or intermodal transport, such as road and rail. Intermodal terminals provide access between different modes of transport, resulting in a stepwise structure of transport cost, as shown in Figure 11.

27

 $^{^8}$ The cost per tonne-km (tonne-kilometre) = the total annual costs / (distance traveled (km) · average weight (tonne)) (Meulen et al., 2023).



Figure 11 Stepwise cost structure of intermodal transport with road and maritime transport. Adapted from Rodrigue (2020). In most cases, biomass needs to be transported by truck to an intermodal terminal to provide access to rail or water transport.



5.3.2. Transport network modelling

An intermodal transport network model was used to calculate the cost of transport that takes into account the actual locations of existing infrastructure including transport networks (road, rail, inland waterways, short sea) and locations of intermodal terminals to shift between modes of transport. This Biomass Intermodal Transport model (BIT-UU) has been applied to multiple case studies at EU level and national level, amongst others:

- To calculate biomass transport cost to model international trade of solid biomass in the EU to 2020 for different renewable policy scenarios (Hoefnagels, Resch, et al., 2014; Lamers et al., 2015)
- Input for the Green-X model (TU Wien) used to model renewable energy deployment scenarios, including biomass trade, as input for the impact assessment of policy options for the Renewable Energy Directive recast (PWC, 2017).
- To examine the impact and interrelationship of economies of scale, intermodal transport, integration with existing industries, and distributed supply chain configurations for advanced biofuel production with HTL in Sweden (de Jong et al., 2017).

BIT-UU runs in ESRI's ArcGIS Network Analyst extension (ESRI, 2024), which has the option to calculate the least-cost routes between a series of predefined origins and destinations. The results are Origin-Destination (OD) matrices that include the total cost of transport (sum of fixed and variable transport cost in €/t) and distances traveled over each network (road, rail, inland waterways, sea) for each possible origin - destination combination that are input to the spatially explicit supply chain model.

The transport network consists of connection points (nodes) and links (line segments). The nodes represent actual locations on how to access transport links. The line segments represent the connection between these nodes and the related attribute data:



- Mode of transport (road, rail diesel, rail electric, inland waterway, sea)
- Distance (km)
- Country (linked to labour cost, fuel excise duty and VAT)
- Maximum travel speed (km/h)
- Loading/unloading cost (for terminal connectors)

The attribute data is combined with transport cost parameters for each mode of transport to calculate transport cost as explained in section 5.3.3. The road, rail, inland waterways, and short sea transport networks and data sources in BIT-UU used in this study are shown in Figure 12.

Figure 12 Transport network topology of the EU used in the ArcGIS Model with links (or segments) of road, rail, inland waterways and short sea shipping. The included supply, demand, and terminal nodes that define the connections and access to these links are not shown for visual reasons.

Network layer	Main source	
Road	TRANS-TOOLS (JRC, 2009) and OpenStreetMap (OSMF, 2023)	
Rail (electrified, diesel)	OpenStreetMap (2023)	
Inland waterways	TRANS-TOOLS (JRC, 2009)	
Short sea shipping	RRG Database (RRG, 2008)	
Intermodal terminals	Terminal database (ETISPLUS, 2013)	

5.3.3. Transport cost parameters in BIT-UU

The variable (proportional to distance) and fixed cost (do not vary by distance, but result from handling activities in transport terminals) which are used in the BIT-UU model are summarized in Figure 13 and Figure 14 respectively. We assumed similar cost structures for 2030 and 2050 based on the existing transport fleet and infrastructure. Detailed information about these cost structures is provided in Annex C.

Inland transport costs are based on the study Cost Figures for Freight Transport (Meulen et al. 2023) which provides insights into costs for road, rail, inland waterways and maritime transport in the Netherlands. For this study, these costs were adjusted to make them representative for the studied region (EU-27 + UK) based on the following changes:

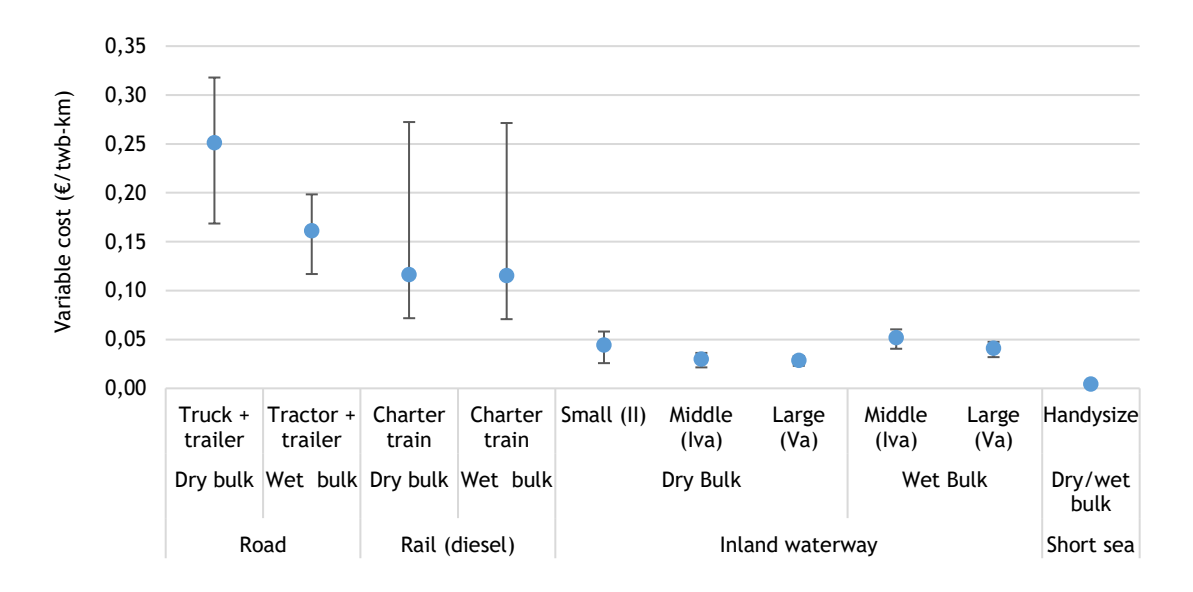


- Cost figures in Meulen et al. (2023) were adjusted from €₂₀₂₁ to €₂₀₂₃ based on HICP indices.
- Fuel consumption figures were calculated based on JRC (Edwards et al., 2017). Fuel costs were calculated based on country-specific VAT and excise duties.
- Labour costs for road, rail, and inland shipping were calculated based on country-specific labour costs figures (EUROSTAT 2024).
- Variable rail costs were calculated based on country-specific rail cargo tariffs.

The uncertainty bars show the cost ranges between all EU member states and the UK based on different fuel prices (including excise duty and VAT) and country-specific labour costs. The BIT model calculates the country-specific transport cost parameters based on the location of the transport network, except for short sea shipping, which is based on international freight charter rates and fuel prices as provided in Fritsche et al. (2019) that were updated to €2023 (see Annex C).

The variable cost of maritime transport is substantially lower than inland transport, but the fixed costs are higher due to the costlier loading/unloading operations for bulk carriers. The characteristics and cost parameters (e.g., cargo capacity, speed, fuel consumption per ship type) of maritime transport are taken from Fritsche et al. (2019).

EU average variable transport cost (in €2023/twb-km)⁹ per transport mode and transported freight (for both dry and wet bulk)¹⁰ for road, rail, inland waterways, and short sea transport. The uncertainty bars show the cost ranges between EU member states + UK for differences in labour cost, country-specific excise duties, VAT, and rail cargo tariffs used in the BIT-UU model. Details are provided in Annex C.



Transport mode and cargo type

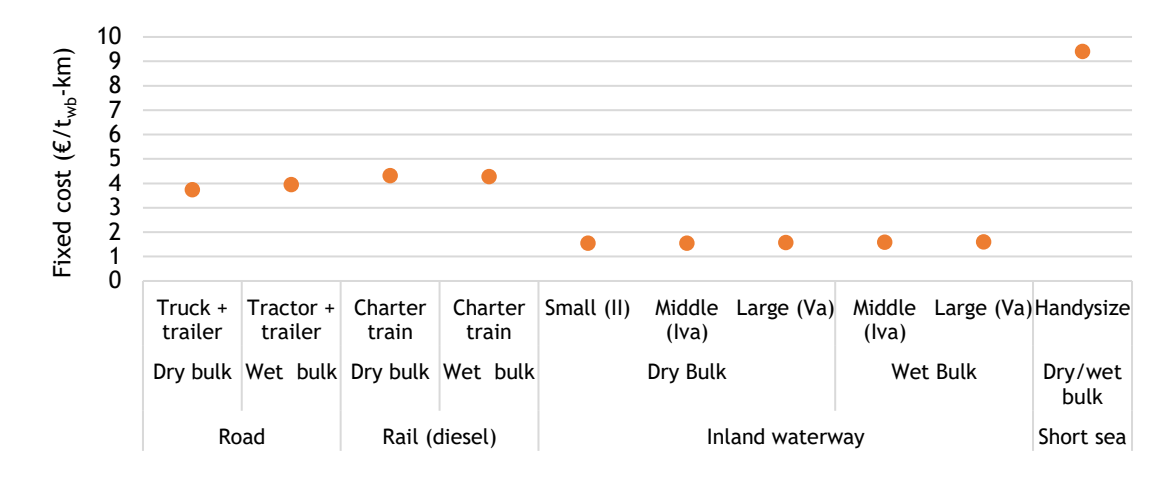
30

⁹ Tonne wet basis is the weight including moisture content. The moisture content varies per feedstock type and is provided in Annex A1.

¹⁰ Wet bulk refers to the transport of liquids in bulk, including biocrude and biofuels. Dry bulk refers to solids transported in bulk, including solid biomass.



Figure 14 EU fixed transport cost (in €₂₀₂₃/t_{wb}) per transport mode and transported freight (for both dry and wet bulk) for road, rail, inland waterways, and shortsea transport. Details are provided in Annex C. All countries were assumed to have similar fixed transport costs.



Transport mode and cargo type

Although wet (liquid) bulk (biocrude and biofuel) and dry (solid) bulk (biomass feedstocks) have different cost structures, the comparison of total fixed and variable costs (in ℓ/t_{wb}) (wet basis), including the moisture content of biomass feedstock) are in similar ranges. However, the overall transport costs for biocrude and liquid biofuels (in ℓ/t_{wb}) are substantially lower due to their higher energy density compared to solid biomass (see Table 8).

Table 8 Biomass feedstock, biocrude, and biofuel characteristics. A detailed table with individual feedstock sub-categories is provided in Annex A1.

Category in supply chain model	LHV (wb) [GJ/t _{wb}]	LHV (dry) [GJ/t _{dry}]	Moisture content [% w/w]
Biomass feedstock			
Agriculture residues	13.7	16.5	15.0
Prunings	10.2	17.2	35.5
Grassy crops	11.8	17.1	24.9
Woody crops	10.0	18.3	40.0
Primary forest residues	9.3	19.0	51.0
Secondary forest residues	14.9	18.4	33.3
Stemwood	11.6	19.1	51.0
Biocrude/biofuel			
Biocrude		33.0	
Biofuel		43.2	



5.4. PROCESS TECHNO-ECONOMICS AND INTEGRATION ECONOMIC BENEFITS

5.4.1. Process Description: Gasification and Fischer-Tropsch synthesis (GFT)

The biomass is first dried to a moisture content of 12% with directly heated rotary driers and then fed into a directly heated, fluidized bed gasifier where it is converted into syngas as described in de Jong et al. (2015) and Zhu et al. (2011). The raw syngas contains impurities like particulates, tars, sulfur compounds, and CO_2 , which are removed through cleaning and conditioning steps, including tar reforming and wet scrubbing. The H_2/CO ratio is adjusted using a water-gas shift reactor.

The clean, conditioned syngas is then compressed and fed into a Fischer-Tropsch (FT) reactor, where it reacts over a catalyst under moderate pressure and temperature. The FT process converts syngas into long-chain hydrocarbons, producing synthetic fuels such as diesel, naphtha, and waxes. These products are then upgraded via hydrocracking and hydrotreating followed by distillation and purification.

Heat from the exothermic FT reaction and hot process streams is recovered to improve efficiency. Unconverted tail gases are used for power generation, resulting in surplus electricity generation which is sold to the local grid.

5.4.2. Process Description: Hydrothermal liquefaction (HTL) and upgrading

The HTL systems are largely based on de Jong et al. (2017) for both centralized and distributed facilities, as shown in Figure 15. Important differences between the centralized and distributed facilities are:

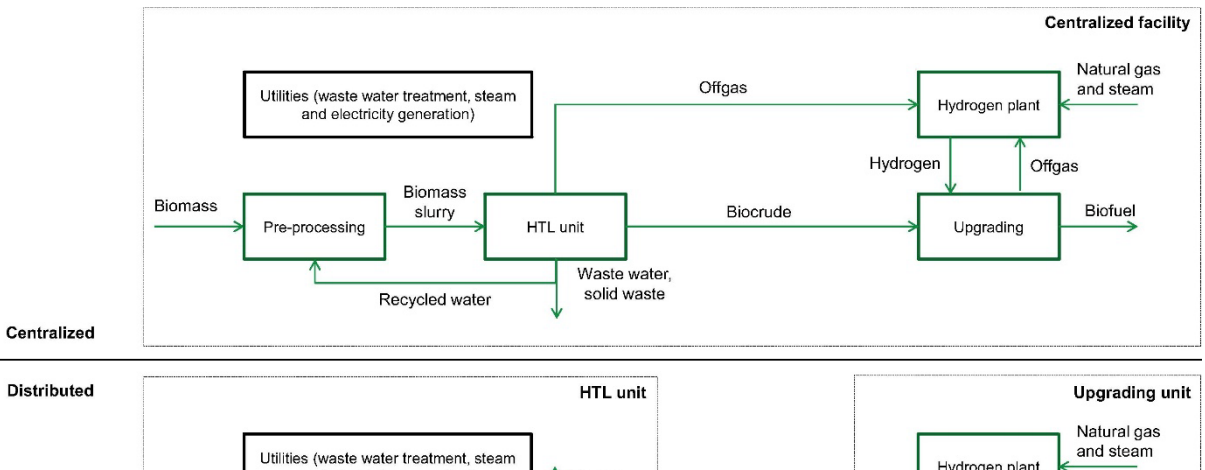
- For the centralised case, offgases produced from the liquefaction process and wastewater treatment are used to produce electricity and steam or hydrogen.
- Upgrading in distributed supply chains at biofuel plants requires more natural
 gas for hydrogen production. At oil refineries, hydrogen is supplied by the oil
 refinery at a price equal to the hydrogen production cost given by the <u>European</u>
 Hydrogen Observatory.
- Excess steam in the reformer can be exported to the host facilities.

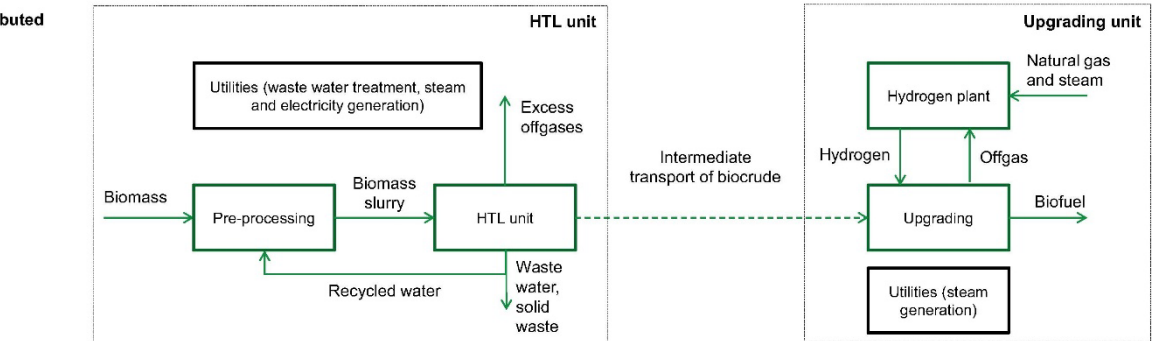
In 2050, the SMR unit is replaced by ex-situ green hydrogen supply for biocrude upgrading for both centralized and distributed supply chain configurations. Offgases are used for electricity and steam generation.



Figure 15

Process configurations for the centralized and distributed HTL conversion systems in 2030 (de Jong et al. 2017). In 2050, the SMR and natural gas used for hydrogen production is assumed to be replaced by ex-situ green hydrogen supply.





5.4.3. Levelized fuel production costs

The biofuel production cost is calculated based on the total investment cost (TCI), operational expenditures (OPEX) and the delivered feedstock costs. Costs and benefits are assumed to be constant over time. Therefore the levelized cost of fuel (LCOF) are calculated as follows (Witcover & Williams, 2020):

$$LCOF = \frac{(\alpha+\theta)*TCI+OPEX+Feedstock\ cost\ (roadside)+feedstock\ transport\ cost}{Biofuel\ produced}$$

For which:

- Θ = scale-dependent OPEX factor (10.2%), and,
- $\alpha = \frac{r}{1-(1+r)^{-n}}$ (Capital recovery factor)

For which:

- r = discount rate
- n = plant lifetime (years)

CAPEX-dependent OPEX cost items include maintenance and repairs, operating supplies, local taxes, and insurance that add up to 10.2% of TCI (de Jong et al. 2017). The production costs are calculated using a discount rate of 10%, a project lifetime of 20 years (annuity factor: 0.117), and a capacity factor of 90%, similar to de Jong et al. (2015, 2017).



5.4.4. Future cost reduction potential

IEA Bioenergy estimated the advanced biofuel production routes' short- and long-term cost reduction potential. Although the report is more detailed for biochemical production routes, it also provides valuable estimates for the cost reduction potential of thermochemical production routes based on expert interviews and experience from existing projects. For thermochemical routes, IEA expects that 10 to 20% cost reductions are achievable from economies of scale, labour requirements, and efficiency improvements. We assumed that these cost reductions would take place after 2030.

Long-term cost reductions were calculated based on the learning curve theory, the empirically observed phenomenon according to which cost tends to reduce by a given percentage for each doubling of cumulative capacity. Figure 16 shows the impact of different learning rates, ranging from 5% to 20%, on cost reductions for FT and biooil processing. Because thermochemical processes used for biofuel production are employed across various industrial applications, they can be regarded as more technologically mature than the process technologies associated with lignocellulosic biomass hydrolysis-based pathways for advanced biofuel production (Brown et al. 2020), (Hurtig et al., 2022). Furthermore, large complex plants have typically lower learning rates than modular technologies that can be produced in bulk, such as photovoltaics (PV) (Junginger & Louwen, 2019). For these reasons, a 5% to 10% learning rate is considered representative.

Brown et al. (2020) calculated the cost reduction for a 10 and 100-fold cumulative capacity growth (Figure 16). Advanced biofuels produced via HTL and FT synthesis are still in the early stages of development. As an example, the total global capacity (operational, non-operational, and under construction) of HTL facilities is limited to 13 kt/y (Sonnleitner & Bacovsky, 2024). It is, therefore, reasonable to assume that the global cumulative capacity could increase at least by a factor of 100 before 2050 to over 1.3 Mt/y. The global capacity of biomass gasification facilities (operational, non-operational, and under construction) is still limited, at around 2 Mt/y (Sonnleitner, 2024). It is, therefore, likely that the cumulative capacity will increase between 10 and 100-fold to 20 to 200 Mt/y by 2050¹¹.

Because cost reductions in this study are considered to take place after 2030, the total cost reduction potential by 2050 is a combination of the short-term cost reduction potential and long-term cost reduction potential proposed by IEA. It was calculated as follows:

Medium-term cost reductions (within 10-15 years) of early-stage technologies is possible as operational experience grows and plant optimization, R&D advancements, scalability, and improved process integration take place. Based on estimates from interviews with biofuel producers and technology providers by IEA (Brown et al., 2020), the short-term cost reduction potentials are:

- Bio-oil and processing: 15% (average of range 10-20%)
- FT liquids: 15% (average of range 10-20%)

34

¹¹ In the IEA Net Zero scenario (IEA, 2021), advanced biofuel capacity is projected to grow from 1.6 to 7 million barrels/day by 2050 of which 90% is expected to be supplied by advanced biofuels. A 100-fold increase would mean that gasification technologies should supply ~60% of global advanced biofuels by 2050.

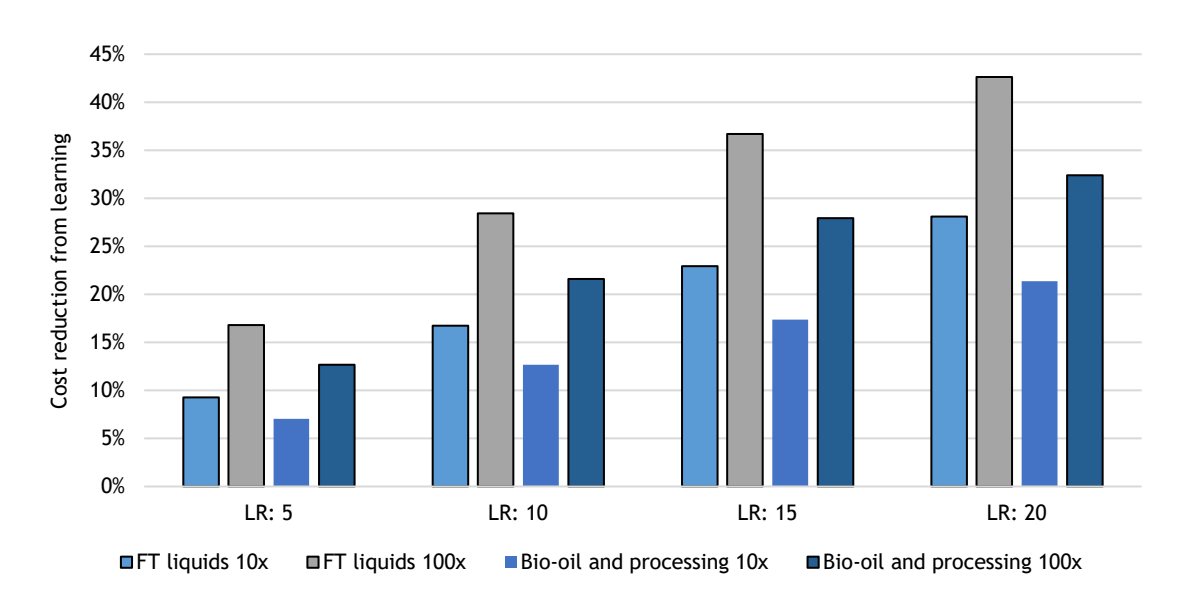


Long-term cost reductions (beyond 15 years) are possible through ongoing learning effects, similar to those already seen for various technologies and represented by learning curves. Achieving significant contributions to global energy needs, as outlined in low-carbon scenarios, would require a substantial increase in technology deployment, leading to substantial experiential learnings:

- Bio-oil and processing: 17% (average LR 5 10, for 100x cumulative capacity increase in Figure 16), beyond short-term cost reductions.
- FT liquids: 18% (average LR 5 10, and average 10 100x cumulative capacity increase in Figure 16), beyond short-term cost reductions.

The total cost reduction potential by 2050, by combining medium-term and long-term cost reductions, is ~30% for both systems.

Figure 16 Impact of increasing learning rates (LR) on cost reduction for a factor of 10 and 100 cumulative capacity increase (Brown et al. 2020). The average LR of 5 and 10 was considered representative for GFT and HTL.



5.4.5. Techno-economic data: Gasification and Fischer-Tropsch (GFT)

The main techno-economic input data for Fischer-Tropsch is presented in Table 9 for 2030 and Table 10 for 2050. The cost of equipment, utilities, and electricity demand and generation for Fischer-Tropsch were taken from de Jong et al. (2015) for an oxygen-blown directly-heated gasifier with a capacity of 2000 tpd (dry) feedstock input that produces 106 ML (million liters) gasoline and 34 ML naptha. Because naphtha is mainly used to produce chemicals that are outside the scope of the model's defined objectives, these outputs were replaced with an overall liquid fuel yield of 38% (energy-based) for 2030 based on JRC (Edwards et al. 2017). Alternatively, a credit could have been given for naphtha production, similar to the cogeneration of electricity. However, in high-demand scenarios, the model favours systems with high biomass-to-liquid fuel, creating an overreliance on HTL systems if co-generation of naphtha was included.

The current overall energy efficiency of GFT, including electricity co-generation etc., ranges from 40% to 55% (Brown et al., 2020), but future advancements in catalyst performance, process optimization, and heat and energy recovery could



raise this to over 60%. Consequently, for 2050, a fuel yield of 45% and an overall conversion efficiency of 51% (including fuel and electricity) are considered realistically achievable.

Table 9 Main input data for Gasification and Fischer-Tropsch (GFT) at reference scale in 2030: 164 MW fuel output (5.2 PJ/y or 124 ktoe/y), 428 MW (13.5 PJ/y or 323 ktoe/y) feedstock input. Details are provided in Annex B3.

Cost item	Unit	Gasific	ation and Fischer-	Tropsch
Host side		Intermodal terminal	Pulp mill / biofuel plant	Oil refinery
Co-location strategy		Greenfield	Co-location	Retrofitting
Product viold 1	t _{biofuel} /t _{biomass (dm)}	0.16	0.16	0.16
Product yield ¹	$GJ_{fuel}/GJ_{biomass}$	0.38	0.38	0.38
Net electricity demand (negative: export to grid)	GJ/GJ _{biofuel}	-0.15	-0.15	-0.15
CAPEX				
Specific capital costs	€/kW _{biofuel}	4425	4084	3697
Total CAPEX	€/GJ _{biofuel}	16.5	15.2	13.8
OPEX				
CAPEX-independent OPEX	€/GJ _{biofuel}	1.6	1.2	1.2
CAPEX-dependent OPEX	€/GJ _{biofuel}	15.1	13.9	12.6
Credits (electricity sales)	€/GJ _{biofuel}	5.4	5.4	5.4
OPEX (excl. feedstock)	€/GJ _{biofuel}	11.3	9.7	8.4
CAPEX + OPEX (excl. feedstock)	€/GJ _{biofuel}	22.9	21.0	19.1

¹⁾ Yield based on wood to liquid hydrocarbons in Edwards et al. (2017) used for default GHG emission calculations from biofuels in EU legislation.

Table 10 Main input data Gasification and Fischer-Tropsch (GFT) at reference scale in 2050: 164 MW fuel output (5.2 PJ/y or 124 ktoe/y), 428 MW (13.5 PJ/y or 323 ktoe/y) feedstock input. Details are provided in Annex B3.

Cost item	Unit	Centralized: Gasification and Fischer-Tropsch			
Host side		Intermodal terminal	Pulp mill / biofuel plant	Oil refinery	Oil refinery (repurpose) ¹
Co-location strategy		Greenfield	Co-location	Retro- fitting	Re-purpose
Product yield ²	t _{fuel} /t _{biomass(dm)}	0.19	0.19	0.19	0.19
Product yield-	GJ _{biofuel} /GJ _{biomass}	0.45	0.45	0.45	0.45
Net electricity demand (negative: export to grid)	GJ/GJ _{output}	-0.13	-0.13	-0.13	-0.13
CAPEX					
Specific capital costs	€/kW _{biofuel}	2973	2744	2484	1963
Total CAPEX	€/GJ _{biofuel}	11.1	10.2	9.3	7.3
OPEX					
CAPEX-independent OPEX	€/GJ _{biofuel}	1.5	1.1	1.1	1.1



CAPEX-dependent OPEX	€/GJ _{biofuel}	10.1	9.4	8.5	6.7
Credits (electricity sales)	€/GJ _{biofuel}	4.6	4.6	4.6	4.6
Total OPEX (excl. feedstock)	€/GJ _{biofuel}	7.1	5.9	5.0	3.2
CAPEX + OPEX (excl. feedstock)	€/GJ _{biofuel}	16.3	14.9	13.6	10.8

¹⁾ Used in the repurposing of oil refineries additional scenario. It assumes a lower Lang factor (3.85) and a 50% reduction (assuming it is already partly economically depreciated) on purchased equipment cost (TPEC) for hydrocracking and product separation units.

5.4.6. Techno-Economic Data: Centralized Hydro-thermal liquefaction (HTL)

The cost of HTL conversion and upgrading are taken from de Jong et al. (2017), who conducted a detailed study on centralized and distributed supply chain configurations for a case study in Sweden. It includes, amongst others, co-location benefits at oil refineries, pulp and paper mills, and existing biofuel plants that are also relevant to this study. A detailed overview of the input data at reference capacity is provided in Annex B3. The main techno-economic input for 2030 and 2050 are given in Table 11 and Table 12 respectively.

Table 11 Main input data centralized HTL and upgrading at reference scale in 2030: 73 MW fuel output (2.3 PJ/y or 53 ktoe/y), 156 MW feedstock input (4.92 PJ/y or 117 ktoe/y).

Cost item	Unit	Centra	lized: HTL + upg	rading
Host side		Intermodal terminal	Pulp mill / biofuel plant	Oil refinery
Co-location strategy		Greenfield	Co-location	Retrofitting
Product yield ¹	$t_{\text{fuel}}/t_{\text{biomass(dm)}}$	0.20	0.20	0.20
Froduct yield	GJ _{fuel} /GJ _{biomass}	0.47	0.47	0.47
Steam sales	GJ/GJ _{biofuel}	0.00	0.00	0.09
Natural gas requirement	GJ/GJ _{biofuel}	0.06	0.06	
Hydrogen requirement	GJ/GJ _{biofuel}			0.15
CAPEX				
Specific capital costs	€/kW _{biofuel}	3441	3144	2501
Total CAPEX	€/GJ _{biofuel}	12.8	11.7	9.3
OPEX				
CAPEX-independent OPEX	€/GJ _{biofuel}	6.9	6.2	8.7
CAPEX-dependent OPEX	€/GJ _{biofuel}	11.7	10.7	8.5
Credits (steam sales)	€/GJ _{biofuel}	-	-	(1.7)
Total OPEX (excl. feedstock)	€/GJ _{biofuel}	18.6	16.9	15.6
CAPEX + OPEX (excl. feedstock)	€/GJ _{biofuel}	31.4	28.6	24.9

¹⁾ Based on a biomass to biocrude yield of 0.247 kg/kg dry wood for a water catalyst at $300 \,^{\circ}\text{C}$ system (Tzanetis et al. 2017) and a biocrude to biofuel yield of $1.06 \, \text{GJ/GJ}$ (de Jong et al. 2017).

²⁾ Future yield estimated based on lower end of the range provided in Brown et al (2021).



Table 12

Main input data centralized HTL and upgrading at reference scale in 2050: 73 MW fuel output (2.3 PJ/y or 53 ktoe/y), 112 MW feedstock input (3.5 PJ/y or 84 ktoe/y). The SMR unit is replaced with ex-situ green hydrogen supply.

Cost item	Unit		Centralized: H	TL + upgrading	
Host side		Intermodal terminal	Pulp mill / biofuel plant	Oil refinery	Oil refinery (repurpose) ¹
Co-location strategy		Greenfield	Co-location	Retrofitting	Repurpose
Product yield ²	t _{fuel} /t _{biomass(dm)}	0.28	0.28	0.28	0.28
Froduct yield	GJ _{fuel} /GJ _{biomass}	0.66	0.66	0.66	0.66
Steam sales	GJ/GJ _{biofuel}		0.09	0.09	0.09
Natural gas requirement	GJ/GJ _{biofuel}				
Hydrogen requirement	GJ/GJ _{biofuel}	0.15	0.15	0.15	0.15
CAPEX					
Specific capital costs	€/kW _{biofuel}	2055	1875	1698	1109
Total CAPEX	€/GJ _{biofuel}	7.7	7.0	6.3	4.1
OPEX					
CAPEX-independent OPEX	€/GJ _{biofuel}	11.8	11.1	10.0	10.0
CAPEX-dependent OPEX	€/GJ _{biofuel}	7.0	6.4	5.8	3.8
Credits (steam sales)	€/GJ _{biofuel}		(1.7)	(1.7)	(1.7)
Total OPEX (excl. feedstock)	€/GJ _{biofuel}	18.8	15.8	14.2	12.2
CAPEX + OPEX (excl. feedstock)	€/GJ _{biofuel}	26.4	22.8	20.5	16.3

¹⁾ Used in the repurposing of oil refineries additional scenario. It assumes a lower Lang factor (3.85) and a 50% reduction (assuming it is already partly economically depreciated) on purchased equipment cost (TPEC) for the hydrotreaters and hydrocrackers.

5.4.7. Techno-Economic Data: Decentralized Hydro-thermal liquefaction (HTL)

The cost of decentralised HTL conversion and upgrading are taken from the same reference with centralised system, de Jong et al. (2017). A detailed overview of the input data at reference capacity is provided in Annex B3.

²⁾ Based on a biomass-to-biocrude yield of 0.345 kg/kg dry wood for a $Na_2CO_3(aq.)$ catalyst at $300 \,^{\circ}C$ system (Tzanetis et al. 2017) and a biocrude-to biofuel yield of $1.06 \, \text{GJ/GJ}$ (de Jong et al. 2017).



Table 13 Main input data for decentralized HTL and upgrading at reference scale in 2030: 73 MW fuel output (2.3 PJ/y or 53 ktoe/y), 112 MW feedstock input (3.5 PJ/y or 84 ktoe/y).

Cost item	Unit		ized: HTL production	Decentraliz upgra	
Host side		NUTS-3	Pulp mill / biofuel plant	Oil refinery	Existing biofuel plant
Co-location strategy		Greenfield	Co-location	Retrofitting	Co-location
Product yield ¹	t _{fuel} /t _{biomass(dm)}	0.25	0.25	0.81	0.81
Product yield	GJ _{fuel} /GJ _{biomass}	0.44	0.44	1.06	1.06
Steam sales	GJ/GJ _{biocrude/fuel}	0.00	0.10	0.00	0.00
Natural gas requirement	GJ/GJ _{biocrude/fuel}				0.16
Hydrogen requirement	GJ/GJ _{biocrude/fuel}			0.15	
CAPEX					
Specific capital costs	€/kW _{biocrude/fuel}	1890	1710	1181	1763
Total CAPEX	€/GJ _{biocrude/fuel}	7.0	6.4	4.4	6.6
OPEX					
CAPEX-independent OPEX	€/GJ _{biocrude/fuel}	3.0	2.7	5.5	3.9
CAPEX-dependent OPEX	€/GJ _{biocrude/fuel}	6.4	5.8	4.0	6.0
Credits (steam sales)	€/GJ _{biocrude/fuel}		(1.9)		
Total OPEX (excl. feedstock)	€/GJ _{biocrude/fuel}	9.5	6.7	9.5	10.0
CAPEX + OPEX (excl. feedstock)	€/GJ _{biocrude/fuel}	16.5	13.1	13.9	16.5

¹⁾ Based on a biomass to biocrude yield of 0.247 kg/kg dry wood for a water catalyst at 300 °C system (Tzanetis et al. 2017) and a biocrude to biofuel yield of 1.06 GJ/GJ (de Jong et al. 2017).

Main input data for decentralized HTL and upgrading at reference scale in 2050: 73 MW fuel output (2.3 PJ/y or 53 ktoe/y), 112 MW feedstock input (3.5 PJ/y or 84 ktoe/y). The SMR unit is replaced with ex-situ green hydrogen supply.

Cost item	Unit		Decentralized: HTL biocrude production		Decentralized: HTL oil upgradi	
Host side		NUTS-3	Pulp mill / biofuel plant	Existing biofuel plant	Oil refinery	Oil refinery (repurpose) ¹
Co-location strategy		Greenfiel d	Co- location	Co- location	Retro- fitting	Re-purpose
Product yield ²	t _{fuel} /t _{biomass(d}	0.34	0.34	0.84	0.84	0.84
		0.62	0.62	1.06	1.06	1.06
Steam sales	GJ/GJ _{biocrude} /	0.00	0.10	0.00	0.00	0.00
Natural gas requirement	GJ/GJ _{biocrude} /					
Hydrogen requirement	GJ/GJ _{biocrude} /			0.15	0.15	0.15



CAPEX						
Specific capital costs	€/kW _{biocrude/fu}	1283	1161	937	801	343
Total CAPEX ⁵	€/GJ _{biocrude/fu} el	4.8	4.3	3.5	3.0	1.3
OPEX						
CAPEX-independent OPEX ⁸	€/GJ biocrude/fu	3.0	2.7	7.1	6.8	6.8
CAPEX-dependent OPEX ⁸	€/GJ _{biocrude/fu} el	4.4	4.0	3.2	2.7	1.2
Credits (steam sales)	€/GJ _{biocrude/fu} el		(1.9)			
Total OPEX (excl. feedstock	€/GJ _{biocrude/fu} el	7.4	4.8	10.3	9.5	8.0
CAPEX + OPEX (excl. feedstock)	€/GJ _{bicrude/fuel}	12.2	9.2	13.8	12.5	9.3

¹⁾ Used in the repurposing of oil refineries additional scenario. It assumes a lower Lang factor (3.85) and a 50% reduction on purchased equipment cost (TPEC) for the hydrotreaters and hydrocrackers

5.4.8. Economies of scale

As the scale of production increases, the average capital cost per unit of production decreases. The cost advantage that can be achieved due to the increased scale is called economies of scale. Within ranges that are system-specific, these cost reductions follow a power-law distribution given by the following formula:

$$(Cost\ of\ equipment)_x = (Cost\ of\ equipment)_{base} \cdot (\frac{Capacity\ x}{Capacity\ base})^{scaling\ factor}$$

Economies of scale are applied for individual units until the maximum scale is reached as shown in Table 15. Individual units are assumed to be built in parallel trains when the maximum scale is reached without scaling benefits (scale factor of 1.0). The scaling factors for HTL plus upgrading are based on de Jong et al. (2017). Maximum capacities were based on the values provided in de Jong et al. (2017). While scaling is limited for the HTL reactor, as a result of heat and mass transfer bottlenecks, SMR, and especially hydrotreaters, can be built at far larger scales (de Jong et al. 2017). For the Fischer-Tropsch plant, an aggregated scaling factor of 0.7 was assumed (Huang et al. 2019). Note that for GFT, the size of individual units is assumed to be limited to the maximum plant size. This means that the maximum capacity of hydrotreaters and hydrocrackers cannot be reached at all locations (see Table 16).

A piecewise linear approximation is used to reflect the non-linear cost trend of economies of scale in the linear (MILP) model (de Jong et al. 2017, Huang et al. 2019). The non-linear curve was split into three linearized segments: small, medium, and large (Table 16). Plant segment sizes were taken from Huang et al. (2019) for centralized systems because they are more realistic compared to the segments in de Jong et al. (2017). De Jong et al. assumed that the maximum input scale would be limited by the maximum scale of a hydrotreater at 61.2 PJ capacity

^{2) 1)} Based on a biomass-to-biocrude yield of 0.34.5 kg/kg dry wood for a $Na_2CO_3(aq.)$ catalyst at 300 °C system (Tzanetis et al. 2017) and a biocrude-to biofuel yield of 1.06 GJ/GJ (de Jong et al. 2017).

 $^{^{12}}$ At 2000 kt_{dry} feedstock input capacity (1173 MW), around 9 gasifiers must be installed in parallel trains considering a maximum capacity of fluidized bed gasifiers at 200 MW_{th} (WBA, 2015), and thermal efficiency of 70-80%.



(2318 MW). In the supply chain model, it was assumed that this capacity can only be reached by upgrading at oil refineries.

Table 15 Scale factors and maximum scale of individual units for HTL (de Jong et al. 2017) and Gasification and Fischer-Tropsch (GFT) (Huang et al. 2019).

Item	Scale factor	Max. scale [PJ _{input} /y]
HTL plus upgrading		
Feedstock handling ¹	0.77	4.92
Biomass conditioning ¹	0.70	4.92
HTL reactor ¹	0.70	4.92
Hydrotreater ²	0.60	61.20
Hydrocracker ²	0.60	61.20
Hydrogen plant	0.79	39.30
Utilities	0.70	61.20
Gasification and Fischer	-Tropsch (GFT)	
All equipment	0.70	37.00

¹⁾ Scale constraints of HTL from de Jong et al. (2017) adjusted to updated biocrude production yield.

For decentralized HTL production, smaller plant segment sizes were assumed. The medium plant size segment starts at the maximum size of the HTL reactor. The maximum plant size of decentralized HTL conversion is assumed to be 1300 $kt_{\rm dry}/y$ feedstock input based on the medium plant segment of centralized production. Note that in both medium and large segments, the effects of economies of scale are limited because HTL units are assumed to be built in parallel trains.

Table 16 Plant segment sizes for 1) Gasification and Fischer-Tropsch and 2) HTL conversion plus upgrading.

Segment	Feedstock/biocrude input kt _{dry} /y (ktoe/y)	Fuel/biocrude output ktoe/y				
		2030	2050			
Gasification	Gasification and Fischer-Tropsch (GFT)					
Small ¹	100 - 600 (44 - 265)	17 - 102	20 - 119			
Medium	600 - 1300 (265 - 574)	102 - 220	119 - 258			
Large	1300 - 2000 (574 - 884)	220 - 338	258 - 398			

²⁾ Hydrotreater and hydrocracker scale constraints for biocrude upgrading are in biocrude input (in PJ/y), based on the output capacity of a single hydrotreater (de Jong et al. 2017).



HTL Conversion plus upgrading (centralised)				
Small	50 - 266 (22 - 118)	10 - 55	15 - 77	
Medium	266 - 1300 (118 - 574)	55 - 269	77 - 376	
Large	1300 - 2000 (574 - 884)	269 - 414	376 - 578	
HTL conversion (decentralised) ²				
Small	50 - 266 (22 - 84)	10 - 37	13 - 50	
Medium	266 - 600 (84 - 265)	37 - 117	50 - 159	
Large	600 - 1300 (265 - 574)	117 - 254	159 - 345	
HTL upgrading at biofuel plant location (decentralised)				
Small	28 - 149 (22 - 118)	24 - 125	24 - 92	
Medium	149 - 321 (118 - 254)	125 - 269	92 - 390	
Large	321 - 494 (254 - 391)	269 - 414	390 - 600	
HTL upgrading at oil refinery location (decentralised) ⁴				
Small	28 - 149 (22 - 118)	24 - 125	24 - 129	
Medium	149 - 727 (118 - 574)	125 - 609	129 - 632	
Large	727 - 1849 (574 - 1462)	609 - 1549	632 - 1608	

¹⁾ The minimum plant size of Fischer-Tropsch was assumed to be 100 kt_{dry}/y input.

Figure 17 provides an example (greenfield case) of the piecewise linear approximation for centralised GFT and HTL in 2030 used in the MILP model to calculate capital investment cost and scale-dependent OPEX. Annex B4 provides a complete overview of all production routes in 2030 and 2050.

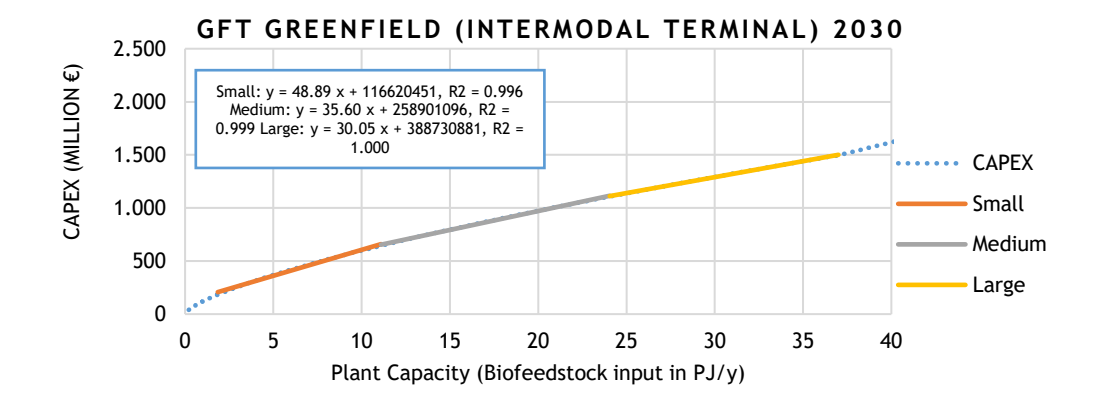
²⁾ The maximum size of distributed HTL production is smaller because of the scaling limitations of distributed production (assumed similar to the Medium segment of centralized HTL production).

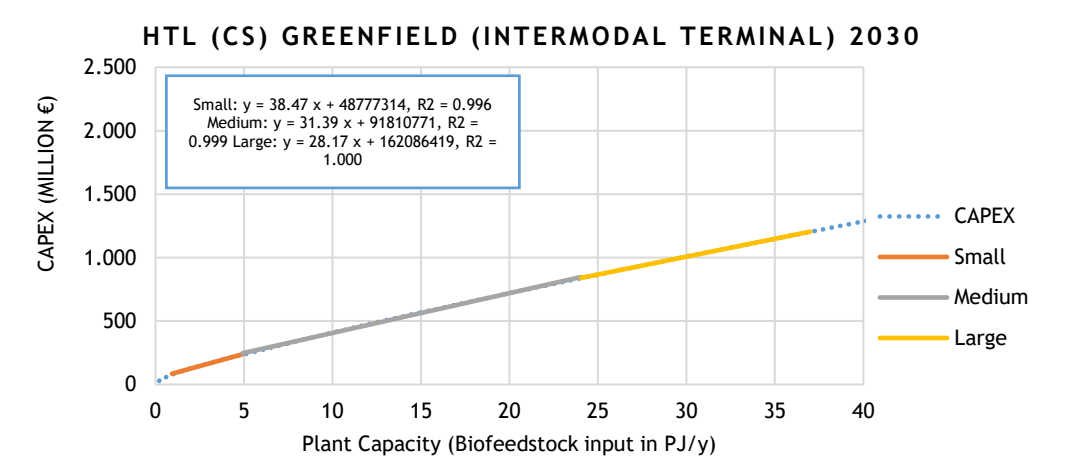
³⁾ Decentralised upgrading input is scaled to similar capacities of biocrude upgrading at centralized HTL production facilities, with the exception of decentralised upgrading at oil refineries (see note 4).

⁴⁾ At oil refineries, upgrading can achieve larger economies of scale. The maximum scale (1462 ktoe) is based on the maximum output capacity of a hydrotreater at 61.2 PJ in de Jong et al. (2017) - indicative size of a refinery's diesel hydrotreater.



Figure 17 Capital cost estimates at three different levels (segment size) for Gasification and Fischer-Tropsch (GFT) and HTL Conversion plus upgrading (centralised (cs)) for greenfield locations in 2030. The other cases are provided in Annex B4.







6. ADVANCED BIOFUEL DEMAND INPUT IN THE MODEL

In the modelling and simulation of biomass supply chains, projected biomass demand for transport and other sectors is a key input factor. The used model is designed to optimize supply chains to meet advanced biofuel demand projections at both EU and national levels. Furthermore, alternative bioenergy applications, such as heat and electricity generation are included, adding a layer of realism to the results. By accounting for competition between these bioenergy sectors, the model provides insights into how competition for these resources can shape and constrain supply chain dynamics.

6.1. ADVANCED BIOFUEL DEMAND FOR TRANSPORT IN EU-27 + UK

The most recent mandates targeting the aviation and maritime sectors, introduced under the Fit for 55 legislative package, together with the updated EU-wide targets of the Renewable Energy Directive III (RED III), define the regulatory landscape shaping the future demand for advanced biofuels in the EU transport sector. While numerous studies have explored the projected demand for advanced biofuels in transport, only a limited number include the latest legislative constraints. Figure 18 presents results from two such studies.

The first, titled "Development of Outlook for the Necessary Means to Build Industrial Capacity for Drop-in Advanced Biofuels", was commissioned by the European Commission (EC, 2024) and is referred to hereafter as the DI Fuel study. Its projections for 2030 and 2050 were developed using the PRIMES-TREMOVE and PRIMES Maritime models. Among various scenarios, the one aligned with the RED III greenhouse gas (GHG) reduction targets was selected for this analysis. The second study, "Study on the potential evolution of Refining and Liquid Fuels production in Europe", was conducted by S&P Global Commodity Insights (S&P, 2025), under commission from Concawe, and assessed the future of the European refining sector in light of current policies and regulations to meet the net zero GHG emission objective by 2050. As part of this study, the projected demand for renewable fuels, including advanced biofuels, was calculated under two scenarios:

- Max Electron: meets all requirements of the Fit for 55 package while surpassing the Heavy-Duty Vehicles CO₂ standards regulation requirements by assuming zero sales of ICE vehicles after 2035 and assumes an accelerated and unprecedented rate of electrification across various modes of transportation
- More Molecule: This scenario has been derived from the Max Electron Scenario
 by relaxing the requirements of the LDV and HDV vehicle standards and
 allowing sales of some new internal combustion engine cars and vans after 2035
 and postponing any electrification in the aviation and marine sectors to after
 2050. In this way, this scenario achieves net zero in 2050 by complementing
 electrification with an increased use of low carbon fuels

According to the DI Fuel study, demand for liquid advanced biofuels (Annex IX-A, excluding biomethane) is projected to reach 19.0 Mtoe by 2030 and 37.6 Mtoe by 2050. The steep increase by 2030 reflects assumptions of delayed electrification, while the more moderate growth to 2050 accounts for widespread adoption of electric mobility in the long term.

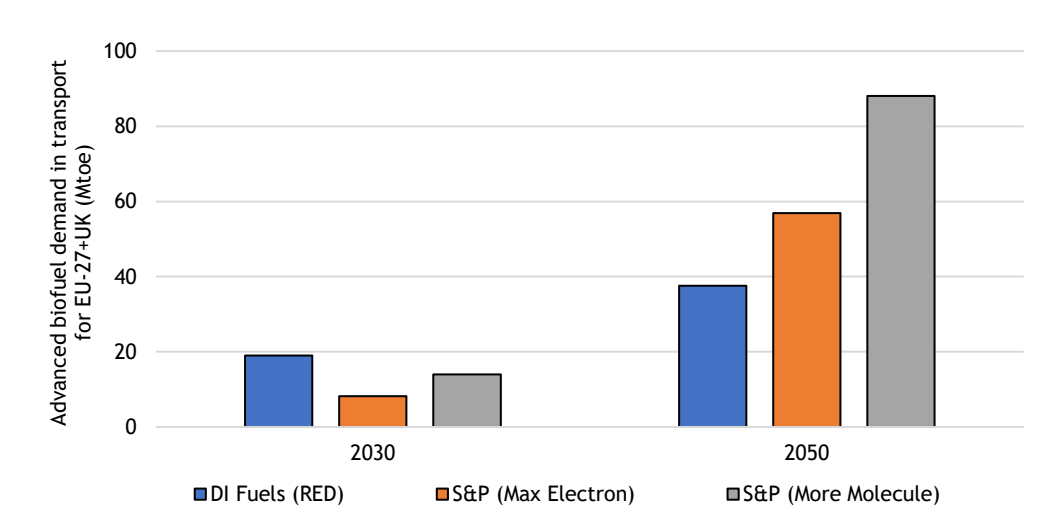


In contrast, the S&P study forecasts lower demand in 2030, equal to 8.2 Mtoe under Max Electron and 14.0 Mtoe under More Molecule. However, its 2050 projections are significantly higher: 56.9 Mtoe (Max Electron) and 88.1 Mtoe (More Molecule)¹³. This divergence illustrates S&P's assumption of a more balanced trajectory, in which renewable liquid fuels play a larger role alongside electrification.

This study adopts an agnostic stance on future demand, recognizing the significant variability in projections, particularly for 2050. Accordingly, the following approach is applied:

- For 2030: The DI Fuels demand of 19.0 Mtoe is used. All the reported demand values are much higher than the current advanced biofuel capacity which makes their realisation very challenging.
- For 2050: The supply chain model is evaluated for both 37.6 Mtoe (DI Fuel) and 88.1 Mtoe (S&P More Molecule). This dual-scenario approach enables an assessment of costs and infrastructure needs across the full spectrum of projected demand reported in the literature.

Figure 18 Projected advanced biofuel demand (excluding biomethane) in the transport sector for the EU-27 + UK for the scenarios of two studies: DI Fuels and S&P (EC, 2024; S&P, 2025)



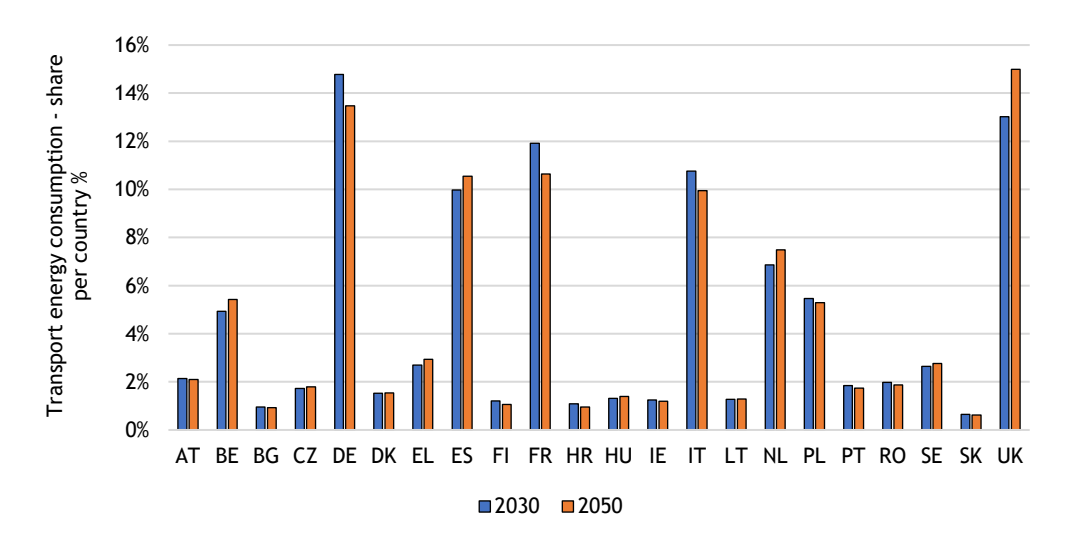
To estimate the advanced biofuel demand at the EU Member State level, alternative methods were employed, as neither the DI Fuel nor S&P studies report projections with country-level granularity. To address this, the relative share of each country's transport energy consumption was calculated using the older country-specific projections from the EU Reference Scenario 2020 (EC, 2021), specifically for transport activity in 2030 and 2050 (see Figure 19).

These country-specific shares were then applied proportionally to distribute the total EU-level advanced biofuel demand (as detailed in Annex D). This approach enabled the estimation of national-level demand figures for advanced biofuels.

¹³ S&P figures also include Switzerland and Norway which are out of the scope of the study. As S&P does not report the country specific figures and these two countries are not expected to largely contribute to the total demand, it is assumed as a simplification that the same total advanced biofuel demand applies to EU-27+UK.



Figure 19 Transport energy share per country within the EU-27 + UK. International maritime bunker fuel demand is included in the figures, which accounts for the high demand in certain smaller countries.



6.2. BIOMASS DEMAND FOR NON-ENERGY USES IN EU-27 + UK

A considerable portion of the calculated available biomass is currently allocated, and expected to remain allocated, to producing various materials and feeds. This includes, for instance, the use of forestry residues for wood-based products and agricultural residues for animal feed. The national-level competing demand for these uses was sourced from the ICL-Concawe study (Panoutsou & Maniatis, 2021). In that study, for each availability scenario (Low, Medium and High), a different percentage of the available biomass was assumed to be directed in these end uses. Detailed tables with the use ratios for each feedstock for both 2030 and 2050 are given in Annex D. Material markets were prioritized over energy uses by excluding biomass demand for materials from the total available biomass.

6.3. BIOMASS DEMAND FOR BIOENERGY (ELECTRICITY/HEAT) IN EU-27 + UK

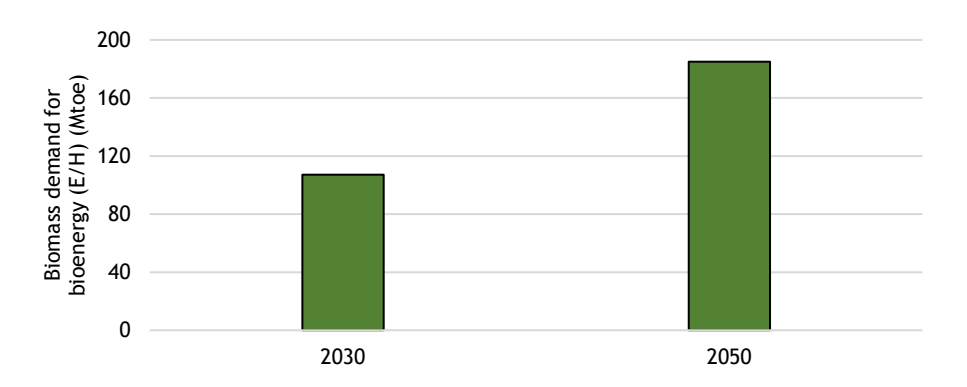
A significant portion of biomass availability is expected to be allocated to energy purposes beyond transport, including electricity and heat (E/H) generation. At the EU level, the bioenergy demand projected in the DI Fuels study was considered (see Figure 20), which was calculated using the PRIMES model (EC, 2024). It is important to note that only lignocellulosic feedstocks are included in the scope of this study (see Table 1), hence any non-lignocellulosic biofeedstock, such as manure, food crops, contributing to the total E/H demand were subtracted. This ensures that only relevant, in-scope feedstocks are considered when estimating biomass availability for the different end-uses.

Additionally, although biowaste streams such as municipal solid waste (MSW) and secondary agricultural residues were not explicitly included in the modelling scope (see Section 2.1), they were indirectly accounted for. Specifically, their supply potential was subtracted from the overall EU bioenergy demand. This approach serves as a mechanism to ease competition between bioenergy and biofuel demands, providing an indirect adjustment to the assumption that not all potentially available lignocellulosic feedstocks were assumed to be accessible for biofuel production in the model.



Figure 20

Biomass demand for bioenergy calculated using the PRIMES model, as reported in the DI Fuels study for the EU-27 (EC, 2024). The original results from the study have been adjusted to reflect the E/H demand based on lignocellulosic biomass considered in this study.



For estimating bioenergy demand for each country, the same method used for the transport sector was applied. Specifically, the projected biomass for bioenergy from the EU Reference 2020 scenario (EC, 2021) was utilized to derive each country's relative share of the total demand reported in the DI Fuels study. The ratio per country is reported in Annex D.

6.4. ADVANCED BIOFUEL AND COMPETING DEMAND LOCATIONS IN THE SUPPLY CHAIN MODEL

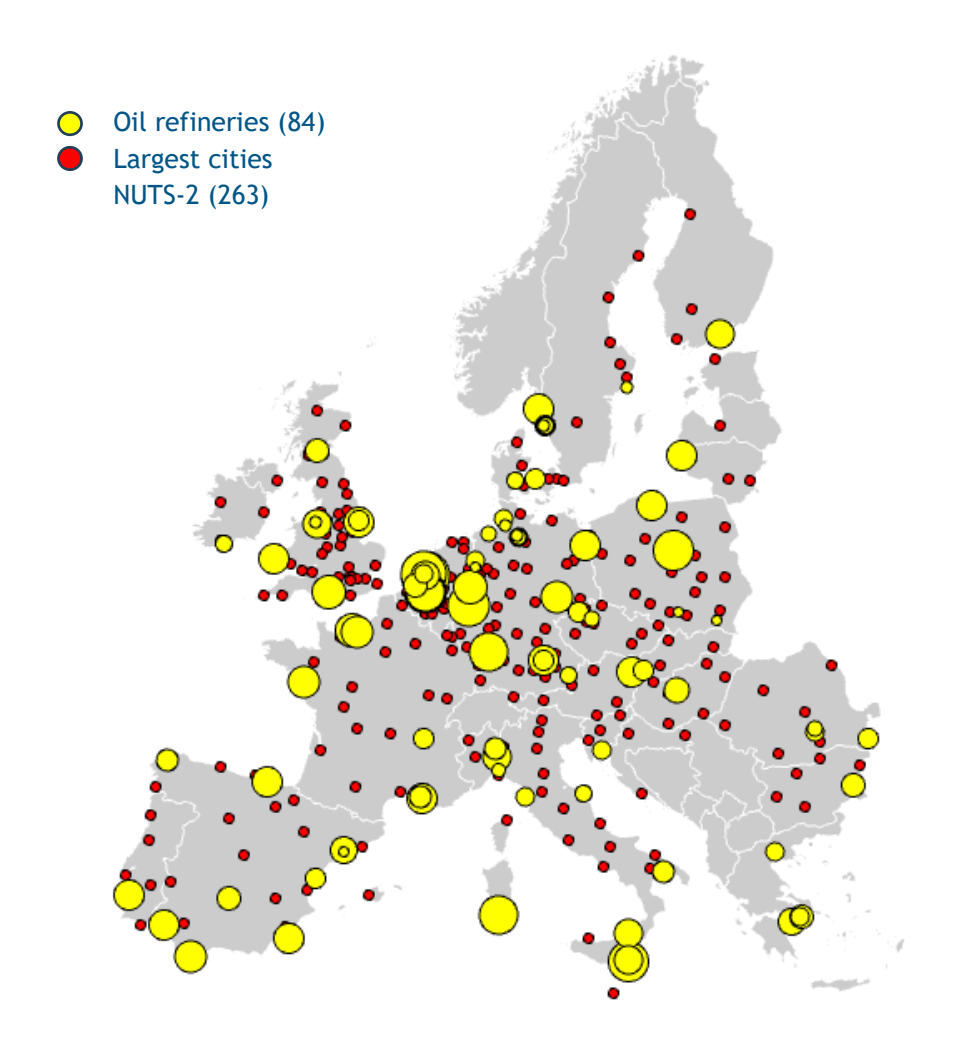
Based on refinery production capacity, advanced biofuel demand per EU country was allocated to existing oil refineries based on the assumption that biofuels will be blended and distributed using the existing transport fuel infrastructure.

Competing bioenergy demand (electricity and heat generation from biomass) was modelled in a simplified way to optimize computational efficiency and reduce memory usage. Competing bioenergy demand was assumed to occur in the largest city in each NUTS-2 region, with population density as a proxy to allocate the share of competing bioenergy demand per country.

Future developments of oil refineries and major cities were not taken into account and the same locations and demand allocation factors were applied to both 2030 and 2050.



Pigure 21 Demand locations for advanced biofuels (oil refineries) and electricity and heat (largest cities NUTS-2 regions). The same locations were assumed for both 2030 and 2050.





7. RESULTS: BIOMASS AVAILABILITY AND COSTS MAPPING

7.1. AVAILABILITY, WATER STRESSES AND COSTS POTENTIAL OF AGRICULTURAL BIOMASS

The availability potential and roadside costs of energy crops and agricultural residues were calculated for this study. A comparison of biomass from agriculture in this study and the ICL-CONCAWE potentials is available in Annex A2.

7.1.1. Availability potential of agricultural biomass

As shown in Figure 22, the total biomass potential in the EU-27 + UK is estimated at 177 million tonnes in 2030, 197 million tonnes in 2040 and 204 million tonnes in 2050 for the Low availability scenario. For the Medium scenario, the total biomass potential is estimated at 222 million tonnes in 2030 and 278 million tonnes in 2050. For the High scenario, the biomass potential is estimated at 272 million tonnes in 2030 and 358 million tonnes in 2050. For each scenario, the highest share of biomass potential corresponds to lignocellulosic energy crops, followed by cereals straw and maize stover. The difference between the scenarios is attributed to annual yield increases, removal rates of agricultural residues, and the shares of potentially available marginal land that complies with RED II/III sustainability criteria and suitability parameters to produce lignocellulosic energy crops.

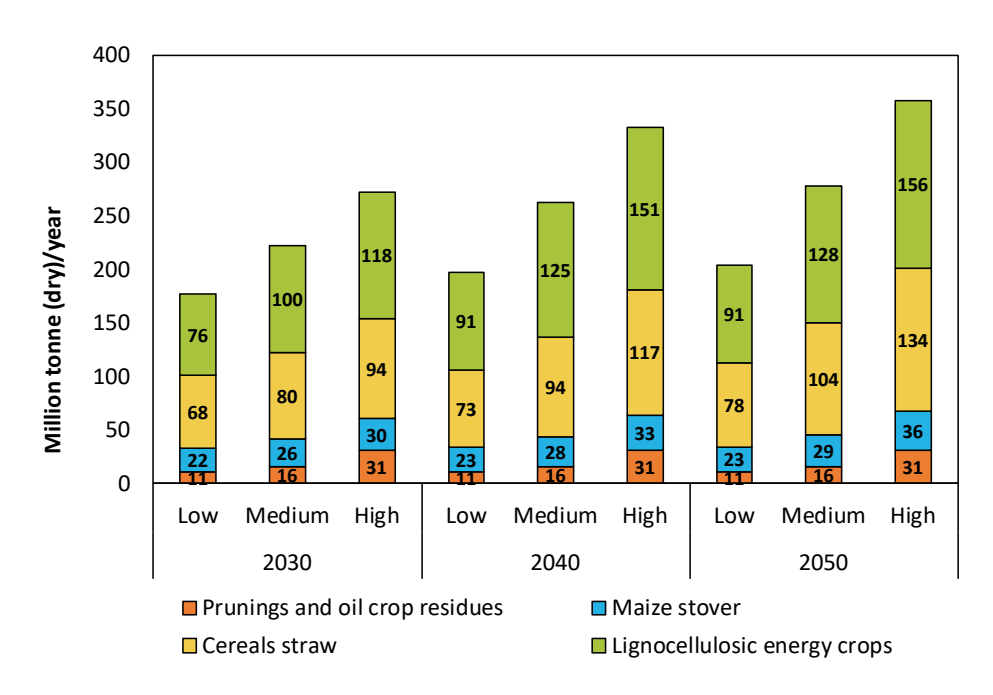
Annual yield increases (mainly) lead to the growth in biomass potentials for agricultural residues over time. For lignocellulosic energy crops, the increase over time is driven by annual yield increases, Land Use Change (LUC) dynamics and variations in climate conditions. For each reference point in time, the LUC dynamics determine the availability of marginal land that complies with RED II/III sustainability criteria and the location of available land. Climate variations influence both the suitability of a location for crop growth and the potential biomass yield. Over time, changes in climate can make areas that were once unsuitable for growing lignocellulosic energy crops viable. To illustrate this, in 2030 there are (approximately) 8 million ha of marginal land available that meet RED II/III sustainability criteria and are suitable for lignocellulosic energy crop production. In 2050, the amount of marginal land that complies with RED II/III sustainability criteria and is suitable for lignocellulosic energy crops production increases to 8.7 million ha.

For agricultural residues, the differences between the biomass potentials are attributed mainly to the amount of primary crops (cereals and maize) projected to be produced on agricultural land. In Europe, cereals such as wheat and barley production are considerably higher than maize. Differences in cereal straw potentials between availability scenarios are primarily due to the varying levels of development projected for cereal crop yields and agricultural management practices (see Annex A2).

The difference in residues biomass potentials for agricultural prunings and oil crop residues are the result of the chosen scenarios from the EU S2Biom project: the Low scenario shows the potential under current practices, the Medium scenario considers the sustainable removal rate to keep soil organic carbon at constant levels and the High scenario represents the maximum removal rate limited by technical constraints. These technical constraints represent the limitations of removal rates driven by harvesting equipment, crop type, growth pattern and variety. These are based on the EU S2Biom User Defined, Base and Technical potentials defined in (Dees, Datta, et al., 2017).



Figure 22 Biomass availability potentials in the EU-27 + UK for the Low, Medium and High availability scenarios.



In terms of individual biomass potentials for lignocellulosic energy crops for the EU27 + UK, miscanthus, switchgrass and Reed Canary Grass (RCG) are the energy crops with the highest potentials (see Figure 23). Note that for the individual biomass potentials for lignocellulosic energy crops presented in the Figure, all available (marginal) land is attributed to only one crop at a time. The difference in biomass potentials between crops arises primarily from the adaptability of each crop to site-specific biophysical conditions and the achievable yield it can provide under those specific conditions. For example, RCG exhibits the lowest water use efficiency and the shortest growth period, resulting in relatively low yields when compared to other crops (see Table 17). Nevertheless, RCGs remarkable tolerance to a broader array of biophysical conditions, such as colder temperatures and reduced precipitation, enables its production in regions unsuitable for other crops. Conversely, giant reed displays the highest water use efficiency, leading to comparatively larger potential yields. However, its capacity to thrive across diverse biophysical conditions is limited, as it struggles under cold temperatures and can only be produced in warm locations. This contrast in adaptability ultimately translates into a lower overall biomass potential for giant reed compared to reed canary grass.

The maximum yield biomass potential (for each location, the lignocellulosic energy crop with the highest attainable yield is selected) is made up largely of miscanthus and giant reed, followed by reed canary grass and eucalyptus, with other crops contributing marginally. Giant reed stands out for its higher water use efficiency, resulting in the highest average yields. As a result, it is the preferred crop in locations where multiple species can be cultivated. Miscanthus and switchgrass exhibit similar growth patterns and adaptability to different biophysical conditions, but miscanthus generally offers higher yield potential. Therefore, miscanthus is prioritized over switchgrass, wherever both crops can be grown. Most sites do not choose willow and poplar, as other crops like giant reed and miscanthus produce higher yields under similar conditions. RCG is only selected in areas where the local biophysical conditions make it the only viable feedstock option.



Figure 23

Biomass potentials (for all markets) of lignocellulosic energy crops, cereal straw and maize stover for the high availability scenario in the EU-27 + UK. The Max-yield biomass potential represents the case based on which the lignocellulosic energy crop with the highest attainable yield is selected for each location. The individual energy crop bars represent the case when all the available marginal land is dedicated to a single crop.

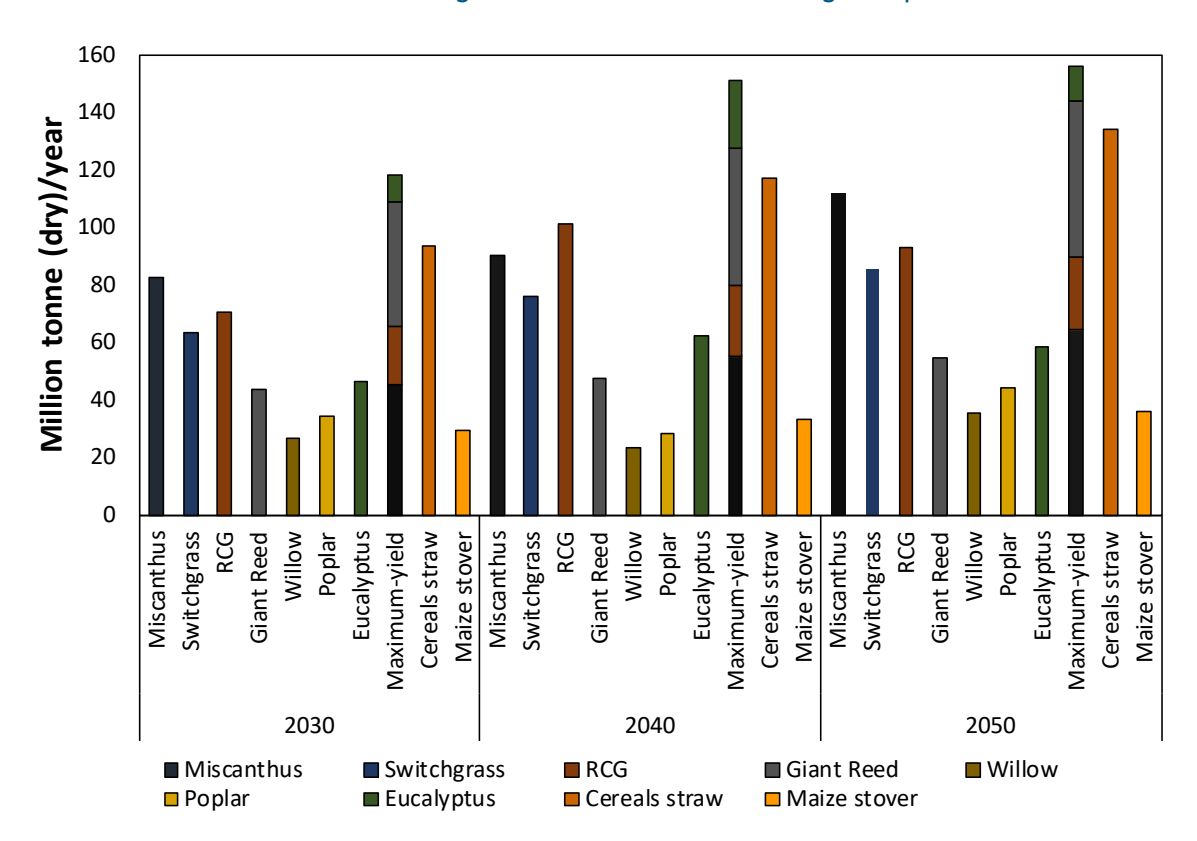


Table 17 Average yield for each crop in the High availability scenario while considering all the potential locations suitable for each crop type in EU-27 + UK.

Crop	2030 (t/ha)	2040 (t/ha)	2050 (t/ha)
Miscanthus	15.6	17.3	19.1
Switchgrass	11.7	13.3	14.3
RCG	8.9	10.4	10.7
Giant Reed	24.0	25.5	28.0
Willow	17.9	18.9	21.1
Poplar	15.9	16.8	18.6
Eucalyptus	17.0	18.6	19.9

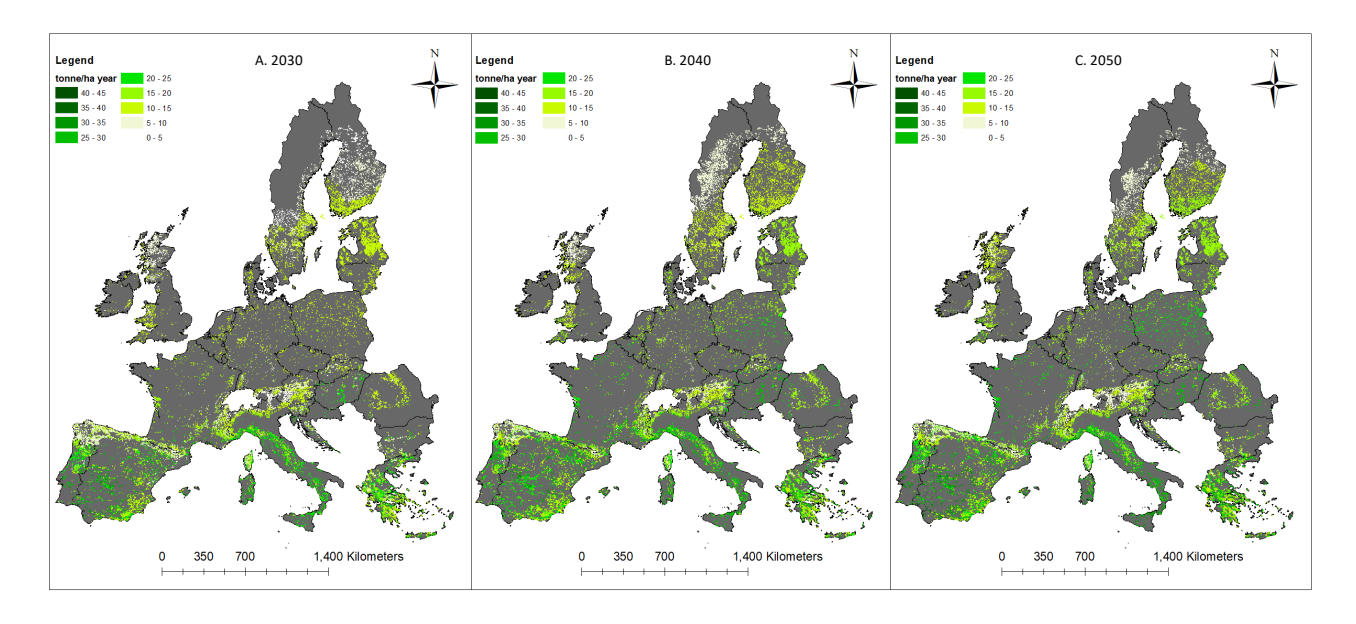


7.1.2. Mapping (spatially explicit results) of biomass availability potential

There is a strong spatial variation of lignocellulosic energy crops biomass potentials over the EU-27 + UK. Figure 24 shows the High scenario's spatially explicit lignocellulosic energy crops biomass potential (maximum yield) over time ¹⁴. The lowest yields are located in regions with severe biophysical conditions, such as low temperatures and acidic soils, which limit biomass growth. This is reflected in Scandinavia, mountainous areas (e.g., the Alps), and north of the UK. The areas with the highest biomass potentials are located in Spain, Italy, Greece and Hungary. These areas feature favourable biophysical conditions for biomass production, especially for giant reed, miscanthus and eucalyptus. Over time, the change in climatic conditions results in some areas previously unavailable for the production of lignocellulosic energy crops becoming available. This is evident in Scandinavia and other places such as Spain, Poland and Germany.

Figure 25 shows the spatially explicit cereal straw High scenario biomass potential over time. Most areas with the highest yields in 2030 are in France, the Netherlands Germany and north of Italy. These countries and regions have a long tradition of cereal production. The lowest yields for 2030 are located in Spain, Scandinavia and Poland. Over time, the increase in cereal yield results in straw output increase for several locations such as in the north of Germany, Poland and Romania. While for lignocellulosic energy crops, the total amount of land available for their production increases over time, for cereals, it decreases. This transition of land dynamics can be seen in places such as the Baltic states.

Figure 24 Spatial distribution of lignocellulosic energy crops (for the Max-yield case) potential over time (t_{dry} /ha year) in the High availability scenario. The Max-yield case refers to the maximum yield biomass potential based on which the lignocellulosic energy crop with the highest attainable yield is selected for each location. The pixel size is enhanced for displaying purposes.



¹⁴ All biomass potential maps and statistics at a country and NUTS-3 level are available in the Annex.



Figure 25 Spatial distribution of cereal straw potential over time $(t_{dry}/ha\ year)$ in the High availability scenario. The pixel size is enhanced for displaying purposes.

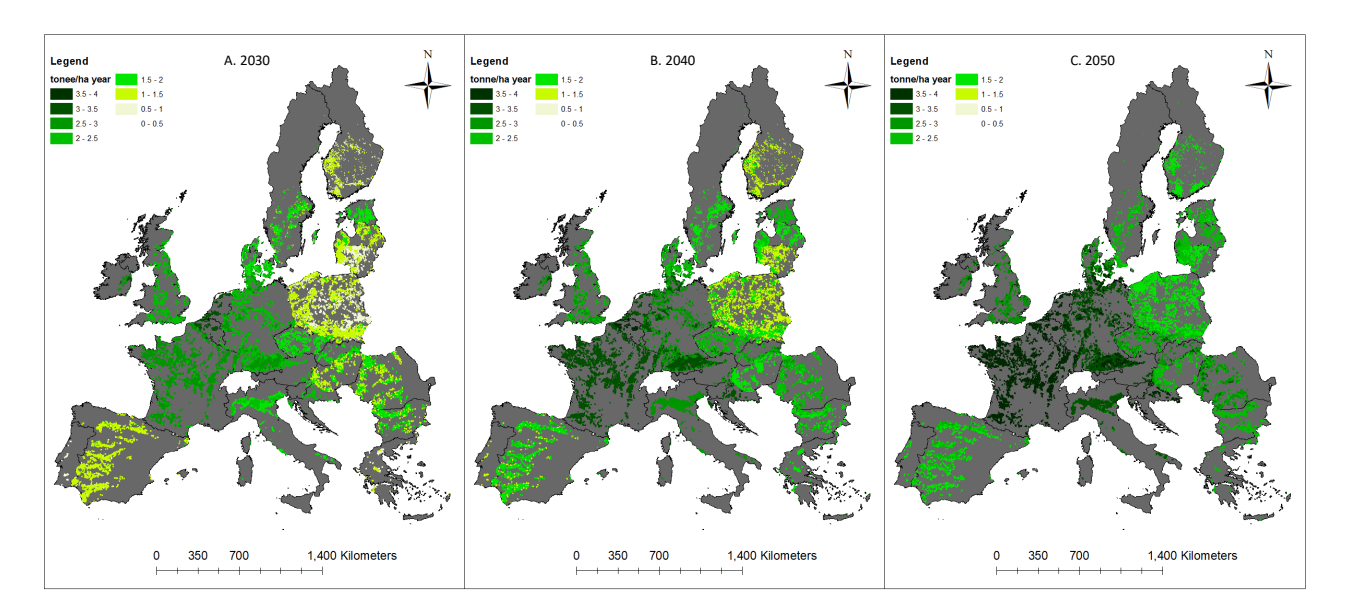
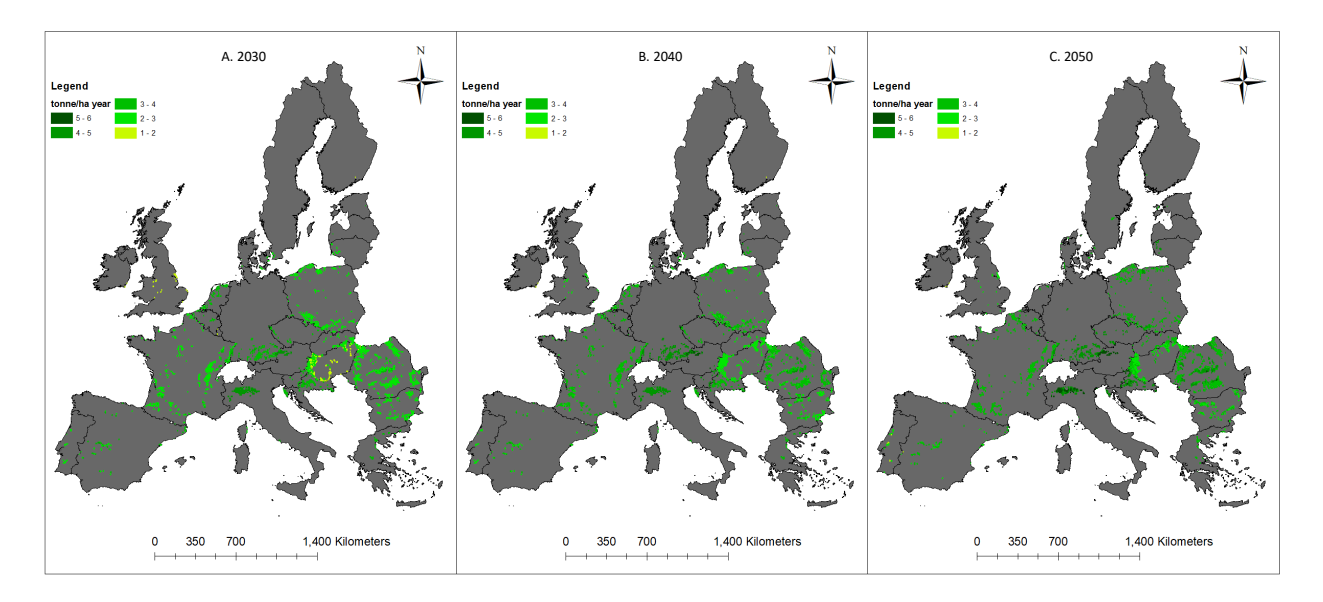


Figure 26 shows the spatially explicit distribution for maize stover in the High scenario over time. The highest yields are found in France, Germany, North of Italy, Hungary and Austria. Different from the other biomass potentials, the availability of maize stover is concentrated in certain countries, given their tradition in the production of maize. Over time, as for cereals, the amount of total agricultural land dedicated to maize production decreases. However, a shift in production areas is also seen, leading to the fact that for some countries, the biomass potential stays relatively unchanged. For example, some new production areas for maize appear in the north of France, Belgium and Germany between 2040 and 2050.



Figure 26 Spatial distribution of maize stover potential over time $(t_{dry}/ha\ year)$ in the High availability scenario. The pixel size is enhanced for displaying purposes.



7.1.3. Water balance (deficit) and impact on energy crop potentials

7.1.3.1. Water balance of lignocellulosic energy crops

The water balance for lignocellulosic crops represents the potential gap between the total precipitation considered in the crop yield calculations and the effective precipitation, which reflects the amount of water that can actually be used by the plants. While this effective precipitation can be estimated using high-level equations based on the total rainfall amount, important factors such as the temporal distribution and intensity of rainfall, as well as soil characteristics and topography, play a crucial role in determining the precise amount of water available for crop use but are not incorporated into the model. Therefore, the water balance figures presented here should be regarded as preliminary insights rather than definitive values or conclusions.

Moreover, the water balance assessment is not directly linked to any of the low, medium, or high scenarios, as these scenarios include yield improvements from management practices or innovations that are applied after the crop growth modelling stage. In contrast, the water balance provides an indication of potential water surplus or deficit based solely on biophysical, climatic, and topographic conditions, without considering any agronomic enhancements or technological interventions.

The lignocellulosic energy crop's EU-27 + UK average biomass water balance varies between -427 mm/year for switchgrass in 2030 and -895 mm/year for giant reed (Figure 27). On average, achieving the biomass yields for switchgrass requires an extra 4270 m³ of water per hectare during the crop's growth cycle, while giant reed requires an additional 8950 m³ of water per hectare. Therefore, the precipitation rates are insufficient to meet (on average) the lignocellulosic energy crops' water demand and achieve the estimated biomass potential yields¹5. Supplying additional water can disrupt water levels and lead to regional water scarcity. The effects of

¹⁵ Results in negative water balance scores

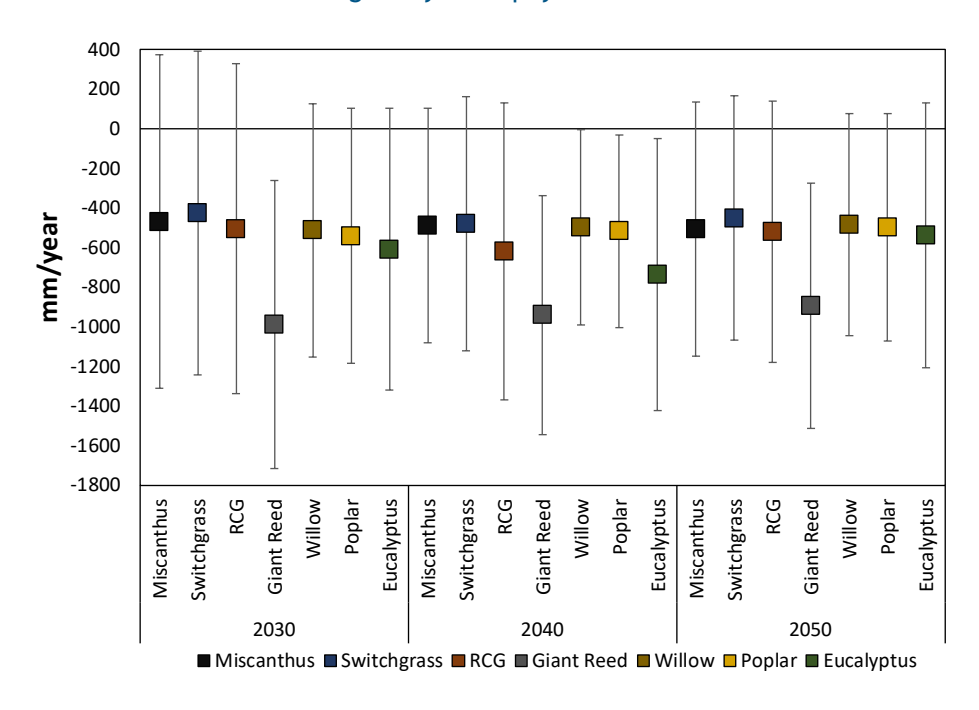


negative water balance or the irrigation costs required to achieve the calculated yield levels were not included in the supply chain analysis. However, these factors are presented here to provide insight into the potential implications associated with the large-scale production of lignocellulosic crops.

Despite that, the average water balance for lignocellulosic crops is negative; there are several locations (except for giant reed) where the precipitation conditions in 2030 are sufficient to provide the required amount of water for each crop to deliver the potential yield. This is shown in Figure 27 by positive water balance scores that fall within the ranges displayed for each crop. However, the locations with positive scores reduce over time, given changes in precipitation and temperature.

The difference in water balance between lignocellulosic energy crops is due to each crop's phenological characteristics that determine the amount of water each crop requires during its growing cycle and the location-specific climatic conditions (mainly precipitation and temperature). For example, giant reed is one of the crops with the highest water requirement during its growing cycle, while other crops such as switchgrass and miscanthus have lower water needs. Changes in temperature and precipitation drive the difference over time in water balance between crops. However, no extreme variations are foreseen for this indicator.

Figure 27 Water balance of lignocellulosic energy crops. The ranges indicate the spatial variability of water shortage due to the heterogeneity in biophysical conditions.



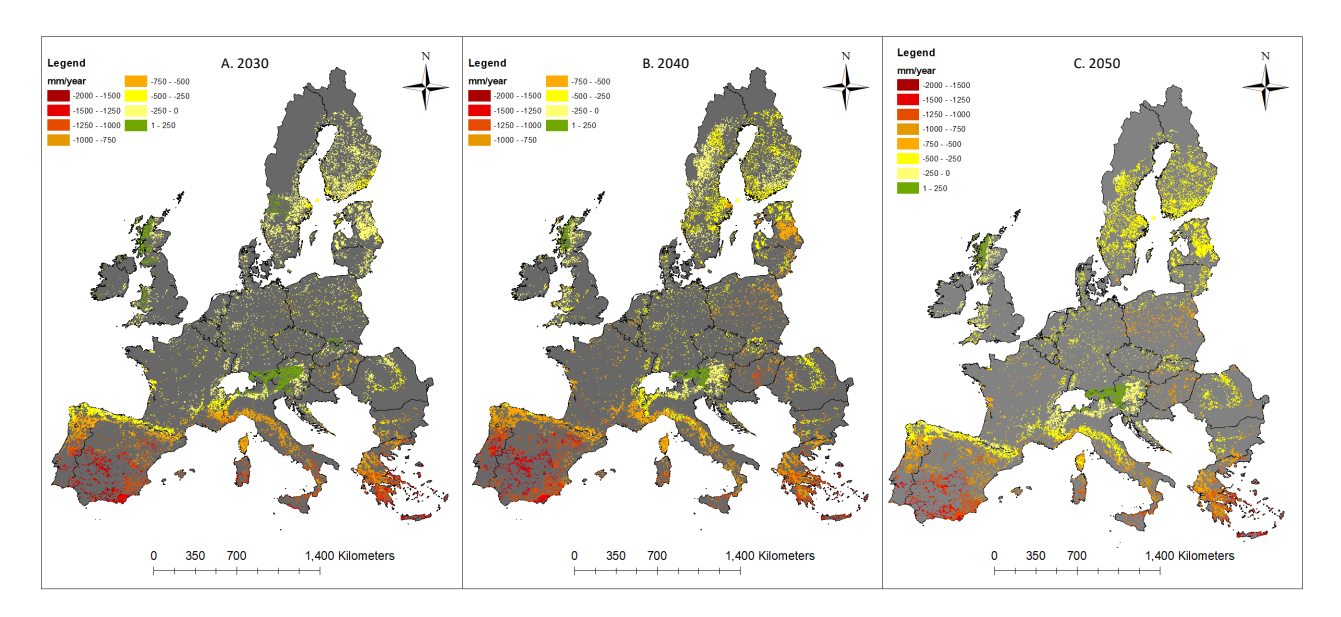
7.1.3.2. Water balance of lignocellulosic energy crops spatially explicit results

As shown in Figure 28, the regions with the highest water deficit (negative water balance scores) are the ones in the Mediterranean; Spain, Portugal, Italy and Greece. In these countries, the precipitation rates are not sufficient to meet the crop's water demand. Over time, the water deficit is projected to increase in countries such as France, Spain, Romania, and Poland, which are led by increasing temperatures and decreasing precipitation rates. However, in other specific locations, such as Latvia, the precipitation rates are expected to increase between



2040 and 2050, and thus, the water deficit will decrease, leading to potentially (somewhat) higher yields.

Figure 28 Spatial distribution of lignocellulosic energy crops water balance over time (mm/year). The pixel size is enhanced for displaying purposes.

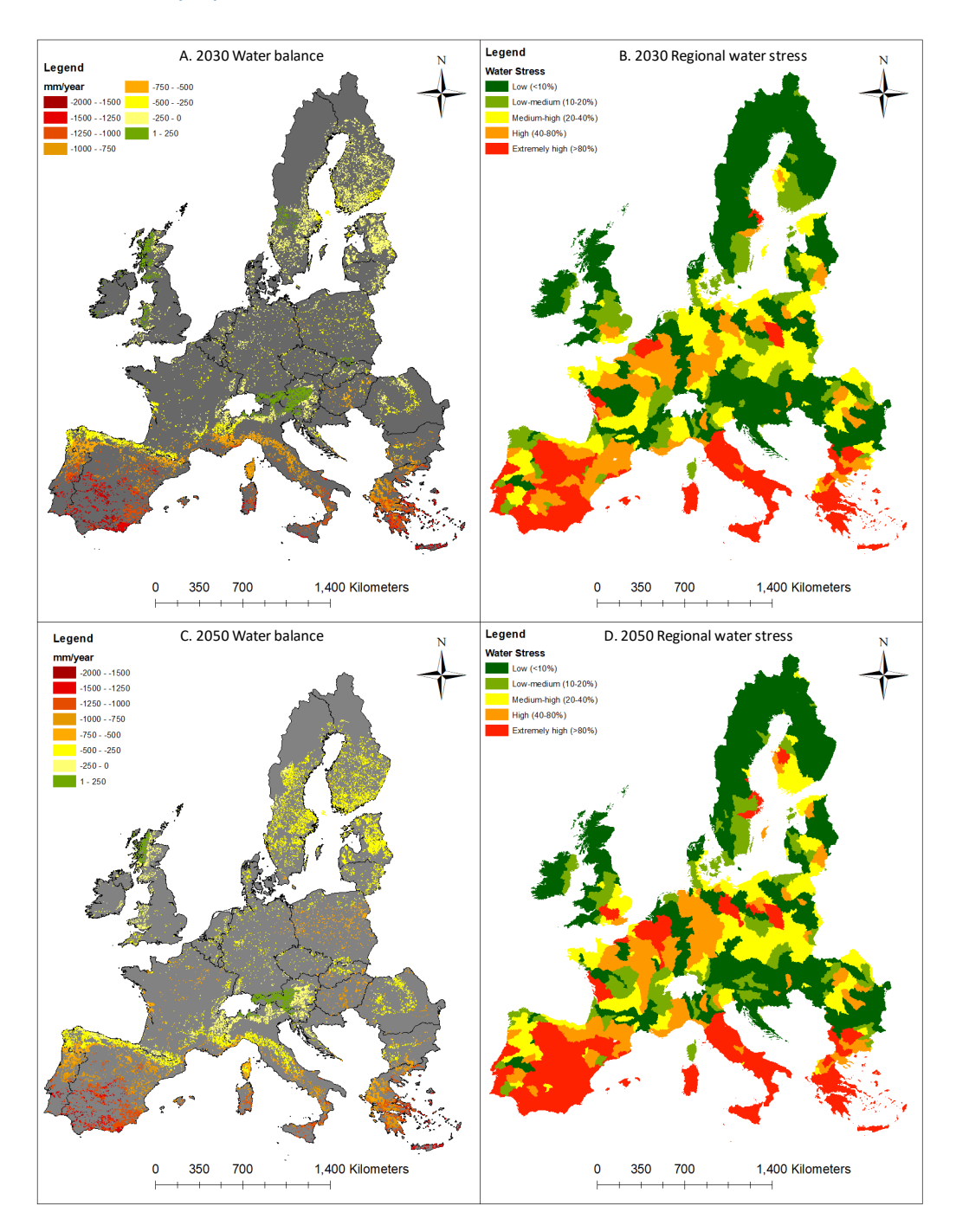


Most of the regions with a large water deficit overlap for 2030 and 2050 with areas expected to undergo very high-water stress (Figure 29). This can be seen especially in the Mediterranean region. In addition, areas in France and Germany that score relatively low water deficit overlap with high water stress areas in 2030 and 2050. Supplying additional water for lignocellulosic energy crop production can disrupt water levels in these regions and lead to additional water stress. Conversely, in other areas, such as Scandinavia, Austria, and parts of the Baltic states, the water stress is projected to be low. Providing water to meet the lignocellulosic energy crops water demand for these areas does not lead to water stress issues compared to southern locations.

As mentioned in the biomass potential section, most of the highest yields are projected in the Mediterranean regions, such as parts of France, Poland, and Hungary. The high-yield locations also overlap with the regions with a large water deficit and high-water stress. However, medium yields can be achieved with relatively low water deficits and in low to medium water stress areas for other regions such as the UK, Austria, and Denmark.



Figure 29 Spatial distribution of lignocellulosic energy crops water balance (mm/year) for 2030 (A) and for 2050 (C). Regional water stress for 2030 (B) and for 2050 (D) (Kuzma et al., 2023). The pixel size is enhanced for displaying purposes.



7.1.4. Roadside cost of agricultural biomass

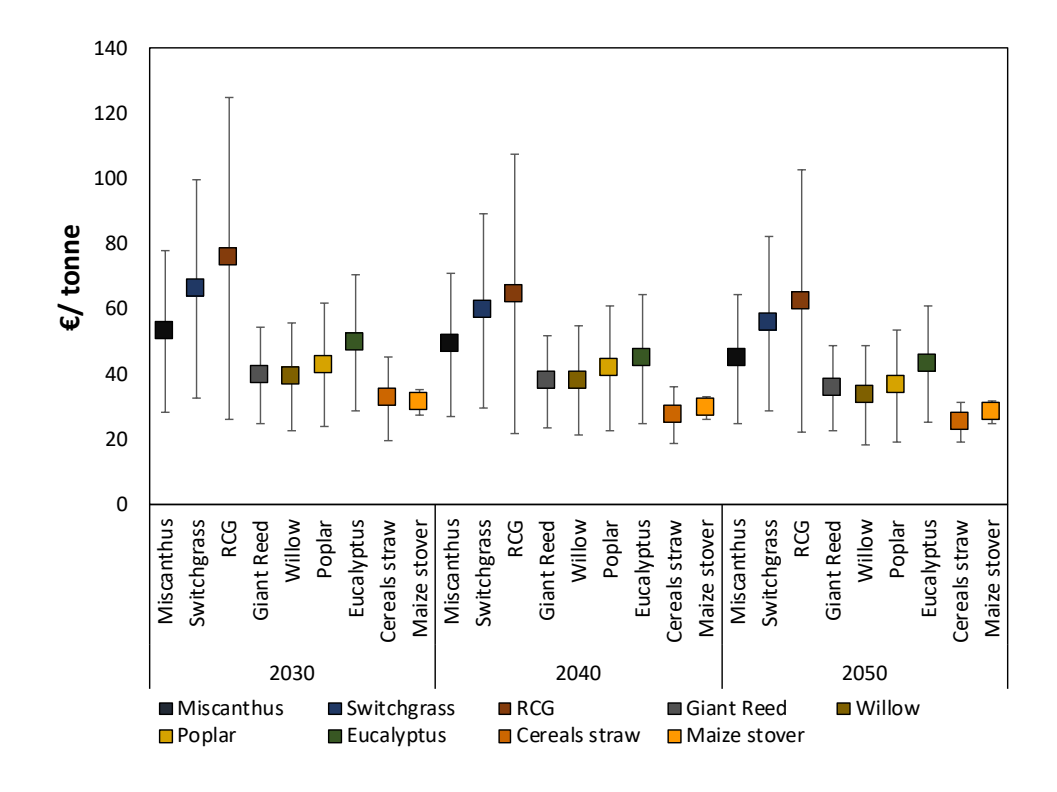
The average production cost of lignocellulosic energy crops for the High scenario in the EU-27 + UK varies between 76 $\ensuremath{\notin}$ t_{dry} for RGC and 39 $\ensuremath{\notin}$ t_{dry} for willow in 2030,



and $63 \ \ \ell/t_{dry}$ for RGC and $33 \ \ \ell/t_{dry}$ for willow in 2050 (see Figure $30)^{16}$. The difference in average costs between biomass types is mainly driven by yield differences and the cost of agricultural activities related to each crop. Over time, yield increases and improved crop management practices lead to cost reductions for all biomass types.

On average, RCG is the crop with the lowest yield and thus shows the highest costs. In some regions, the cost of RCG can go above $120~\mathebox{\ensuremath{ℓ}}/t_{dry}$. Conversely, giant reed is one of the crops with the highest average yield and thus has lower costs than other crops. In addition, harvesting giant reed is less expensive than harvesting other perennial grasses, such as miscanthus and switchgrass. Harvesting such perennial grasses involves more machines than mowing for giant reed. Miscanthus average costs in 2030 stand at $53~\mathebox{\ensuremath{ℓ}}/t_{dry}$. Nevertheless, it can increase to $80~\mathebox{\ensuremath{ℓ}}/t_{dry}$ in locations characterized by lower yields. A review study on miscanthus found that production costs range between $48-138~\mathebox{\ensuremath{ℓ}}/t_{dry}$ (Witzel & Finger, 2016). The average miscanthus cost difference between studies can be attributed to assumptions concerning yields and crop life span. The average switchgrass cost is higher than miscanthus. Both crops show similar harvesting and growing conditions, but switchgrass yields are lower. The costs of harvesting activities related to short rotation coppice are lower compared to perennial grasses harvesting and bailing.

Figure 30 EU-27 + UK average costs of production and harvesting of lignocellulosic energy crops and collection of agricultural residues for the High availability scenario (in $\[mathbb{E}/t_{dry}$). The ranges indicate the spatial variability of cost due to the heterogeneity of yields.



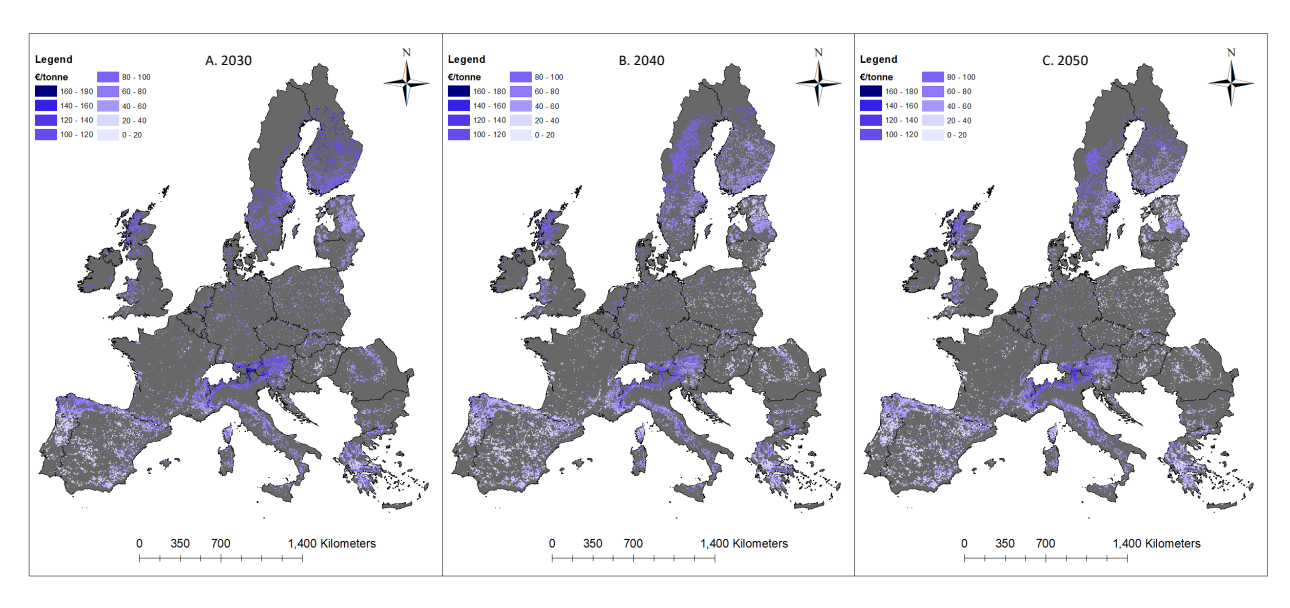
¹⁶ Note that the results are presented for the High scenario to keep consistency with the biomass potentials section. The results for the other scenarios are reported in the Annex.



For cereals straw and maize stover, average costs are estimated at $33 \notin /t_{dry}$ and $31 \notin /t_{dry}$ in 2030, and $25 \notin /t_{dry}$ and $28 \notin /t_{dry}$ in 2050. The cost of agricultural activities related to the collection of different residues is similar. The differences in costs for residues arise mainly from yields and fertilizer inputs (based on the nutrient content of cereals and maize) required to replace the removed nutrients. Several studies and projects have estimated that the costs of cereal straw range from 25 to $45 \notin /t_{dry}$ (Dees, Datta, et al., 2017).

Figure 31 shows a strong spatial distribution over the cost of lignocellulosic energy crops for all points in time ¹⁷. The main differences between costs on a spatial level are related to yields, country-specific labour costs, fuel prices and land rent. For example, Spain shows low costs for 2030, between 20-40 $\rm €/t_{dry}$. As pointed out in previous sections, high yields can be obtained in Spain. In addition, labour costs and land rents are considerably lower in Spain than in other countries. The same combination of drivers results in low costs for Hungary and Greece. Conversely, the prices are higher in countries with low yields and high labour costs. This is the case for Scandinavia, where costs can increase by up to $140-160\rm €/t_{dry}$. In Italy, the costs are higher than in Greece and Spain (countries with similar labour cost conditions), given that land rent costs are higher.

Figure 31 Spatial distribution of lignocellulosic energy crop costs (€/t_{dry}) for the Max-yield case over time. Max-yield refers to the maximum yield biomass potential for each location the lignocellulosic energy crop with the highest attainable yield is selected. The pixel size is enhanced for displaying purposes.



The cost of cereal straw and maize stover is extensively driven by yields. However, labour cost and fuel prices also influence the results to some extent. Countries with higher yield residues, such as France, show lower costs. This can be seen in Figure 32 and Figure 33. For example, cereal straw costs in France are projected between 20-30 €/t_{dry} for 2030; for Poland, costs can be between 40-50 €/t_{dry} , and for Scandinavia, between 45-55 €/t_{dry} .

¹⁷ Note that the results are presented for the High scenario to keep consistency with the biomass potentials section. The results for the other scenarios are present in the Annex.



Figure 32 Spatial distribution of cereal straw costs over time (ξ/t_{dry}) . The pixel size is enhanced for displaying purposes.

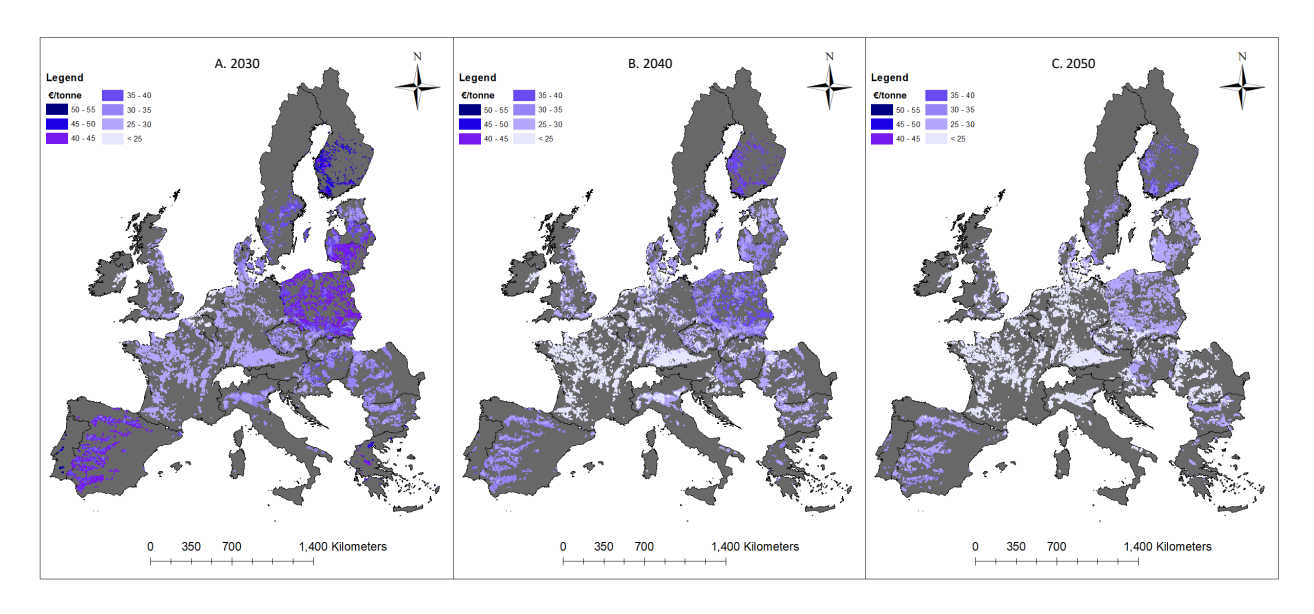
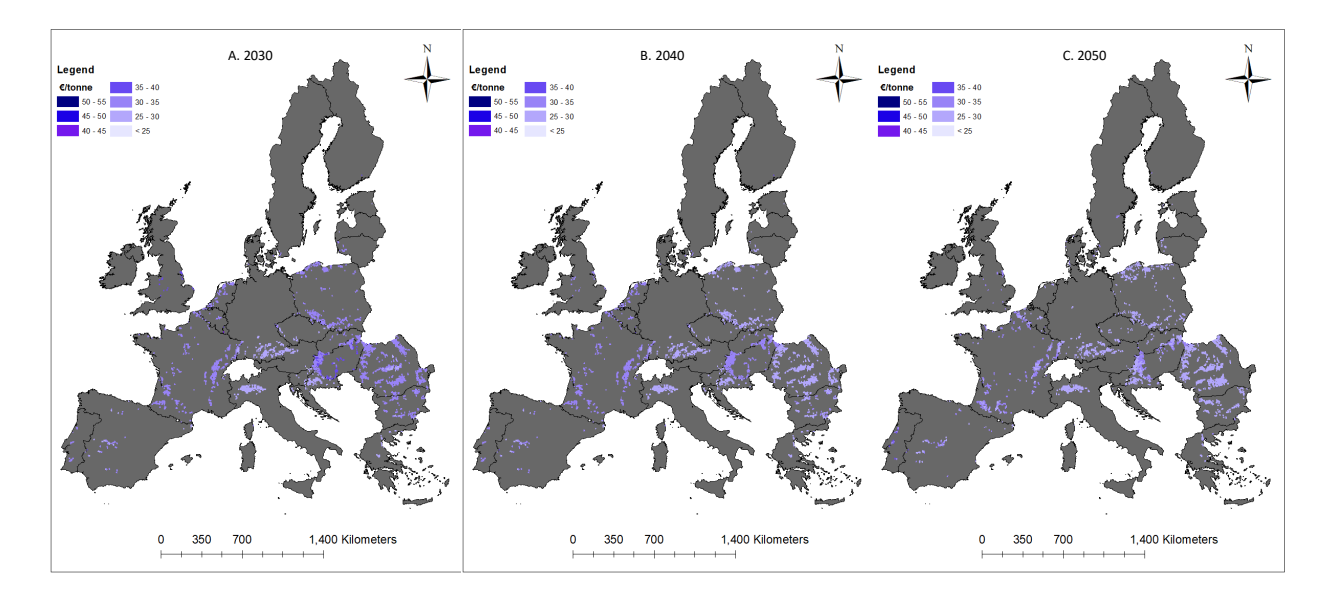


Figure 33 Spatial distribution of maize stover costs over time (€/t_{dry}). The pixel size is enhanced for displaying purposes.



7.2. AVAILABILITY AND COSTS POTENTIAL OF FOREST BIOMASS

7.2.1. Availability potential of forest biomass

The availability potential of forest biomass consists of stemwood, primary forestry residues and secondary forestry residues, with the availability figures taken from the ICL-Concawe study (see Figure 34) (Panoutsou & Maniatis, 2021). The potential is also given in energy units (Mtoe) in Figure 35.



The total availability potential for all markets (materials, energy, etc.) in the Medium availability scenario is estimated to be 632 Mt (dry)/y in 2030 (scenario range: 558 - 659 Mt (dry)/y), increasing to 672 Mt (dry)/y (scenario range: 590 - 726 Mt (dry)/y) by 2050. The estimated potential from stemwood, including fuelwood for energy, shows minimal changes over time because it is based on the average maximum sustainable harvest over 50 years (Panoutsou & Maniatis, 2021). The difference between the Low and High availability scenarios for all markets, comes mainly from differences in measures to increase stemwood availability. The availability scenarios of forest biomass for bioenergy show larger variations because of the differences in shares of forest biomass available to bioenergy in the scenarios (see Table 4 and Table 5).

Figure 34 Availability potential of forest biomass available for all markets in 2030 and 2050 in million tonnes dry (Mt_{dry}/y) in the different availability scenarios.

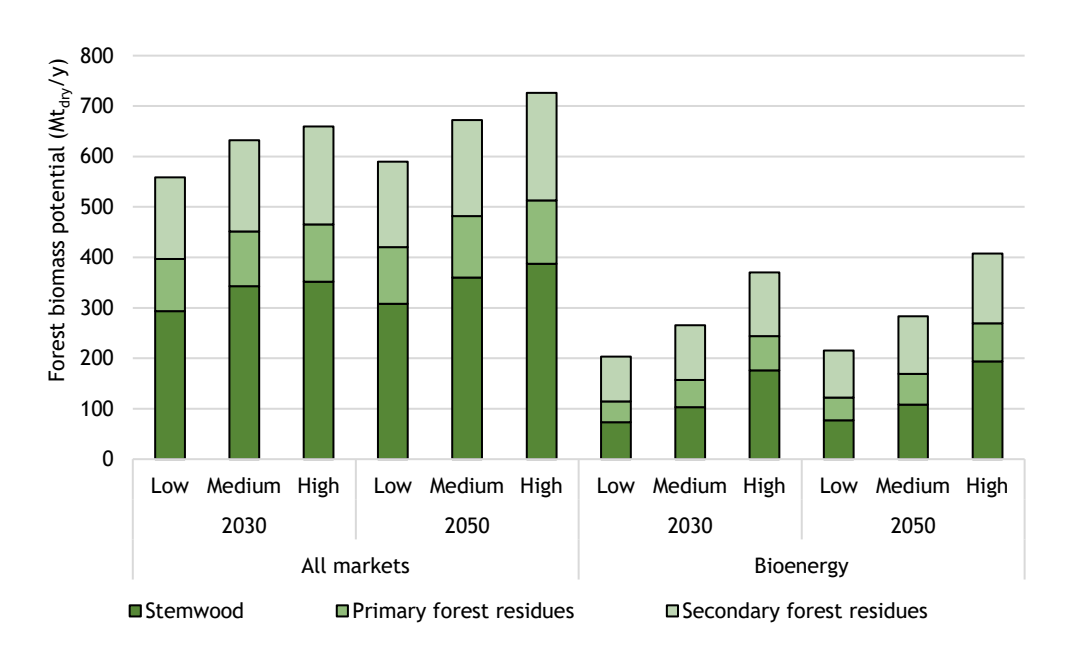
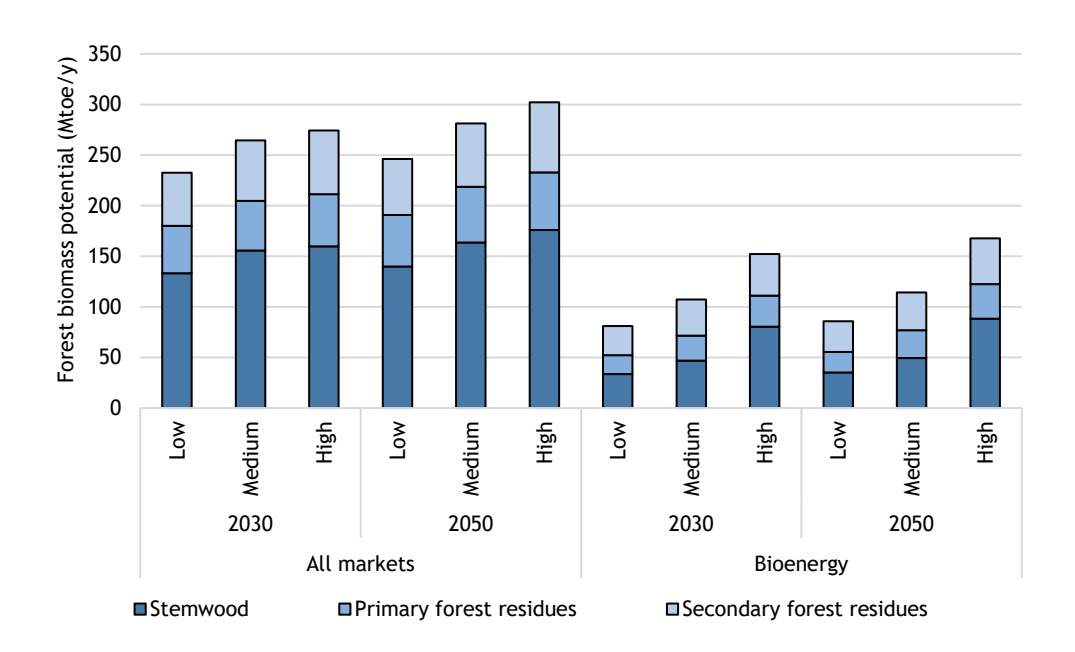




Figure 35

Availability potential of forest biomass available for all markets in 2030 and 2050 (in Mtoe/y). Note that the potential in energy units deviates slightly from the ICL-Concawe study because it is calculated from feedstock-specific energy densities (Table 8) whereas ICL-Concawe assumed an average LHV of 2.5 t_{dry}/toe for all feedstock categories.



7.2.2. Mapping (spatially explicit results) of biomass supply and costs potential

The availability potential of forest biomass for all markets is mapped to NUTS-3 level for 2030 in Figure 36 and 2050 in Figure 37. Both stemwood and primary forestry residues are mapped based on the forest density in each region (see Section 3.3.1) resulting in a similar pattern at NUTS-3 level. The availability potential of stemwood for all markets is more significant than primary forestry residues, but the majority is utilized in material markets and not available for bioenergy. Secondary forestry residues are mapped based on wood processing industries in each NUTS-3 region from the S2Biom project (see Section 3.3.2). It shows that forest processing industries are often located in relatively high forest-density regions. This results in competing demand but also increased availability of secondary forest resources such as sawmill residues.

The mapping of roadside costs of forest biomass is given in Figure 38. Note that the roadside cost of forest biomass does not reflect on market competition. The costs of stemwood and primary forestry residues are calculated using an Activity Calculation method based on the efforts and costs to make it available at the roadside (Dees, Elbersen, et al., 2017). The same roadside costs were assumed for both 2030 and 2050. Cost differences result from country-specific cost factors such as labour cost and productivity levels (see Annex A1). It is acknowledged that additional factors such as inflation, labour market dynamics, and technological developments (e.g. automation) could further influence future costs.



Figure 36 Stemwood, primary forestry residues, and secondary forestry residues availability potentials for all markets at NUTS-3 level for 2030 in kilo tonnes dry material (kt_{dm}/y).

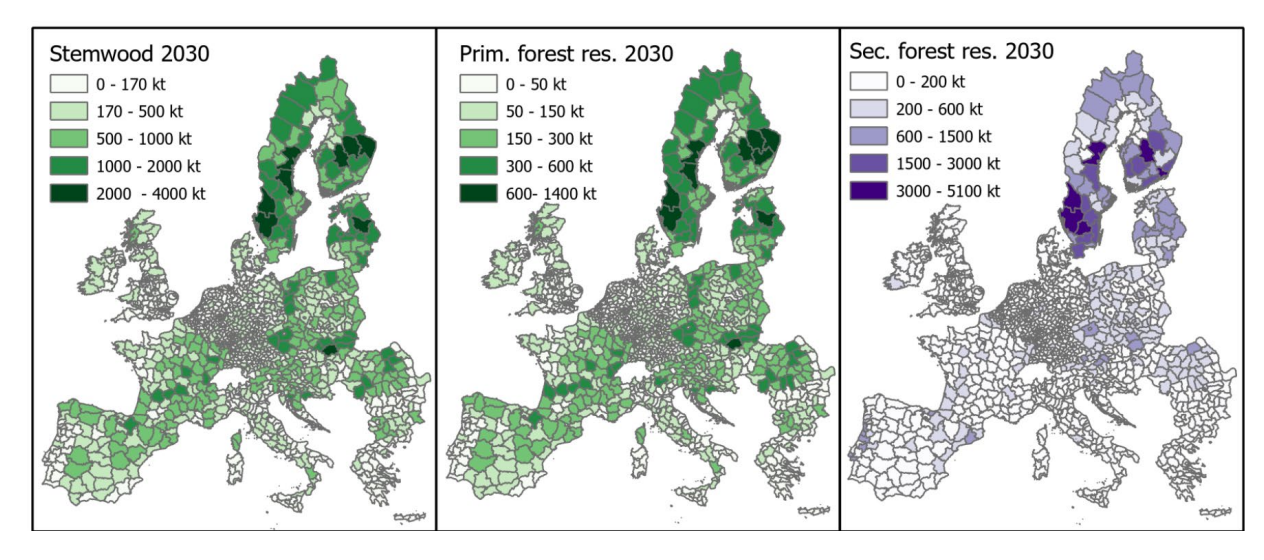


Figure 37 Stemwood, primary forestry residues, and secondary forestry residues availability potentials for all markets at NUTS-3 level for 2050 in kilo tonnes dry material (kt_{dm}/y).

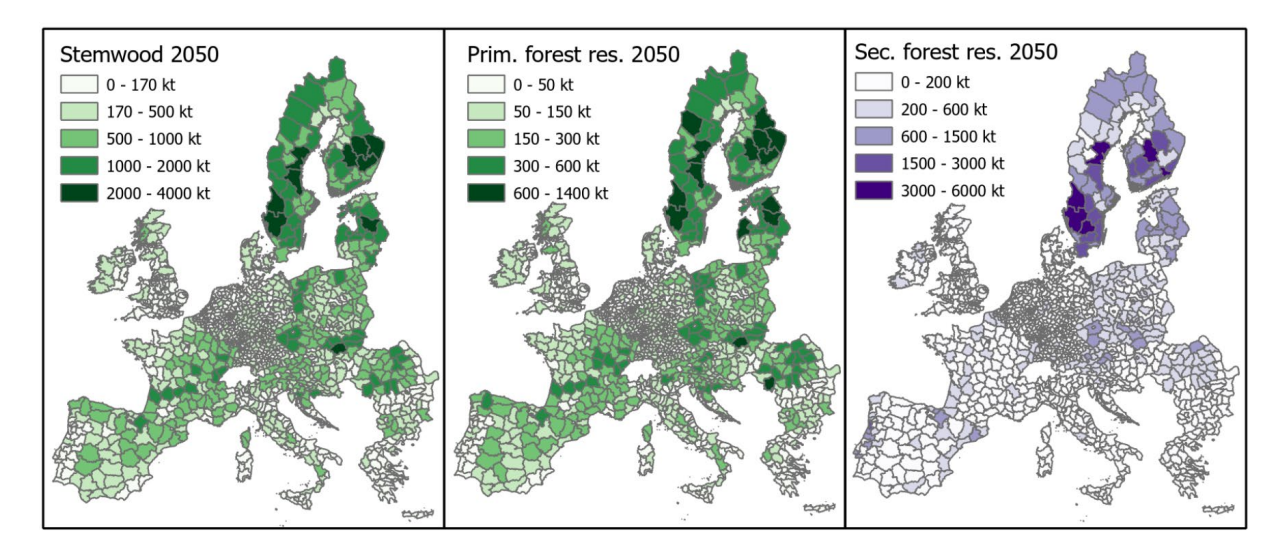
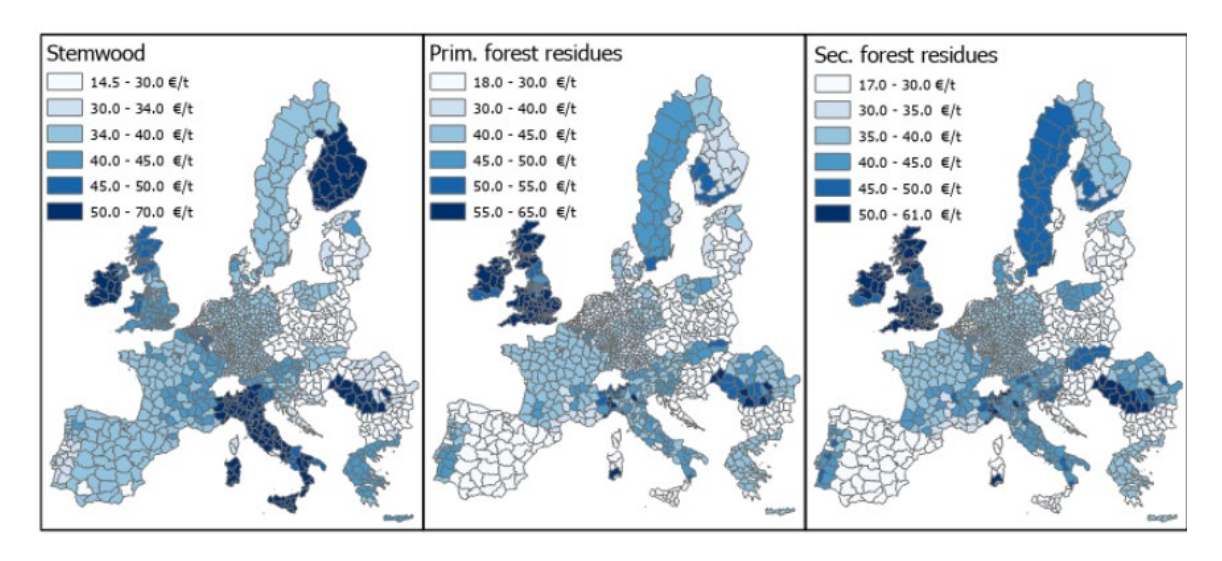




Figure 38 Roadside cost of stemwood, primary and secondary forestry residues in € per tonne dry material (€/t_{dry}). Costs are assumed to remain constant between 2030 and 2050.



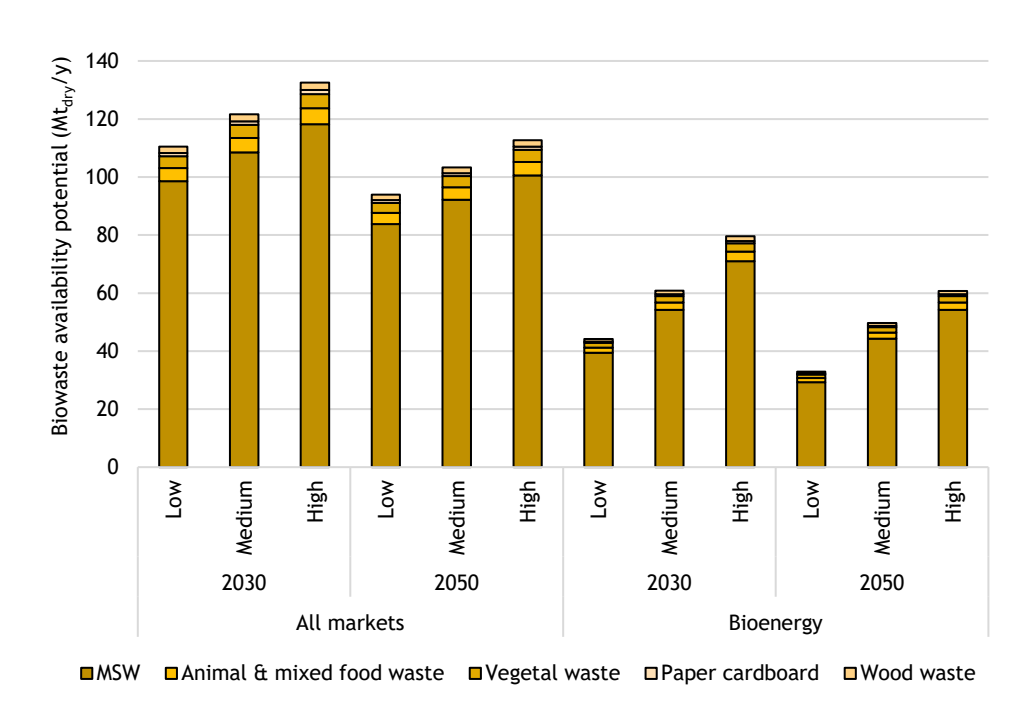
7.3. AVAILABILITY AND COSTS POTENTIAL OF BIOMASS WASTE

7.3.1. Availability potential of biomass waste

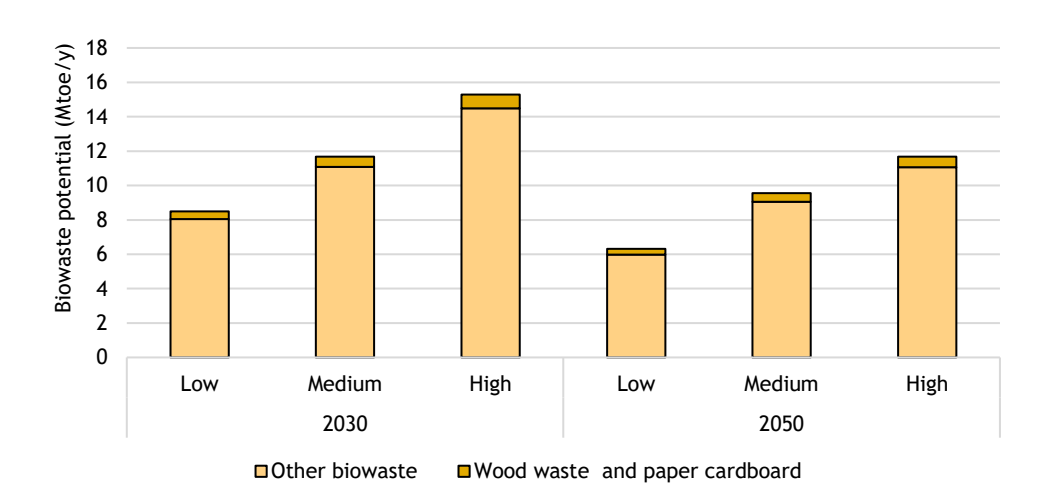
The availability potential of biowaste for all markets in the EU-27 plus UK ranges from 110 - 133 Mt (dry) by 2030, reducing to 94 - 113 Mt (dry) by 2050 due to waste reduction measures (increasing recycling) (Panoutsou & Maniatis, 2021). Biowaste available for bioenergy is estimated to be 44 to 80 Mt (dry) in 2030, which is projected to be reduced to 33 to 61 Mt (dry) by 2050. Almost 90% of the biowaste potential consists of MSW, which is excluded from advanced biofuel production in this study. The biowaste categories available to advanced biofuel production (wood waste and paper cardboard waste) add up between 1.3 - 2.4 Mt (0.4 - 0.6 Mtoe) by 2030 and between 1.0 - 1.8 Mt (0.3 - 0.6 Mtoe) by 2050 (Figure 39 and Figure 40). Advanced collection and separation systems could increase the availability potential of biowaste suitable for advanced biofuel production, but was beyond the scope of this study.



Figure 39 Availability potential of biowaste available for all markets in 2030 and 2050 in million tonnes dry (Mt_{dry}/y) in the different availability scenarios.



Availability potential of biowaste available for bioenergy in 2030 and 2050 in Mtoe/y for the different availability scenarios. Wood waste and paper cardboard waste is included in the supply chain model. Other waste (MSW, animal & mixed food waste, and vegetal waste) is assumed to be available for electricity/heat but not included in the model.

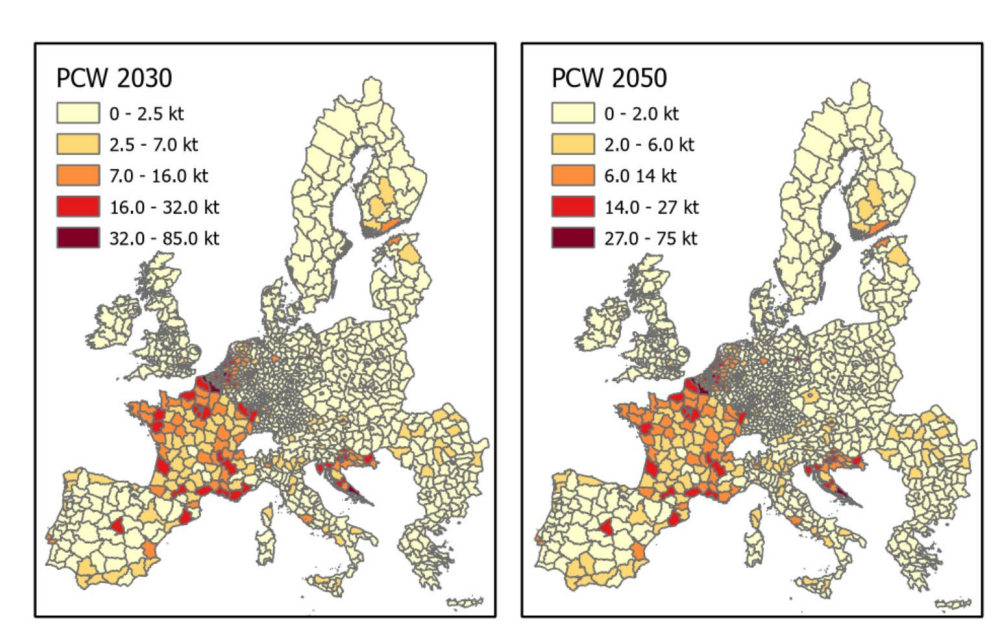




7.3.2. Mapping (spatially explicit results) of biomass availability potential

The availability potential of post-consumer wood and cardboard at NUTS-3 level in Figure 41 shows the challenge of these feedstock categories available in low quantities at geographically spread locations. Mapping is based on population density (see Section 3.4) rather than actual supply locations, but it is a good proxy for the distribution of biowaste categories. Biowaste is assumed to be available at the point of collection without cost.

Figure 41 Post-consumer wood waste and cardboard waste available for all markets at NUTS-3 level in 2030 and 2050.



7.4. BIOMASS FROM IMPORTS

7.4.1. Supply potential and price

Solid biomass import (wood pellets) potentials from outside the EU were taken from the ICL-Concawe study. No differentiation was made between the availability scenarios because the focus of this study is on domestic supply potentials. Furthermore, imported pellets are, in most cases, more expensive than domestic solid biomass supply in the EU and are therefore not fully utilized in the demand scenarios making a detailed distinction between the availability scenarios less relevant. In this study, we assumed a price of 8.0 €/GJ for both 2030 and 2050, available in European ports, based on the current CIF-ARA spot price of 150 US\$/t¹⁸ (Figure 43). Although spot prices of pellets are volatile as a result of market conditions, fuel prices, freight rates, and exchange rates, the assumed price is considered representative of an average cost-price plus profit margin (Fritsche et al., 2019).

66

¹⁸ Energy density wood pellets: 17.2 GJ/t, exchange rate: 0.92 €/US\$.



Figure 42 Solid biomass import potential to the EU-27 +UK 2020 - 2050 (Panoutsou & Maniatis, 2021).

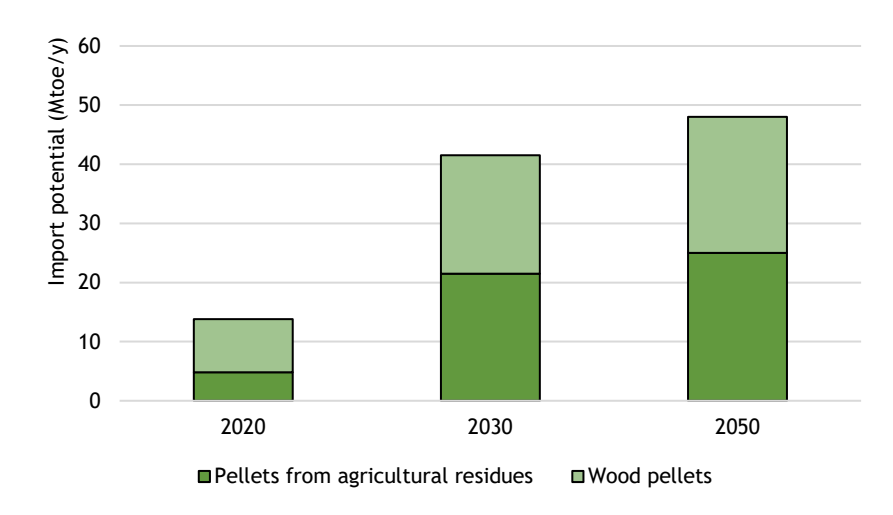
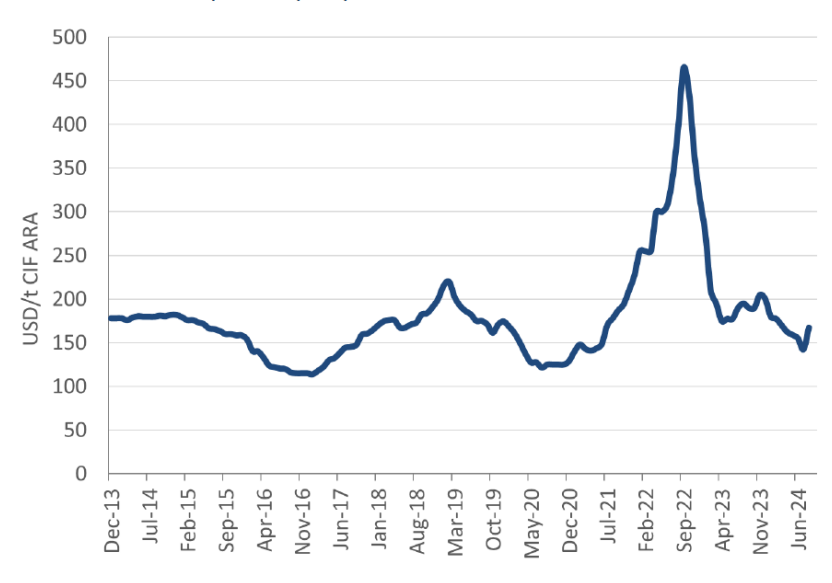


Figure 43 Development of industrial wood pellet spot prices between 2013 and 2024 (Gauthier, 2024).

Industrial wood pellet spot prices, USD/t CIF ARA



Source: Hawkins Wright

7.4.2. Mapping (spatially explicit results) of biomass import potential

Importing solid biomass from overseas requires dedicated infrastructure in terminals to handle wood chips or pellets. The distribution of imported solid biomass was based on the total freight throughput at the most important European ports. Pellets from these ports can be transported to any end-use location in the supply chain model using inland transport infrastructure.



14 ■2030 ■2050 Pellet import supply potential (Mtoe) 10 8 6 4 2 Port of Presentation of Managing Hause by Port of Roller days. A Dot of Artiner, the Livering Bedding Port of London, r. i.ed windsdom Andre of Infriedrate Integral Prized. A Port of Horote & Learning 0 Januar & Johnson & Spain or Jodge Agencia. .. air Pok of water sport take Port of Barcalora, Coan Ar ou trumbsdam, rutering by Dentary Ard Cabrish. Del Central Genoa hadd

Figure 44 Distribution of pellet imports in 2030 and 2050 over ports in the EU-27 plus UK.

7.5. TOTAL BIOMASS SUPPLY POTENTIAL

7.5.1. Total supply potential available to advanced biofuels and competing bioenergy demand

Figure 45 shows the combined availability potential of forest biomass, agricultural biomass, and biowaste for bioenergy in the Low, Medium, and High availability scenarios. The total domestic availability potential ranges from 213 to 314 Mtoe in 2030 and increases to 222 to 318 Mtoe by 2050 (Table 18). The feedstock categories in the supply chain model scope cover 61% to 74% of the total domestic potential, as black liquor, manure, secondary agricultural residues, oil crop residues, and municipal biowaste are outside of the scope of the supply chain modelling.

Black liquor could, in principle, also be used to produce advanced biofuels but is, similar to the DI Fuels study (EC, 2024), assumed to be used for electricity and heat generation. Also, wet organic residues and wastes, such as manure and many secondary agricultural residues, could be used to produce transport fuels, for example, biogas via anaerobic digestion. Finally, municipal solid waste, the largest biowaste category (Figure 40), was also excluded from advanced biofuel production. These systems and associated logistical challenges, including pre-processing, were beyond the scope of this study.

Imported wood and agri-pellets add 17% to 24% to the domestic feedstock potential but are relatively expensive compared to most domestic solid biomass sources.



Figure 45

Total domestic biomass availability potential for bioenergy in 2030 and 2050 for the different biomass availability scenarios in the EU-27 plus UK. The shaded columns are feedstock categories excluded from the supply chain model, with their availability values coming from the ICL-CONCAWE study.

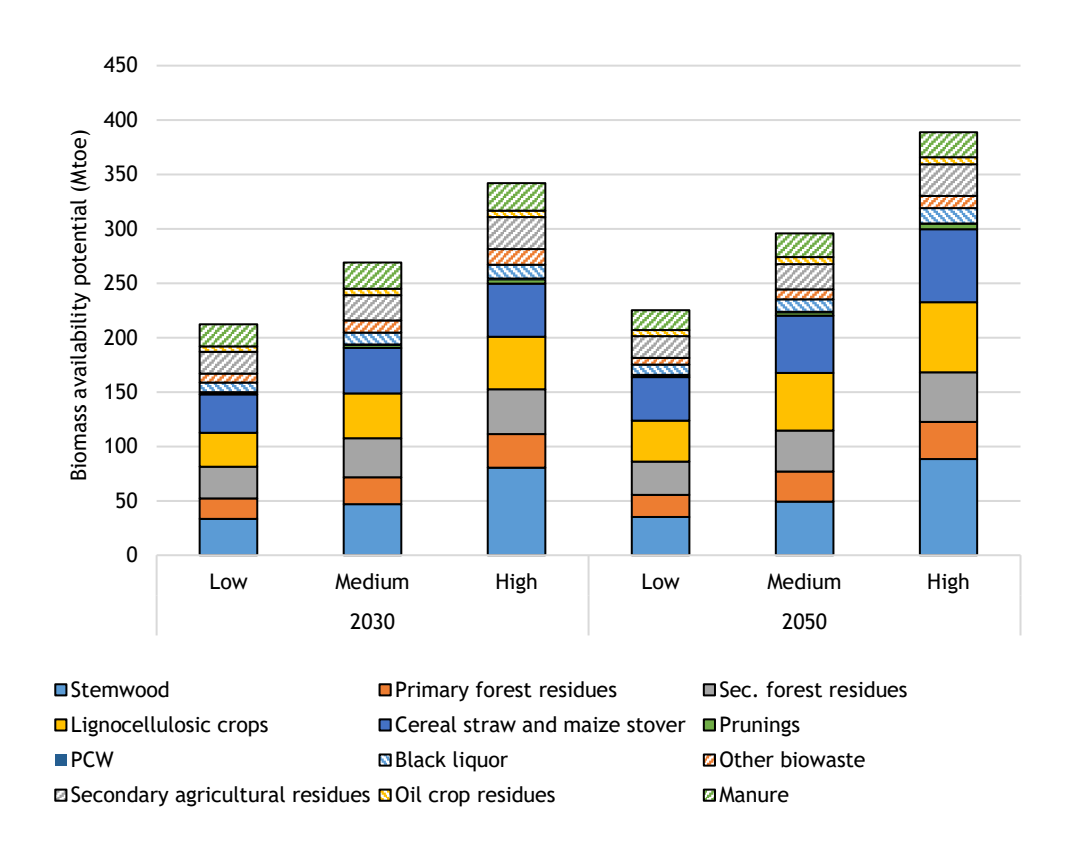


Table 18 Total biomass availability potential (Mtoe) for bioenergy in 2030 and 2050 in the different biomass availability scenarios.

Parameters		2030		2050			
	Low	Medium	High	Low	Medium	High	
Total domestic supply	212.2	269.1	342.0	225.1	295.9	388.7	
Domestic supply in the scope of this study	149.9	193.6	254.3	165.9	223.6	305.1	
Supply in model incl. pellet imports	191.4	235.1	295.8	213.9	271.6	353.1	

7.6. ROADSIDE COST-SUPPLY CURVES

Figure 46, and Figure 47 present the cost-supply curve for biomass, illustrating the relationship between the cost of cultivating or collecting biomass and the quantity that can be supplied at the roadside under the Medium availability scenario. These curves reflect the varying costs associated with the cultivation, harvesting, and collection of different biomass quantities, providing insight into how different feedstocks are prioritized economically as total biomass supply for EU-27 + UK increases.



Although forest residues are cheapest at some locations, agricultural residues are available in larger volumes at relatively low cost in both 2030 and 2050. In contrast, energy crops were calculated to be the most expensive feedstock in 2030, making them the lowest-priority option for mobilization when considering supply from a biomass cost perspective. When included in the supply, they cause a steep rise in overall supply costs. However, results for 2050 show that energy crops have the most significant potential for cost reduction, mainly resulting from yield increases (see section 7.1.4). By 2050, energy crops could reach similar cost levels as forest biomass. These cost-supply curves (transport costs not included in them), along with their geographical locations, serve as inputs to the supply chain model, which calculates the total cost of delivering biomass to biofuel plants, factoring in roadside costs as well as transport and handling expenses.

Figure 46 Domestic roadside cost-supply curve of feedstock categories available to advanced biofuel production and competing uses in the EU-27 plus UK. Medium availability scenario, 2030.

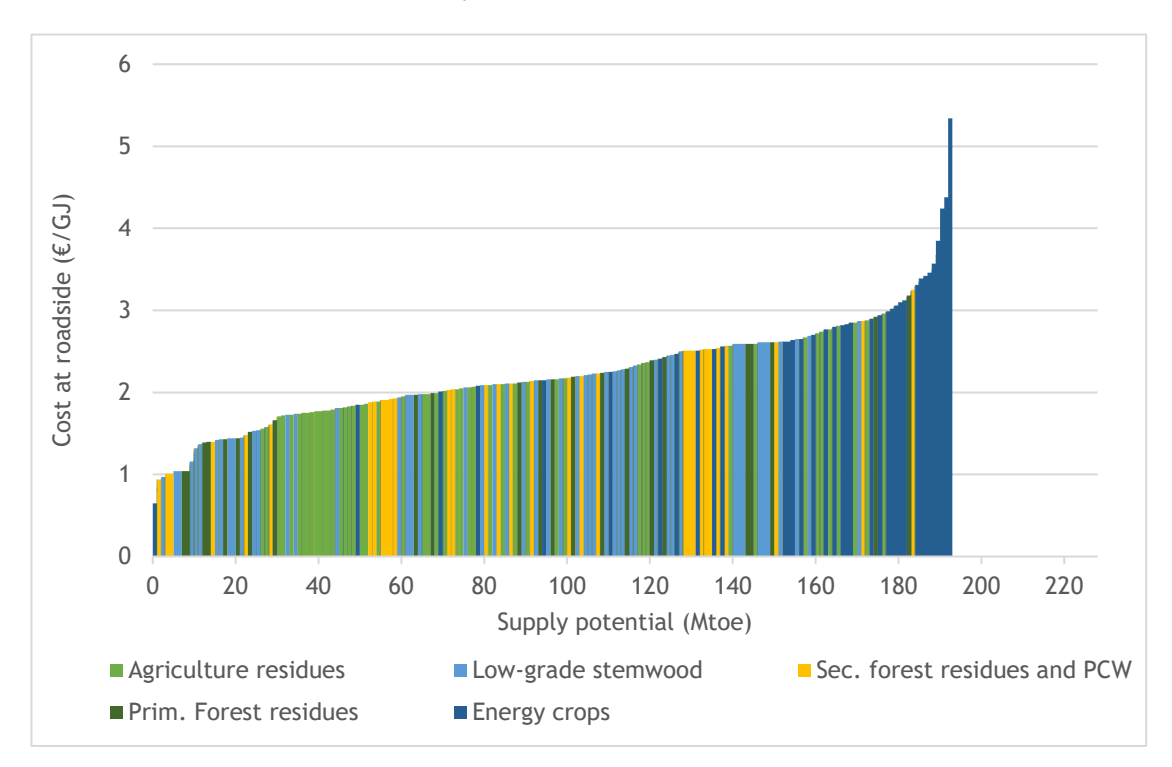
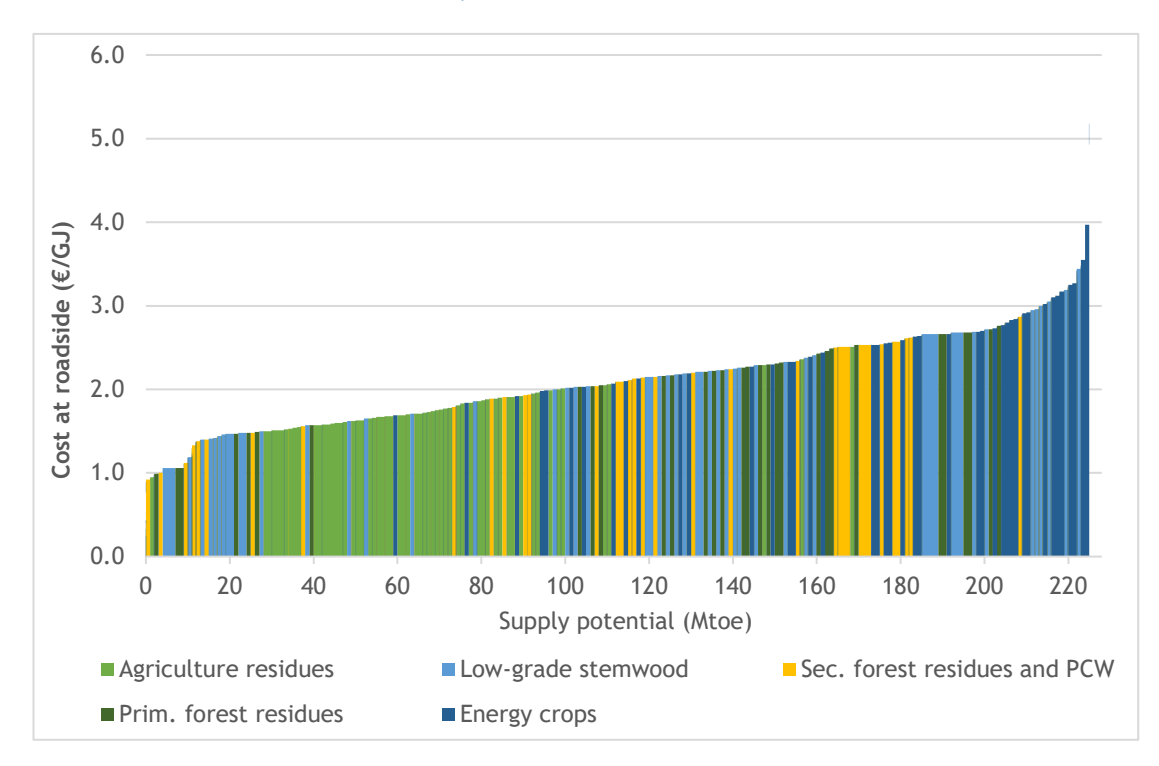




Figure 47 Domestic roadside cost-supply curve of feedstock categories available to advanced biofuel production and competing uses in the EU-27 plus UK. Medium availability scenario, 2050.





8. OVERVIEW OF THE BASE AND ALTERNATIVE SCENARIOS

The scenarios used in the supply chain model to calculate advanced biofuel deployment and costs are summarized in Table 19. The Base scenarios for 2050 explore variations in advanced biofuel demand based on DI Fuels (EC 2024) and the S&P (High-Demand) scenarios (see Section 6.1). The option to repurpose existing oil refinery hydroprocessing units to upgrade biofuels is evaluated in the 2050 Repurpose scenario. Alternative biomass availability scenarios (Low and High) evaluate the impact that biomass availability variations would have. The 2050 S&P High-Demand scenario is infeasible with Low biomass availability. Domestic Annex IX-A fuel demand and competing demand (E/H) are applied to the supply chain model.



Table 19 Overview of bioenergy supply and bioenergy demand, and main assumptions in the Base and Alternative scenarios.

Scenario name	Integration strategy ¹	Feedstock availability scenario	Total domestic availabilty ²	Biomass available in model ³	Annex IX A biofuel demand ⁴	Domestic IX A biofuel demand in model	Bioenergy demand (E/H) ⁶	Competing demand (E/H) in model ⁷
			[Mtoe biomass supply]	[Mtoe biomass supply]	[Mtoe biofuel demand]	[Mtoe biofuel demand]	[Mtoe biomass demand]	[Mtoe biomass demand]
Base scenarios								
2030	Default	Medium	269.1	193.6	19.3	18.3	107.3	70.4
2050 Low Demand (LD)	Default	Medium	295.9	223.6	37.6	33.8	185.0	126.1
2050 High Demand (HD)	Default	Medium	295.9	223.6	88.2	74.9	185.0	101.4
2050 Repurpose (RP)	Repurposing at refineries	Medium	295.9	223.6	37.6	33.8	185.0	126.1
Alternative biomass availabrelated scenarios	oility							
2030 (Low)	Default	Low	212.2	149.9	19.3	18.3	107.3	70.4
2030 (High)	Default	High	342.0	254.3	19.3	18.3	107.3	70.4
2050 LD (Low)	Default	Low	225.1	165.9	37.6	33.8	185.0	101.4
2050 LD ((High)	Default	High	388.7	305.1	37.6	33.8	185.0	126.1
2050 HD (High)	Default	High	388.7	305.1	88.2	79.3	185.0	101.4

¹⁾ Default: NUTS3: Greenfield, Intermodal terminal: Greenfield, pulp mill: co-location, biofuel plant: co-location, oil refinery: retrofitting. Repurposing at an oil refinery changes the integration strategy at oil refineries to repurposing. Integration at other locations remains similar to the default.

²⁾ Total domestic biomass available for bioenergy, including secondary agricultural residues and biomass wastes (e.g., municipal biowaste, black liquor)

³⁾ Total domestic biomass available for advanced biofuel production and competing demand for electricity and heat for the considered biofeedstocks in this study.

⁴⁾ Total Annex IX A biofuel demand, excl. biomethane. Based on DG-RTD (2023): for 2030 and low demand (37.6 Mtoe) scenario in 2050. Based on S&P and Concawe (2024): high demand (88.2 Mtoe) scenario in 2050.

⁵⁾ Total domestic Annex IX A biofuel demand (excl. biomethane) in the supply chain model, assuming 5% imports of liquid advanced biofuels in 2030 and 10% in 2050.

⁶⁾ Total biomass demand for electricity and heat generation. Based on DG-RTD (2023) FF55_RED (2030) and FF55_ESR (2050) scenarios. This number covers only lignocellulosic biomass. Non-lignocellulosic biofeedstocks, such as food crops, gaseous fuels, black liquor, and manure, are not in the scope of the study. Hence, their contribution according to the scenarios was not considered when accounting for E/H demand.

⁷⁾ Competing lignocellulosic biomass demand for electricity and heat generation in the supply chain model. Calculated from total biomass demand for electricity and heat generation, assuming that 8% (16.8 Mtoe) is covered by solid biomass imports in 2030, increasing to 10% (29.9 Mtoe) and 15% (44.8 Mtoe) by 2050 for the low demand and high advanced biofuel demand scenarios, respectively. In addition, it is assumed that the availability potential of lignocellulosic biofeedstocks not considered in the supply chain modelling (namely, secondary agricultural residues and municipal biowaste), is mobilized by 50% in 2030, increasing to 75% by 2050 (and 100% in the 2050 HD and 2050 LD (Low) scenarios) for E/H to reduce the pressure that transport biofuel demand would have by relying on the set of considered feedstocks (see also explanation in section 6.3).



9. RESULTS: ADVANCED BIOFUEL SUPPLY CHAINS

The biomass availability and demand scenarios developed for this study (outlined in Table 19) were run with the dedicated Mixed-Integer Linear Programming (MILP) supply chain optimization model. The objective was to determine the economically optimal biomass supply chain network across the EU-27 and the UK in both 2030 and 2050. It is important to emphasise that the results presented are not forecasts of how future biomass supply chains will necessarily evolve. Rather, they provide valuable insights into key structural trends, such as the potentially optimal locations for the development of advanced biofuel production hubs, the range and breakdown of biomass-to-advanced biofuel costs and the cumulative build-up of costs required for domestic production to meet future demand and the supply configurations required to achieve system-wide efficiency. To support this analysis, the following figures have been developed and are presented in the subsequent sections:

- Cost-supply curve: Illustrating how upstream costs (biomass production and transport) accumulate as biomass is increasingly mobilised to meet target demand levels
- **Technology mix:** A summary of the biorefining conversion technologies selected as optimal under each scenario
- **Cost breakdown per pathway:** Highlighting the major economic components within each biomass-to-biofuel pathway and supply chain configuration
- Map of advanced biofuel production sites across EU-27 + UK: Showing the spatial distribution of facilities, calculated as optimal by the model
- **Technology scale deployment per country:** Bar charts showing what conversion technologies and at what scale are employed at country level
- Mobilisation per feedstock: Bar charts showing the amounts of biomass mobilised, separately for each feedstock
- Trade flow charts: Country-level bar charts and maps detailing imports and exports of raw biomass, biocrude, and drop-in advanced biofuels

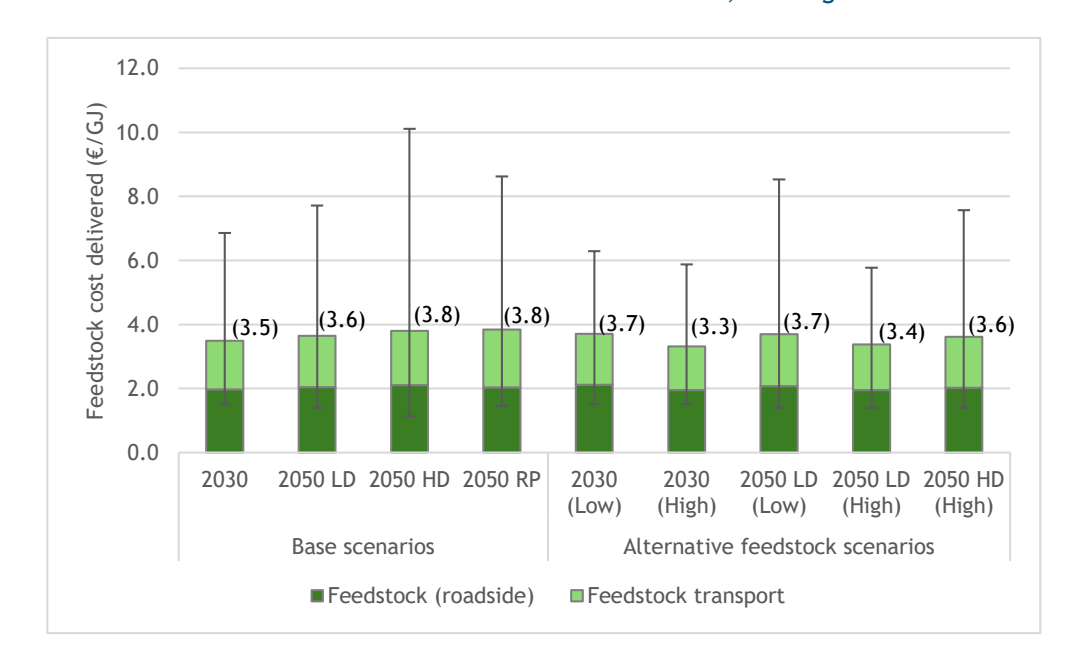
9.1. COST-SUPPLY CURVES

This section presents the weighted average cost of feedstock delivered to biomass conversion to biocrude/biofuel plants. Afterward, the detailed cost-supply curves for the delivered feedstock cost at the biorefinery gate, as a function of cumulative biomass mobilisation under different demand and availability scenarios for the years 2030 and 2050 offer insight into how upstream costs (biomass roadside plus transport costs) evolve with increasing biomass use across EU-27 + UK and highlight the critical thresholds shaping efficient bioenergy deployment.

Figure 48 shows that both the feedstock cost at the roadside and the biomass feedstock transport costs are important cost components of the total feedstock cost delivered. Transport costs contribute on average 43% to 47% to the total feedstock cost delivered to biocrude/biofuel plants in the scenarios. The variability across scenarios shows that when biofuel demand is high (e.g., 2050 HD) or biomass availability is limited (Low alternative scenarios), the system must rely on more expensive or harder-to-access feedstocks. However, because most biomass is still available at lower costs, the overall effect on the average system cost remains relatively small.



Figure 48 Weighted average feedstock cost delivered to biocrude/biofuel plants in the Base and Alternative feedstock scenarios in the EU-27 + UK (in €/GJ biomass delivered). The error bars show the ranges between the minimum and maximum cost of feedstock delivered. LD: Low Demand, HD: High Demand.



Biomass supply in 2030

Figure 49 presents the cost-supply curves for 2030 under the three biomass availability scenarios, Low, Medium, and High, covering the total demand for advanced biofuels. Geographic factors, particularly the location of biomass sources and demand centres, are the primary determinants of upstream costs. The analysis reveals that supply costs to biorefineries remain relatively stable up to a certain threshold and beyond this threshold, the curve becomes significantly steeper, indicating:

- Low-cost, easily accessible biomass sources become exhausted, and
- The system must increasingly rely on higher-cost or logistically complex feedstocks, such as biomass from peripheral or fragmented regions and/or feedstocks requiring long-distance transport, and multimodal logistics

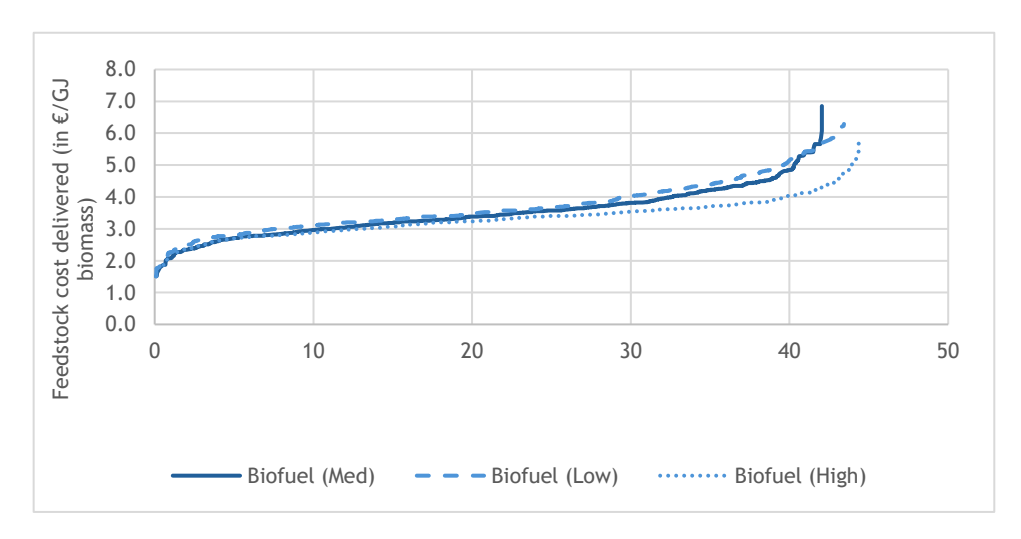
For example, in the cost-supply curve for advanced biofuels, the threshold at which supply costs begin to rise significantly occurs at approximately 35 Mtoe of cumulative biomass mobilisation. However, it is important to highlight that this study concentrates on optimising supply costs, and the results may therefore differ from how biomass and biofuel markets could actually evolve, including potential changes in market pricing dynamics, which lie beyond the scope of a cost-focused analysis. In competitive markets, commodity prices, biomass in this case, could rise considerably if there is competition for the same resource and end-use sectors have sufficient purchasing power to secure supplies by offering biomass producers the highest possible profits.

When transitioning between biomass availability scenarios, only modest shifts in the cost-supply curve are observed, both in terms of the threshold point and the associated supply costs. For instance, when moving from the Medium to High biomass availability scenario, the threshold shifts from approximately 35 Mtoe to



40 Mtoe for the advanced biofuels curve. This reflects the improved ability to distribute biomass more widely across Europe, as there is a higher likelihood of sourcing and transporting feedstock in a more economically efficient manner.

Figure 49 Cost-supply curve of delivered feedstock (biomass roadside + transport costs) to meet the demand for advanced transport biofuels in the EU-27 + UK by 2030. Results are shown for the three biomass availability scenarios: Low, Medium (Med), and High.



Biomass supply in 2050

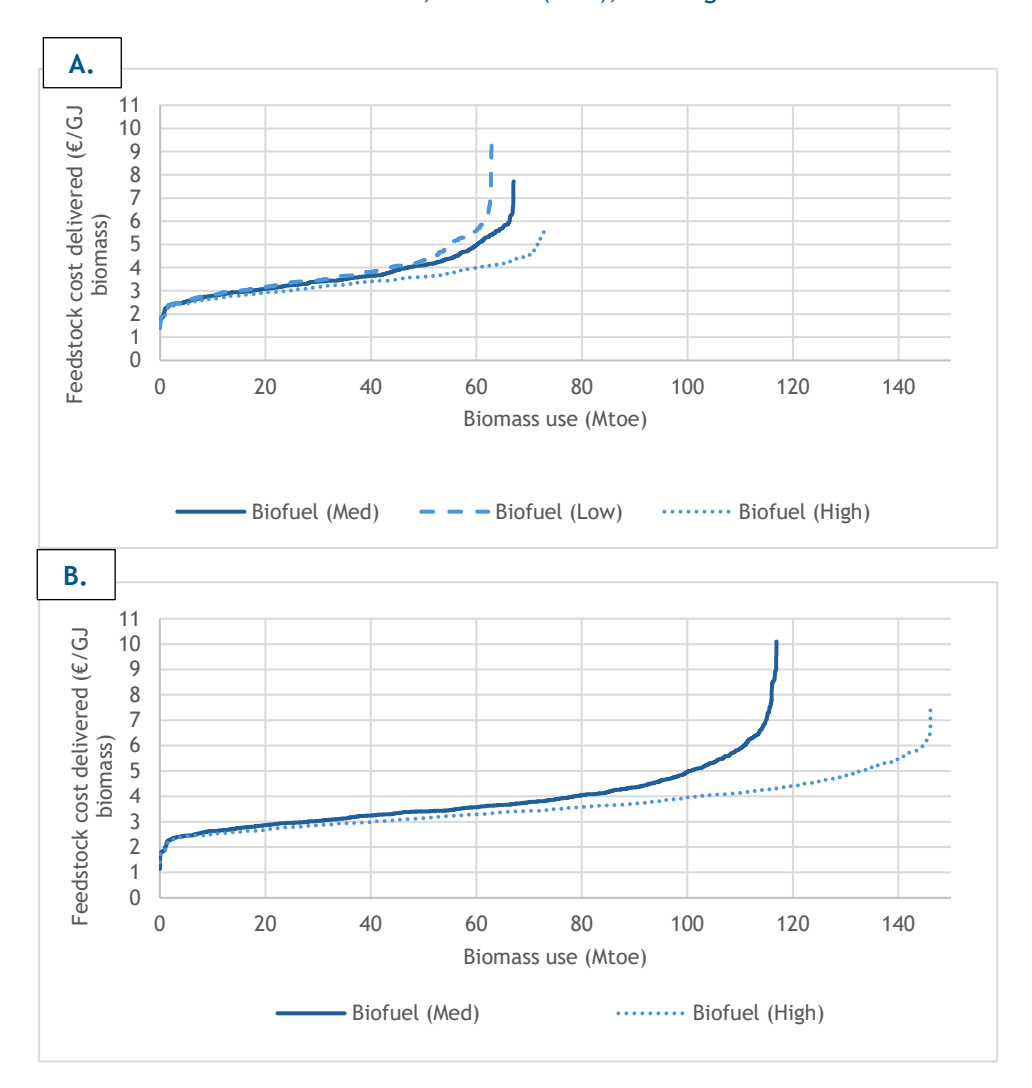
The cost-supply curves for the Low and High biofuel demand scenarios in 2050 are presented in Figure 50. While the overall trends remain consistent with those observed in 2030, there are notable changes in both the total supply costs and the threshold points at which costs begin to rise more steeply. For the Medium biomass availability scenario, the threshold point for advanced biofuels shifts is approximately at: 50 Mtoe in the Low demand scenario and 90 Mtoe in the High demand scenario.

Increased biofuel demand leads to a rightward shift in the inelastic, or capacity-constrained, segment of the supply curve. This shift is predominantly a consequence of greater investments in decentralized biofuel production infrastructure, thereby facilitating access to a wider range of local biomass. Notably, the High advanced biofuel demand scenario sees 80% of biofuels produced in decentralized facilities, contrasting with 34% in the Low advanced biofuel demand scenario. This upward shift for the threshold, along with the generally lower supply costs within the same biomass mobilisation range compared to 2030, reflects the increase in available biomass across Europe by 2050. Enhanced availability improves the system's ability to source and transport biomass more efficiently, thereby delaying the onset of more expensive feedstock mobilisation and reducing the average cost per unit of delivered biomass.



Figure 50

Cost-supply curves of delivered feedstock (biomass roadside + transport costs) to meet the demand for advanced transport biofuels in the EU-27 + UK by 2050 for: A. Low advanced biofuel demand (37.6 Mtoe), B. High advanced biofuel demand (88.2 Mtoe). Results are shown for the three biomass availability scenarios: Low, Medium (Med), and High.



9.2. BIOREFINING TECHNOLOGY MIX AND ADVANCED BIOFUEL PRODUCTION COSTS

9.2.1. Conversion technologies selection

The calculated optimal capacity distribution of Gasification and Fischer-Tropsch (GFT) and Hydrothermal Liquefaction (HTL) plants across the EU is shown in Figure 51 for both the 2030 and 2050 Base scenarios. The error bars indicate the variability in technology allocation resulting from the Alternative Scenarios, which account for different biomass availability assumptions (i.e. the Low and High availability cases). Figure 52 shows the number of biocrude and biofuel plants per technology/supply chain configuration that need to be built across Europe to achieve the calculated processing capacities. More detailed bar charts showing the results separately for each biomass availability-biofuel demand scenario are given in Annex F1.



Technology mix in 2030

Base Scenarios:

For the Base scenario, the modelling results indicate a balanced mix between centralised GFT facilities, typically integrated with existing refineries, and decentralised (ds) HTL systems located near biomass sources. In total, 72 plants are selected, broken down as follows: 25 GFT at oil refineries, 2 HTL (cs) at biofuel plants, 39 biocrude producing HTL (ds) at pulp mills or biofuel plants, and 6 upgrading units at refineries. However, as shown in the following section, the average cost difference between centralised GFT and HTL is below 10%, which makes technology selection highly sensitive to geographic context and infrastructure availability. Given that GFT currently has a higher TRL than HTL, it could potentially be the more readily deployable and preferred option in the near term. Hence, while no definitive conclusion can be drawn on the preference between centralised GFT and HTL, since small changes in input assumptions could tip the balance, the differentiation between centralised (GFT or HTL) and decentralised HTL remains robust. This distinction is primarily driven by geographic factors and the spatial distribution of biofuel demand across Europe.

While the assumed GFT process is a little less costly, its deployment is constrained by feedstock accessibility in some cases. Some high-demand countries, such as the Netherlands, lack sufficient domestic biomass resources, limiting the feasibility of localised GFT plants. As a result, these countries depend on biomass or biocrude intermediates imported from other regions. These factors drive the selection of decentralised HTL systems in biomass-rich countries (Scandinavia and Iberian Peninsula), where feedstock is converted into biocrude near the source. The biocrude is then transported over long distances to refineries located in high-demand regions for final upgrading to drop-in biofuels. This highlights the interconnected and transnational nature of the EU biofuel supply chain, where cross-border trade flows are critical for optimising system efficiency.

Alternative Scenarios:

Under Alternative scenarios for 2030 (Low and High biomass availability), small changes in technology allocation are observed. The model still selects a balanced combination of GFT and decentralised HTL systems as the optimal supply chain configuration. This consistency arises from the fact that, even under the Low availability scenario, biomass availability remains sufficient relative to demand, resulting in no major differences in plant siting or technology choice.

Technology mix in 2050

Base Scenarios:

In 2050, the composition of the optimal technology mix changes significantly depending on the demand scenario. For the Low demand Base scenario, the modelling results show a strong preference for GFT pathways (66% of the total advanced biofuel production capacity), particularly those integrated into oil refineries. This preference is driven by the substantially lower total process costs associated with GFT in 2050: up to 35% lower than decentralised HTL (ds) systems. The cost advantage is largely due to greater CAPEX reductions applied to GFT between 2030 and 2050, reflecting the benefits of technological learning for this capital-intensive pathway. In addition, the role of GFT expands beyond refineries and is applied at terminals, pulp mills, and biofuel plants, despite the higher process costs associated with these locations. These non-refinery sites are generally closer



to biomass resources, helping to reduce feedstock logistics costs and improve overall system efficiency.

In parallel, HTL decentralised systems continue to play a significant role, though they represent a smaller share of total capacity (34% for the Low-demand case) compared to 2030. These systems are primarily co-located in biofuel/pulp-mill plants which are close to biomass-rich areas. The geographic focus for HTL (ds) remains on Iberian Peninsula and Scandinavia, where biomass availability is high and biocrude can be efficiently exported to fuel upgrading hubs in Western Europe.

In the Repurpose scenario, evaluated under the Low-demand case, where repurposing hydroprocessing units in refineries is assumed feasible, the model shows a further preference for centralised GFT plants over decentralised HTL systems. This outcome is driven by the fact GFT is more efficient from a process cost perspective. However, the high transport costs associated with centralised GFT plants limit their wider deployment across Europe. Through repurposing, GFT regains some advantage, as the lower CAPEX for hydrocrackers can partially offset the increased transport costs. However, it is important to note that, unlike hydrotreaters, which are standard equipment found in all refineries, hydrocrackers are not universally present across the refining fleet but such site-specific considerations were not part of the scope of this study.

However, as moving from the Low to the High-demand Base scenario, the structure of the optimal supply chain network changes significantly. Transitioning from one demand scenario to another has a large impact on technology selection, plant siting, and intra-EU trade dynamics.

In the High demand scenario, the model identifies decentralised HTL as the dominant pathway, accounting for over 80% of total capacity: 197 biocrude-producing HTL decentralised plants followed by 38 upgrading plants. In contrast, GFT becomes a less favoured option (12 plants in total). This shift underscores that the efficiency of a centralised versus decentralised configuration is highly dependent on the scale of biofuel demand, which in turn determines how to best exploit the biomass resources in Europe.

The preference for HTL under high demand conditions is driven by two main factors:

- 1. Higher yields of HTL compared to GFT, which become critical when attempting to maximise output from limited feedstock.
- 2. The decentralised configuration enables the full utilisation of dispersed biomass resources across the EU, avoiding bottlenecks and inefficiencies associated with long-distance transport of solid biomass to centralised facilities.

Without this decentralised strategy, the alternatives would involve: Long-distance transport of solid biomass across the EU, or increased reliance on biofuel imports from outside the EU. Both alternatives are more expensive and less efficient than the decentralised system selected by the model. In essence, decentralisation allows for greater flexibility, accommodating fragmented feedstock availability while keeping logistics and system costs under control.

Repurposing was not modelled for the High demand scenario, but it can be qualitatively concluded that enabling repurposing would not significantly alter the strong preference for decentralised HTL systems. In the Low demand case, enabling repurposing resulted in a 13% increase in the share of GFT systems. However, a



smaller increase is anticipated under high-demand conditions, due to greater transport distances and the associated cost penalties linked to deploying additional centralised GFT plants, which cannot be offset by potential repurposing benefits. Furthermore, shifting towards a larger number of GFT plants, which have lower biofuel yields compared to HTL, would increase biomass supply requirements beyond the modelled available EU domestic resources. This would necessitate reliance on costly pellet imports from outside the EU, which is not an economically favourable solution.

Alternative Scenarios:

Just as changes in demand significantly reshape the supply chain network, similar effects are observed when biomass availability varies. A critical driver in both cases is the biomass availability-to-biomass demand ratio, which determines how stretched or constrained the system becomes.

When the availability/demand ratio is high (applies to the Low demand - High availability Alternative scenario, ratio = 1.9), the supply chain begins to resemble the Low-demand Base scenario described earlier. Under these conditions, the system has flexibility to optimise logistics, and the model tends to favour centralised configurations, particularly GFT integrated with existing refineries. Centralisation becomes cost-effective due to more available feedstock and opportunities for economies of scale. Conversely, as the availability/demand ratio declines (applies to the Low demand - Low availability Alternative scenario, ratio ≈ 1.0), the system starts to mirror the High-demand Base scenario, where resource constraints necessitate greater distribution of processing capacity. In this context, the model shifts towards decentralised configurations, such as HTL (ds), which allow for the maximum utilisation of locally available biomass and reduce dependence on long-distance transport of solids or on imports.



Advanced biofuel/biocrude production per plant type (in Mtoe/y) in the Base scenarios for 2030 and 2050. The error bars show the ranges of the Alternative biomass availability scenarios (Low, High). LD: Low-Demand, HD: High-Demand, RP: Repurpose.

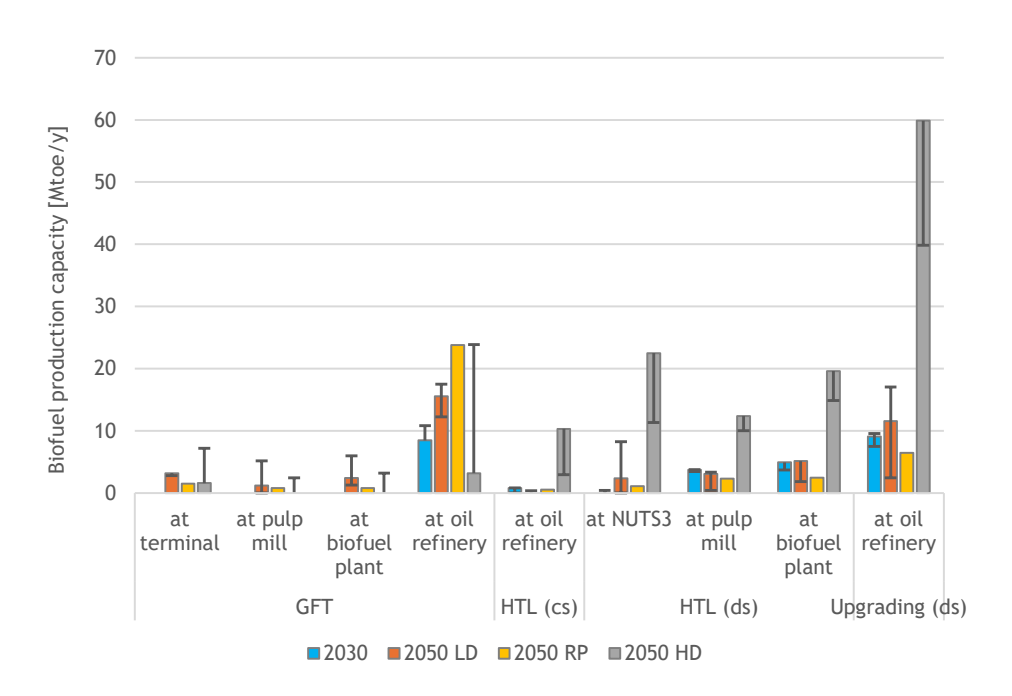
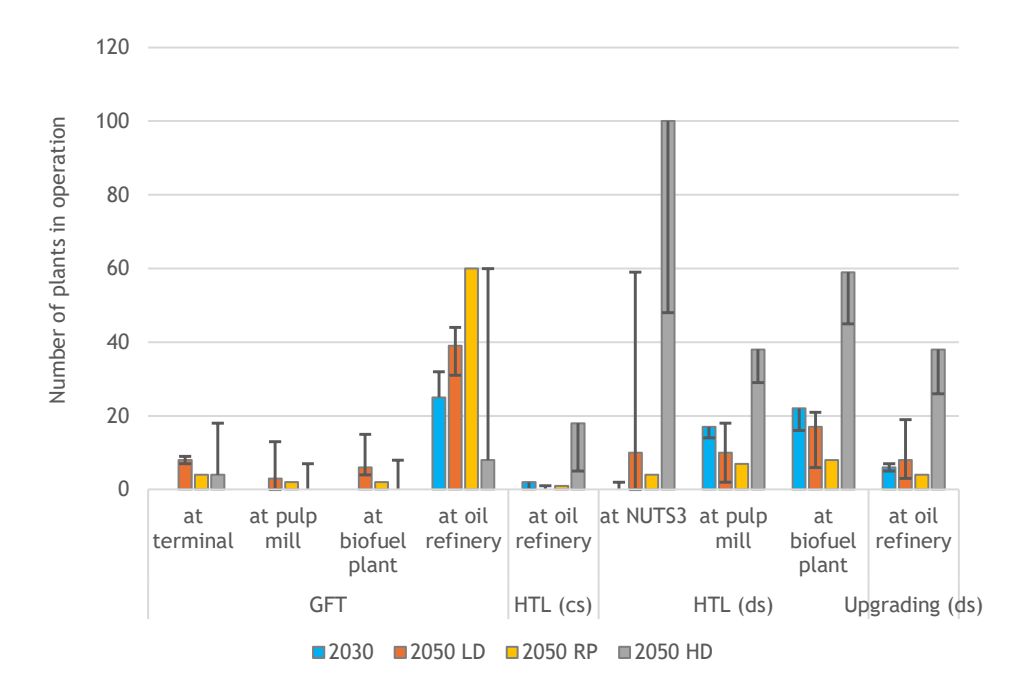


Figure 52 Number of biocrude (HTL (ds)) and advanced biofuel plants (GFT, HTL (cs), Upgrading) in the Base scenarios for 2030 and 2050. The error bars show the ranges of the Alternative biomass availability scenarios (Low, High).





9.2.2. Advanced biofuel production costs

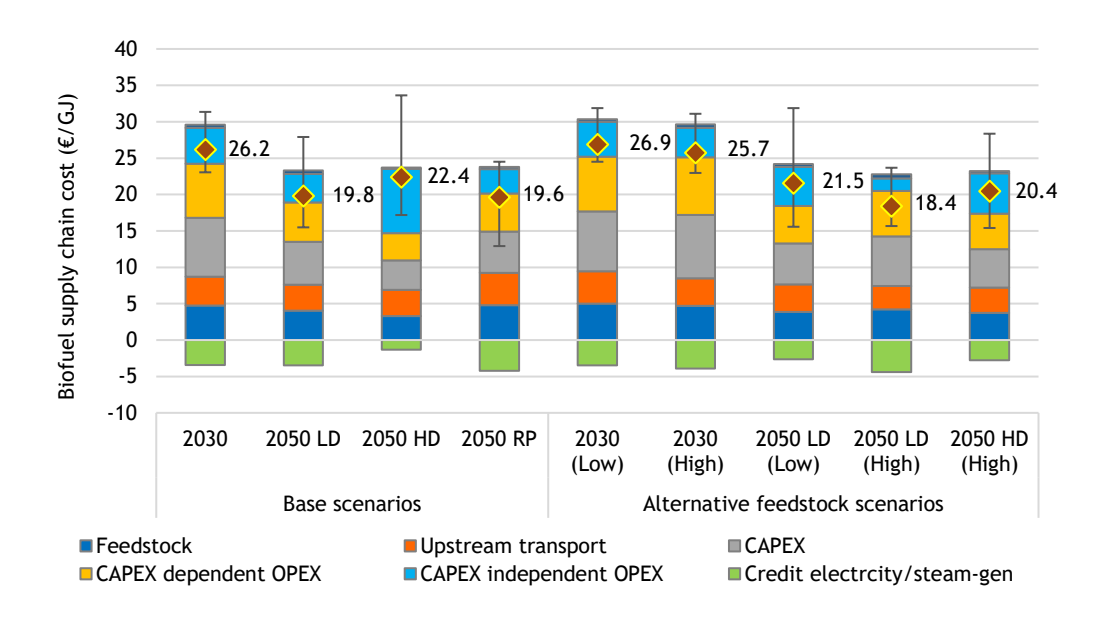
Average costs per scenario:

The average advanced biofuel production costs per modelled scenario are presented in Figure 53. For the year 2030, cost variation across the Low, Medium, and High biomass availability scenarios is moderate, with the deviation between the lowest and highest values being ~25 %. For the Medium availability scenario, the average biofuel production cost (including all pathways) is estimated at 26.2 €/GJ_{biofuel}.

By 2050, biofuel production costs decrease across all scenarios, primarily driven by technological learning and the resulting CAPEX reductions for both GFT and HTL technologies. Among the Base scenarios, the least expensive production cost is observed in the Repurpose scenario, where existing hydroprocessing units are repurposed to process biofuels, lowering capital investment costs. This is followed by the Low demand scenario. These findings reinforce the key trend explained before: the higher the ratio of biomass availability to biomass demand, the greater the system's flexibility in sourcing cheaper biomass, and selecting the least expensive conversion pathway, typically centralised GFT where economies of scale and integration benefits can be realised. In contrast, scenarios with tighter biomass constraints force the system toward decentralised configurations and more complex logistics, increasing the overall cost per unit of biofuel.

At this point, it should be noted that the calculated process costs are consistent with the values reported in the scientific literature. However, in industrial practice, total project costs are typically higher due to the early commercialisation stage of these technologies and additional factors such as site infrastructure, owner's costs, and financing during construction. Therefore, the results are presented on a comparative basis to assess the impact of different scenarios on supply chain costs and drivers rather than as an absolute cost assessment.

Figure 53 Average biofuel production cost in the Base and Alternative scenarios. The error bars show the ranges between the minimum and maximum biofuel production costs calculated in the scenarios.





Cost ranges per pathway:

Figure 54 and Figure 55 present boxplots illustrating the cost ranges per scenario and technology, highlighting the variability that emerges under different demand and supply conditions.

For both Gasification and Fischer-Tropsch (GFT) and Hydrothermal Liquefaction (HTL) pathways, cost variability becomes more pronounced in 2050 compared to 2030. This is primarily a result of the increasingly stretched supply chain due to the larger biofuel demand, which requires sourcing biomass from a broader range of locations.

In the case of GFT, the scenario showing the widest cost range is the 2050 Repurpose (RP) case. As detailed in earlier sections, the capital cost advantages associated with repurposing existing hydroprocessing units strongly favour GFT over HTL in this scenario, leading to an increased reliance on GFT which accounts for approximately 80% of the total conversion capacity. This broad deployment naturally introduces greater cost variability across the system.

For HTL, cost ranges are even more pronounced, particularly under the high biofuel demand scenarios in 2050, where differences between the least costly and most expensive supply chains can exceed $10~\rm C/GJ_{biofuel}$. As discussed, the high demand pressures in 2050 necessitate the mobilisation of biomass from remote or fragmented sources, making decentralised HTL systems the preferred configuration for cost-effective processing. However, while decentralised HTL can offer certain benefits under these high-demand conditions, this does not mean it comes without additional cost burdens.

Figure 54 Median, quartiles, and minimum/maximum ranges in supply chain cost of GFT in the Base and Alternative feedstock scenarios.

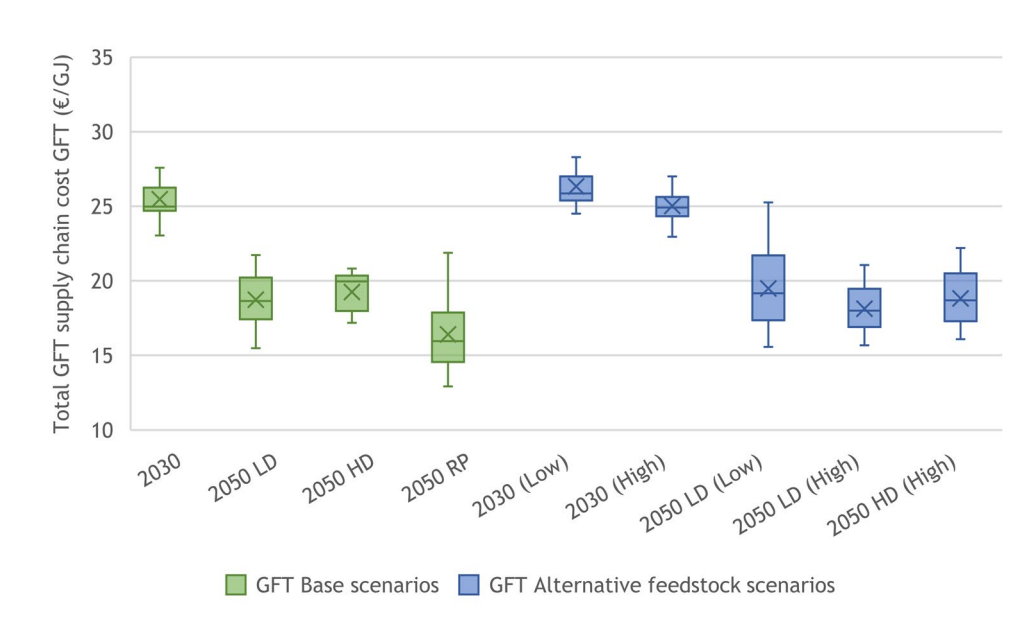
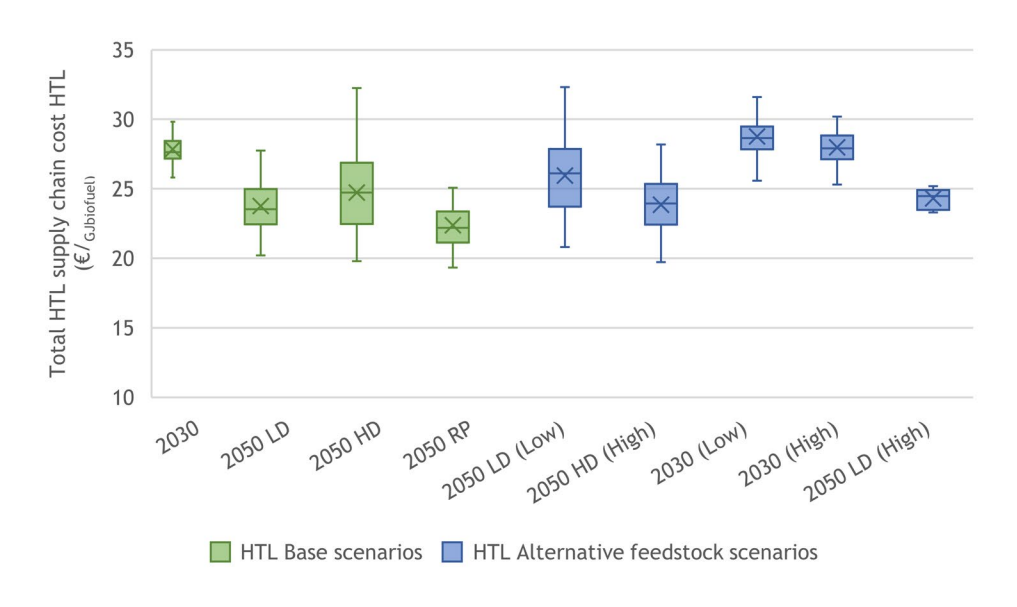




Figure 55 Median, quartiles, and minimum/maximum ranges in supply chain cost of centralized and distributed HTL in the Base and Alternative feedstock scenarios.



Cost drivers per pathway:

Figure 56 and Figure 57 present the supply chain cost ranges for the Base and Alternative feedstock scenarios. The detailed cost structures of each pathway are provided in Annex F3.

From a cost perspective, Gasification and Fischer-Tropsch (GFT) is a capital-intensive pathway, with the CAPEX of GFT accounting for the largest cost component in the selected GFT pathways. However, integration with existing industrial facilities, particularly oil refineries, offers substantial cost savings through retrofitting and shared infrastructure. In this study, refinery integration for GFT emerges as the most cost-effective option, yielding an average biofuel production cost of 25.2 $\mbox{\ensuremath{\mathsf{C}}/GJ_{biofuel}}$ in 2030 and 18.1 $\mbox{\ensuremath{\mathsf{C}}/GJ_{biofuel}}$ in 2050. A key insight is that due to the capital intensity and strong economies of scale, all GFT plants selected by the model operate at their maximum capacity (biofuel output ≈ 400 ktoe/y in 2050¹), highlighting the importance of scale maximization within the technological limits in reducing unit costs.

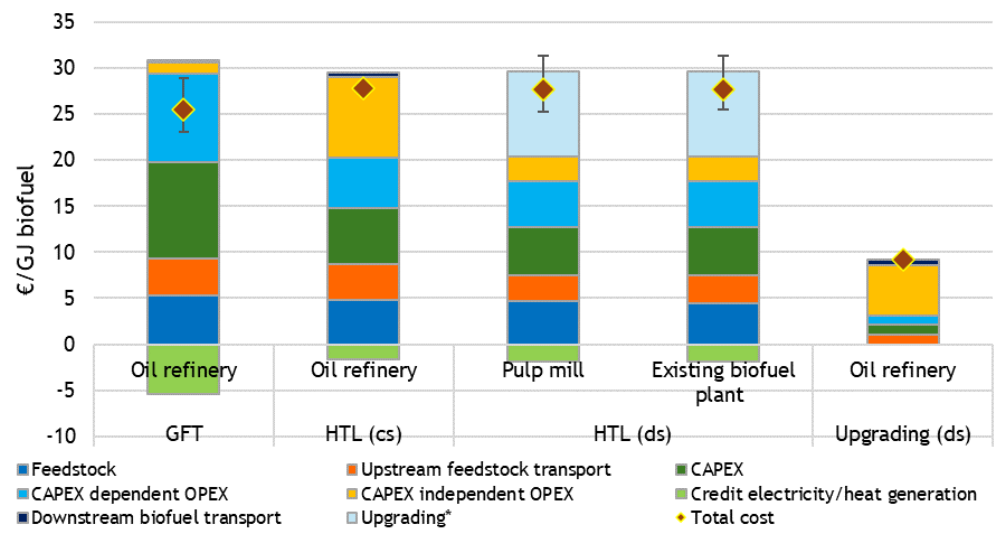
In contrast, hydrothermal liquefaction (HTL) is an OPEX-dominated technology. However, HTL benefits from its higher biofuel yields than GFT, enhancing its competitiveness in cases with high biomass delivery costs. The model reveals no significant cost difference between siting HTL units within dedicated biofuel plants or pulp mills and site selection is driven by biomass proximity. It is also worth noting that for 2030 a few centralized HTL plants are selected. Nonetheless, the relatively small cost gap between centralised GFT and HTL in 2030 suggests that in real-world engineering practice, long-term deployment will likely be shaped more by technological maturity than by marginal cost differences.

¹ Maximum capacity was set according to Huang et al. 2019, taking a maximum feedstock input of 2 Mt_{dry}/y.



While conversion process costs dominate both pathways, feedstock supply and transport remain significant cost components. For instance, in the refinery-integrated GFT scenario, feedstock production contributes 5.2 $\[\in \]$ / GJ_{biofuel} in 2030 and 4.6 $\[\in \]$ / GJ_{biofuel} in 2050, while its transport adds 4.1 $\[\in \]$ / GJ_{biofuel} in 2030 and 3.9 $\[\in \]$ / GJ_{biofuel} in 2050.

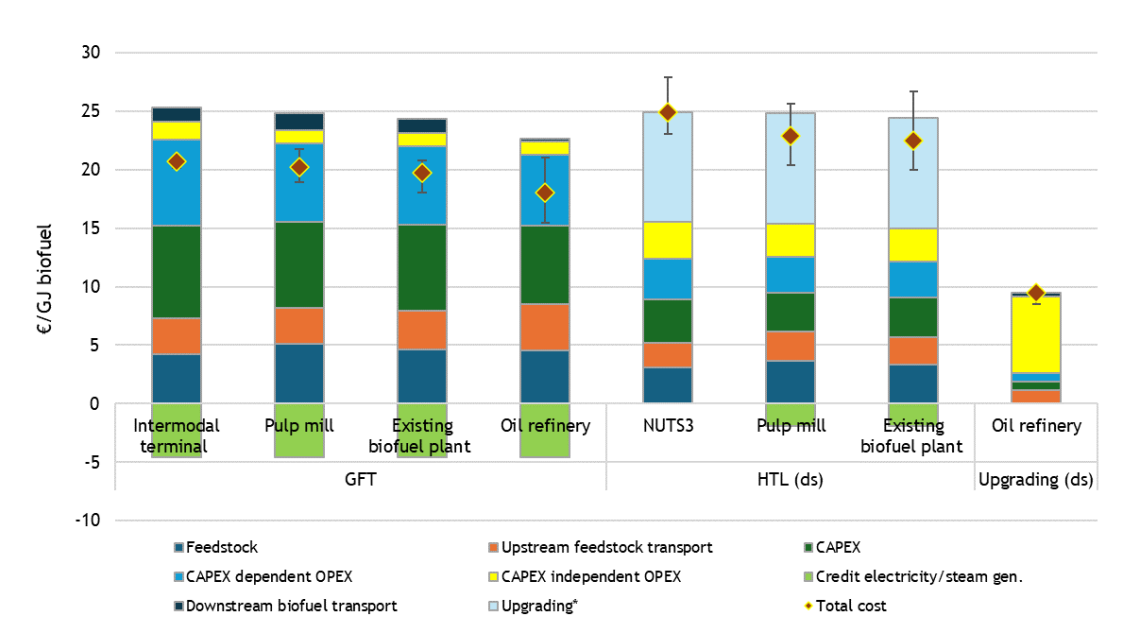
Figure 56 Breakdown of each pathway costs into the different components and average biofuel production cost per pathway/configuration. Base scenario, 2030.



^{*)} Average distributed upgrading and downstream fuel transport cost

Figure 57

Breakdown of each pathway costs into the different components and average biofuel production cost per pathway/configuration. Low-demand Base scenario, 2050.



 $^{^{\}ast})$ Average distributed upgrading and downstream fuel transport cost



9.3. GEOGRAPHICAL DISTRIBUTION OF BIOREFINERIES

In this section, the geographical distribution of the optimal conversion technology mix calculated by the supply chain model will be presented for the Base scenarios in 2030 and 2050. The results for the other Alternative scenarios are included in Annex F4 as reference.

Distribution in 2030 (Base scenario):

For 2030, the spatial distribution of the aforementioned biorefining technologies and configurations is presented in Figure 58 and Figure 59. In total, 72 plants are calculated, split as follows: 25 GFT at oil refineries, 41 HTL biocrude producing units at biofuel plants or pulp mills and 6 upgrading units hosted at existing refineries, hydroprocessing biocrude to drop-in fuel.

As previously explained, countries with limited domestic biomass resources but high biofuel demand and developed refining and port infrastructure, such as the Netherlands and the UK, rely on the import of biocrude via maritime transport. In contrast, countries like Finland, Sweden, endowed with high biomass availability but relatively small biofuel demand, host many decentralised HTL plants. These facilities convert local biofeedstocks into biocrude (primarily forest residues), which is then shipped to port-based upgrading facilities in other member states. Upgrading facilities, especially those located at strategic refineries in Rotterdam (Netherlands) and Normandy (France), play a central role as they serve as distribution hubs for drop-in fuels across Western Europe. An additional observation concerns Germany, Spain and France, which exhibit a broad technology mix. These large countries encompass both inland areas, where feedstock logistics favour local processing and distribution and maritime-connected regions, which enable integration into the wider shipping-based biofuel economy.



Figure 58 Spatial distribution of modelled biocrude and biofuel plants required for advanced biofuels in the EU-27+UK. Base scenario, 2030.

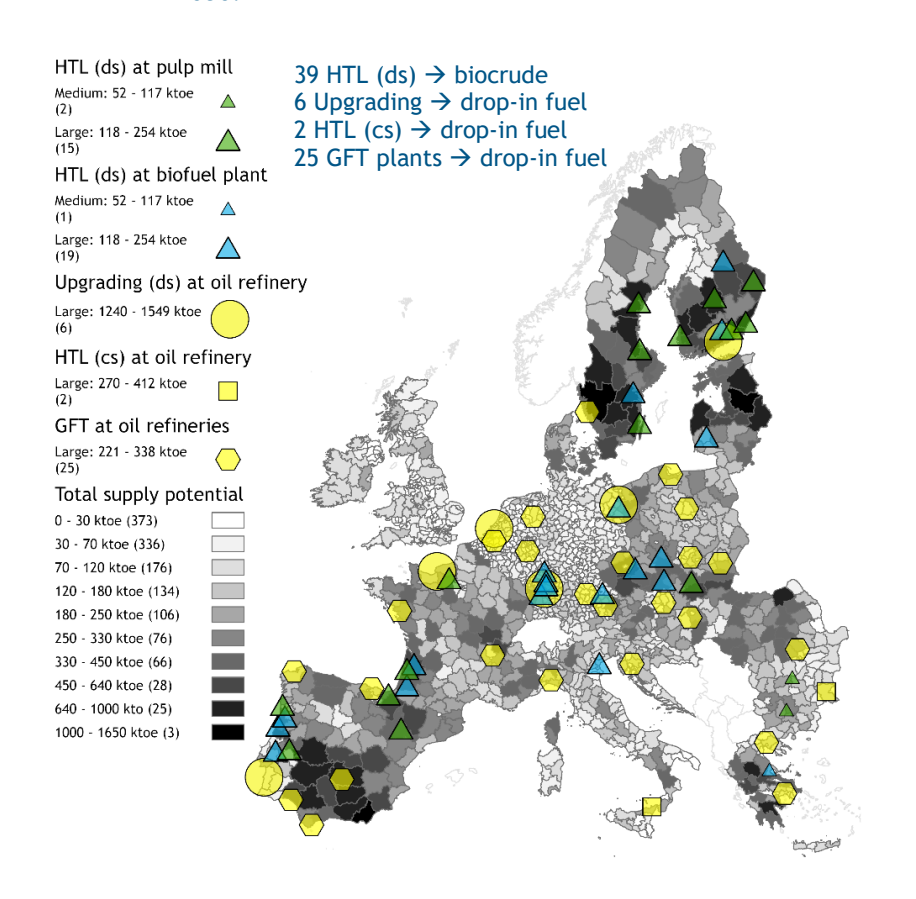
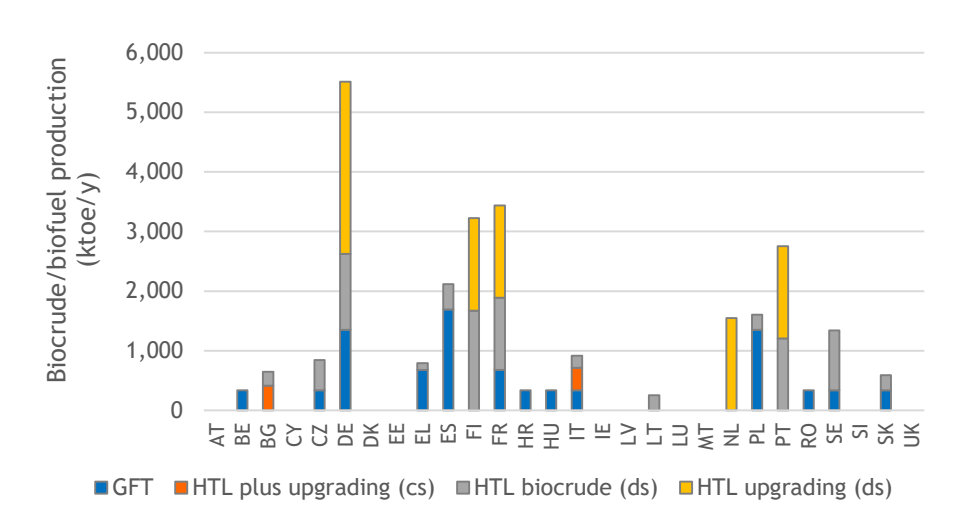


Figure 59 Distribution of biocrude and biofuel production per country in the EU-27+UK. Base scenario, 2030.





Distribution in 2050 (Base scenarios):

For 2050, the analysis focuses on the Base scenarios: Low-demand, High-demand and Repurpose. The results are shown in Figure 60, Figure 61,

Figure 62, Figure 63, Figure 64, Figure 65. The outcomes for the Alternative scenarios are provided separately in Annex F4. Unlike 2030, the optimal technology mix, and supply chain configuration strategy in 2050 are shown to be highly sensitive to the selected scenario, primarily due to the larger variations in biomass demand.

The Base scenarios presented here showcase fundamentally different system behaviours and supply chain architectures. The Alternative scenarios which are based on different levels of biomass availability, are expected to approximate one of these Base cases, depending on the biomass availability-to-biomass demand ratio. As explained previously, this ratio is a key determinant of the optimal supply chain system configuration. When the ratio is high, the model favours centralised supply chains, particularly those based on GFT plants integrated with refineries. When the ratio is low, the system shifts toward decentralised HTL configurations, which allow for distributed conversion of fragmented biomass resources, minimising long-distance transport penalties and better utilising the EU's domestic biomass resources.

For the reason explained above, the Low-demand case gives 101 plants in total, comprising: 56 centralised GFT, 37 HTL biocrude-producing decentralised plants and 8 upgrading plants in existing refineries. On the other hand, the High demand case results in 265 plants, specifically: 12 centralised GFT, 18 centralised (cs) HTL, 197 biocrude-producing decentralised (ds) HTL, followed by 38 upgrading plants.

These figures highlight the magnitude of infrastructure investment required, especially under the High-demand scenario, which necessitates a more than two-fold increase in facility count compared to the Low-demand case. The maximum biofuel output per centralised biorefinery has been assumed at ~ 400 ktoe/year, which, although significantly larger than the current state-of-the-art in the advanced biofuels industry, may look small if production at the scale in the High-demand scenario is to be realised. If larger biorefineries (beyond 400 ktoe/year) were constructed, the modelled High-demand case would begin to resemble up to an extent the Low-demand case in terms of plant distribution and technology mix, as the increased scale would allow a re-consolidation of capacity into fewer, larger facilities.

In the Repurpose scenario, as outlined in earlier sections, the potential to repurpose hydrocracking units in existing refineries offers a more important CAPEX benefit compared to repurposing hydrotreatment units being used for HTL biocrude upgrading. This economic benefit further strengthens the presence of centralised GFT. As a result, decentralised biocrude-producing HTL systems play a more limited role, emerging only in regions such as the Iberian Peninsula and Scandinavia. As showcased in all scenarios, these areas remain strategic hubs for biocrude production and export, enabling the supply of upgrading facilities Western Europe and helping meet the EU-wide advanced biofuel demand through maritime trade.

Summary of trends per geographical region in Europe

Summarising, as the model transitions from 2030 to 2050, several important trends emerge regarding the spatial distribution of biomass/biofuel infrastructure and the strategic role of different EU countries in the evolving supply chain. These insights highlight how resource availability, logistics, and biofuel demand levels shape regional investment priorities.



North-western Europe - Upgrading Hubs:

Countries such as the Netherlands and the United Kingdom, despite their limited domestic biomass resources, consistently emerge as key locations for upgrading facilities. These countries leverage their maritime infrastructure and strategic port access (e.g., Rotterdam) to import biocrude from biomass-rich regions such as Scandinavia and the Iberian Peninsula. As a result, they are well-positioned to become early movers in biofuel deployment, with upgrading plants likely to be among the first constructed facilities in the transition to advanced biofuels.

Scandinavia and the Iberian Peninsula -Biocrude Hubs

Scandinavian and Iberian countries exhibit strong potential to host both centralised plants, particularly under Low-demand scenarios, and decentralised HTL facilities. These regions benefit from high biomass availability, established maritime routes and strategic positioning for distributing biocrude or any other liquid intermediate across Europe. Their consistent role in both 2030 and 2050 scenarios highlights their importance as primary producers of intermediate energy carriers, making them ideal candidates for early investment in such infrastructure.

Eastern Europe - Rising Importance under High Demand

While Eastern European countries play a limited role in 2030 and 2050 Low-demand scenario, their strategic importance increases significantly under high demand conditions in 2050. These countries, many of which have relatively high biomass availability for their size, can take advantage of their access to the Baltic Sea to become notable exporters of biocrude.

Germany and France - Diversified, High-Capacity Systems

Countries such as Germany and France, due to their size, biomass availability, and location, must invest in a diverse portfolio of technologies: For low demand scenarios, they can build centralised GFT plants by utilising domestic or biomass resources from neighbouring countries. However, under high demand scenarios, the dispersion of feedstock and increased transport requirements necessitate also a decentralised approach, including the development of biocrude production facilities near biomass sources.

Central Europe (e.g. Austria, Czech Republic) - Demand-Sensitive Behaviour Central European countries such as Austria and Czech Republic display a more demand-sensitive supply chain configuration: Under lower demands, they can leverage domestic and biomass from neighbouring countries to support centralised GFT facilities. When demand increases, they shift to decentralised HTL systems, as long-distance biomass transport becomes cost-prohibitive. This adaptability allows these countries to play a supporting but strategic role, depending on how EU-wide demand evolves.

Mediterranean Region - Transitional Role

Mediterranean countries, particularly Italy and Greece, demonstrate flexibility in their roles depending on demand levels: Under low demand scenarios, countries like Greece can efficiently transport their own solid biomass to centralised GFT facilities. As demand grows, these countries must adopt a hybrid system, combining centralised and decentralised approaches. A notable trend in Greece is the emergence of decentralised biocrude production for the High-demand scenario in 2050, not solely to meet domestic demand, but also to supply biocrude to larger Mediterranean countries such as France, Spain, and Italy, which may struggle to meet elevated demands with their own resources.



Figure 60 Spatial distribution of modelled biocrude and biofuel plants required for advanced biofuels in the EU-27+UK. Low demand - Base scenario, 2050.

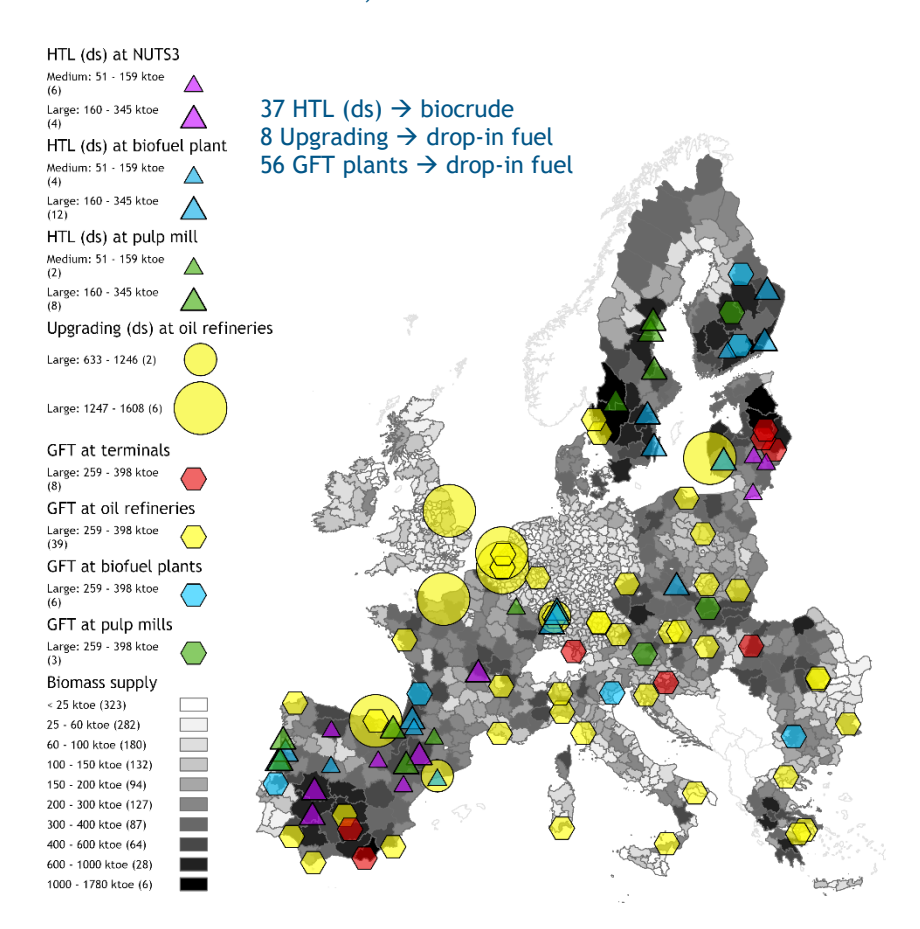


Figure 61 Distribution of biocrude and biofuel production per country in the EU-27+UK. Low demand - Base scenario, 2050.

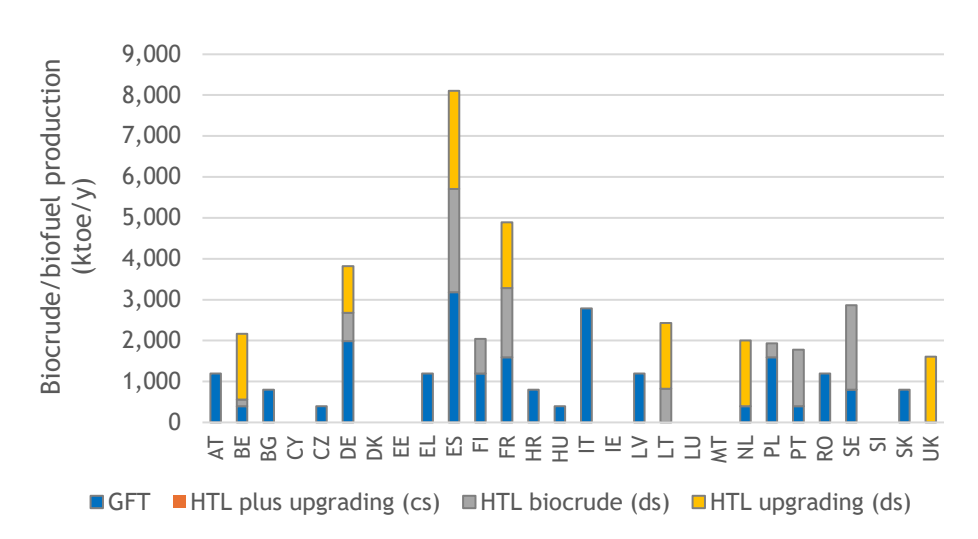




Figure 62 Spatial distribution of modelled biocrude and biofuel plants required for advanced biofuels in the EU-27+UK. High demand - Base scenario, 2050.

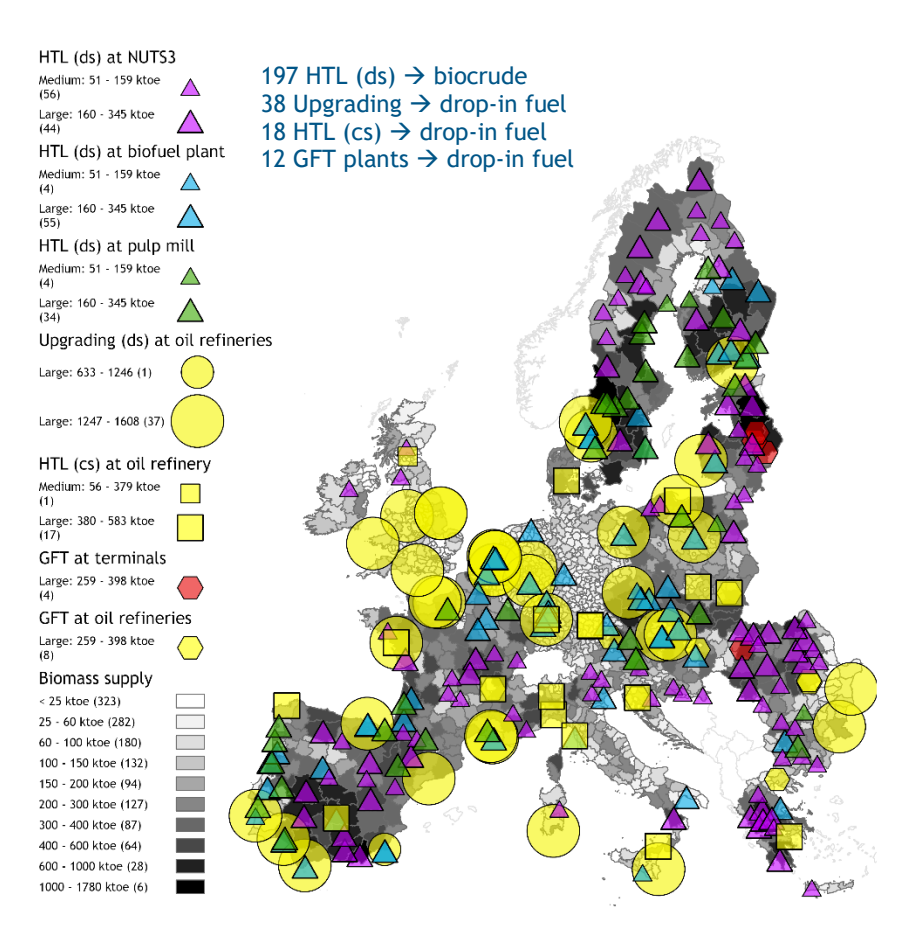


Figure 63 Distribution of biocrude and biofuel production per country in the EU-27+UK. High-demand Base scenario, 2050.

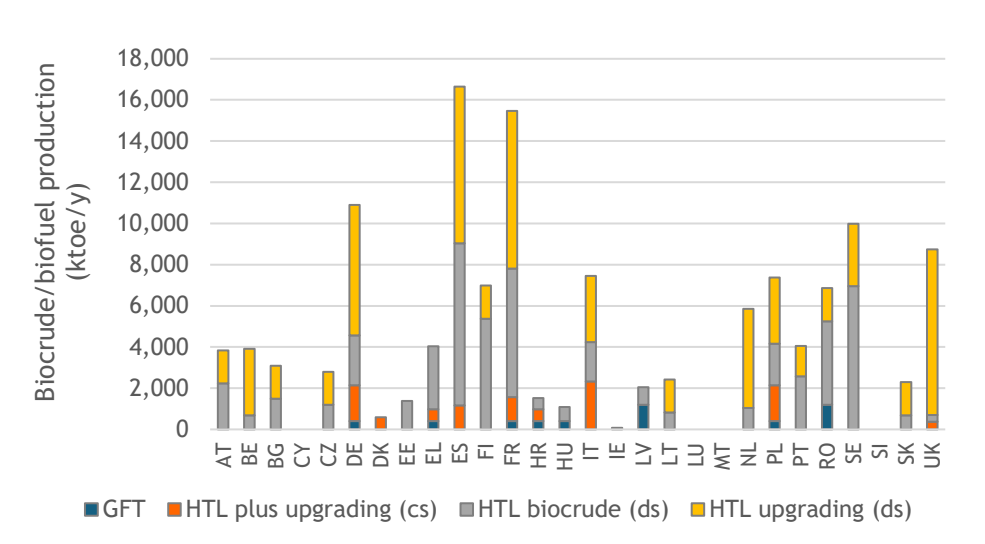




Figure 64 Spatial distribution of modelled biocrude and biofuel plants required for advanced biofuels in the EU-27+UK. Repurpose scenario, 2050.

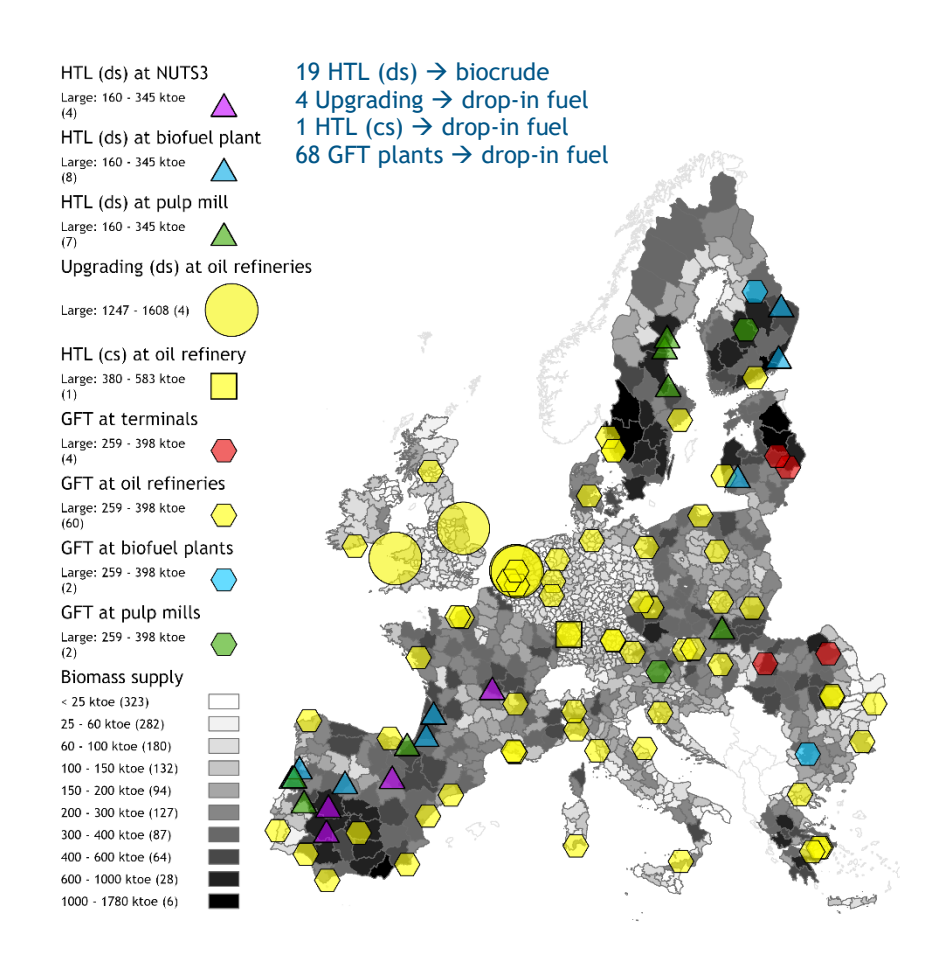
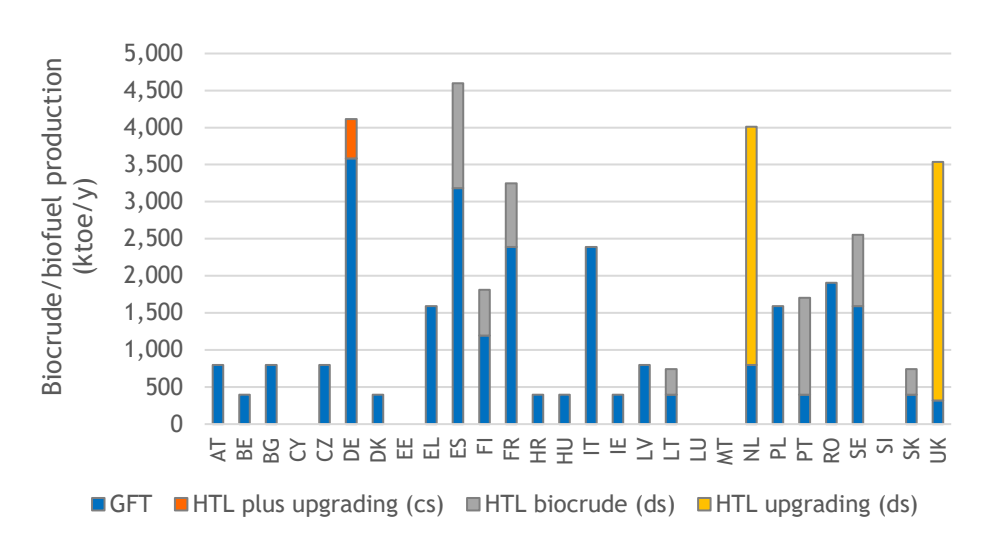


Figure 65 Distribution of biocrude and biofuel production per country in the EU-27+UK. Repurpose scenario, 2050.





9.4. BIOMASS/BIOFUEL CONSUMPTION AND TRADE DYNAMICS

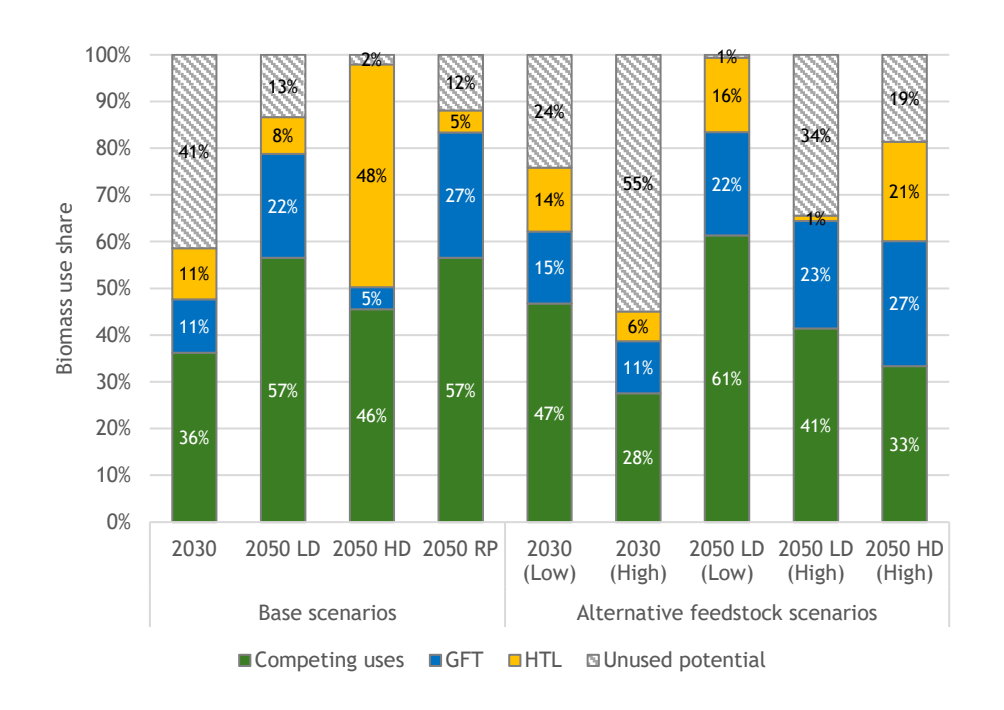
This section presents a detailed analysis of domestic consumption and inter-country trade flows of solid biomass, biocrude, and drop-in biofuels across the EU-27 + UK for the 2030 and 2050 scenarios. While trade patterns were briefly discussed in earlier sections, the following offers a deeper examination of trade dynamics and their implications for supply chain optimisation.

Biomass consumption in the Base and Alternative feedstock scenarios

Figure 66 and Figure 67 show that the total domestic biomass supply in the EU-27 + UK is sufficient to cover the domestic² demand for drop-in biofuels and competing uses for electricity and heat in the scenarios. Nevertheless, 2050 scenarios show that the unused potential is limited, in particular in the High fuel demand (HD) or low feedstock availability scenarios. As a result of the constrained supply, technology selection shifts from GFT to decentralised HTL pathways that have a higher feedstock-to-fuel conversion efficiency.

It is important to highlight, though, that the scope of this study excluded certain lignocellulosic biofeedstocks, such as manure, secondary agricultural residues, sewage sludge and new feedstocks listed under Annex IX like intermediate crops, from the modelling. Including these feedstocks would increase the amount of available biomass for biofuels and could potentially significantly ease supply chain constraints. In addition, integrating green hydrogen into conversion routes such as GFT can significantly increase the conversion yield and reduce biomass use share, however the integration of RFNBOs was outside the scope of this study.

Figure 66 Biomass utilization as a fraction of the total domestic availability potential in the Base and Alternative scenarios in the EU-27 + UK.



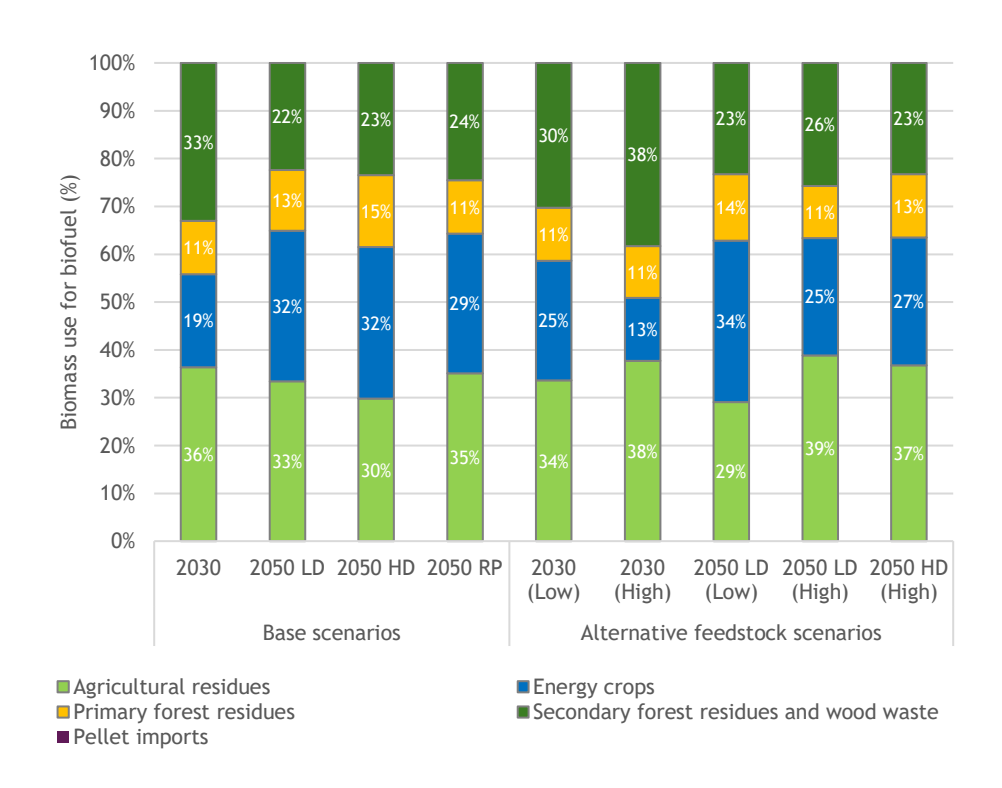
² Note that part of the demand for biofuels and competing uses is already assumed to be covered by imports (outside EU) and was not modelled (see Table 19).



Energy crops play a substantial role in biofuel production in all scenarios (see Figure 67), increasing from almost 1/5th by 2030 to up to almost 1/3rd by 2050. These crops could potentially reduce the pressure on lignocellulosic biomass markets, including forest biomass, but the current production is still very low, and the development of novel crop cultivation takes time (Hoefnagels & Germer, 2018).

Pellet imports are not used in any of the scenarios, despite the high feedstock utilization rates in 2050. This can be explained by the modeling approach used. Wood and straw pellets are available at 8 €/GJ in selected port terminals, which is substantially higher compared to the domestic feedstock supply cost at roadside. The on-site advantages of pellets, including better handling and storage characteristics and avoiding the need for drying and grinding compared to wood chips or other biomass sources, were not taken into account in the model. The potential role of imported biomass is therefore likely underestimated in these scenarios.

Figure 67 Biomass utilization for advanced biofuels (excluding electricity/heat) per feedstock type in the Base and Alternative feedstock scenarios in the EU-27 + UK.



Intra-EU biomass trade in the Base scenarios

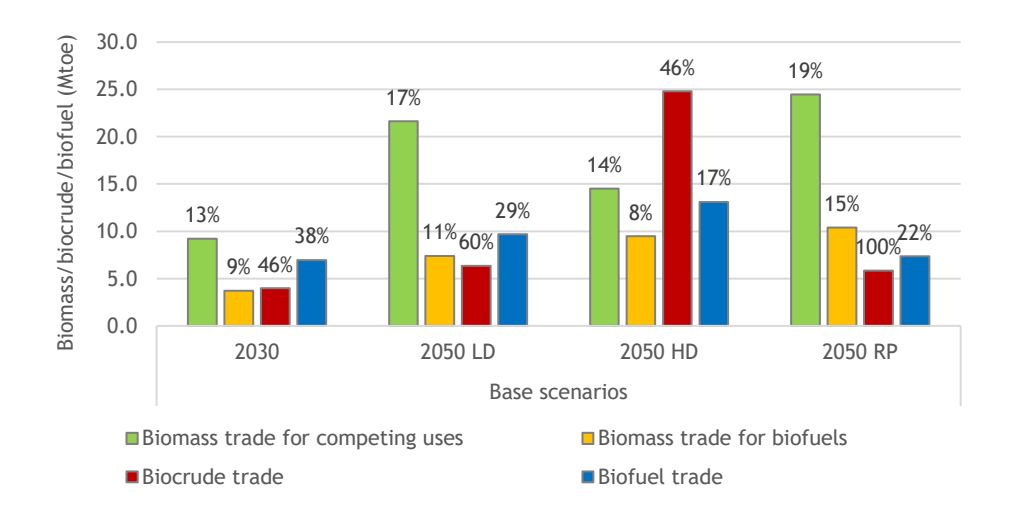
Biomass used for biofuel production is largely sourced from domestic sources with intra-EU trade ranging between 9% (2030) and up to 15% (2050 RP scenario) of total biomass supply for biofuels (see Figure 68).

For competing bioenergy uses, particularly electricity and heat (E/H), biomass trade volumes are the largest in absolute terms compared to other traded goods. However, their relative share compared to total biomass for bioenergy demand is among the lowest at around 20%, since most biomass used for E/H is sourced domestically within each country. Trade becomes more prominent in advanced biofuel supply chains, more specifically for liquid intermediates and drop-in biofuels



that can be transported over longer distances at lower cost due to their higher energy density. For example, 50% of the biocrude produced at decentralised HTL plants is exported to other countries for upgrading, and under certain conditions (such as in the Repurpose scenario), this figure rises to 100%, highlighting the central importance of cross-border liquid biofuel flows within the EU supply network.

Figure 68 Inter- country (EU-27+UK) trade of biomass, biocrude, and biofuel trade in the Base scenarios. The % labels show the share of trade relative to the total demand of the respective flow (biomass, biocrude, biofuel).



Intra-EU Trade flows in 2030 (Base scenario):

Figure 69 to Figure 71 present the inter-country trade flows of biomass, biocrude, and drop-in biofuels across the EU-27 + UK for the base scenario (Medium biomass availability) in 2030. In addition, biomass trade flows related to E/H, but also the flows for the Alternative scenarios, are also included and analysed in Annex F5 to provide a complete picture of bioresource movement.

Notably, the majority of solid biomass trade is localised, with most countries relying primarily on their domestic feedstock resources (91%). This is due to the low energy density of solid biomass, which leads to high transport costs per unit of biofuel produced for long distances. A few exceptions include trade between neighbouring countries, for example, Hungary and Slovakia.

Trade becomes more important in the form of biocrude, especially for countries with limited domestic biomass availability, and developed port and refining infrastructure. For example, as discussed before, the Netherlands, despite limited feedstock availability, imports a significant amount of biocrude. With Rotterdam as the largest port in Europe and a major refining hub, it is ideally positioned to receive biocrude shipments from Scandinavia, Baltic countries and the Iberian Peninsula. Maritime logistics make this cost-efficient and scalable. Other countries, with large upgrading units deployed, such as Portugal, also import biocrude from Italy, Greece, and Bulgaria, making use of short sea shipping routes.

Trade of drop-in biofuels is even more widespread and major exporting countries include Finland, Portugal, and Germany, where their important volumes of biomass resources and established upgrading facilities enable surplus production. Importing



countries such as the UK, Italy, and Belgium benefit from port access for efficient shipping logistics.

Figure 69Biomass trade flows among countries in the EU-27+UK of biomass used for biofuels (in ktoe biomass). Base scenario, 2030. Arrows point trade at country level and not the exact location of supply or demand.

Exporting country	Importing country	Flow (ktoe biomass)	Share (% total trade)	Solid biomass trade for biofuels (T)	Spinifer Transles Operand
HU	SK	694	19%		
NL	BE	466	13%		Nonway
FR	DE	459	12%		Open Orenza
AT	DE	448	12%	The state of the s	
PL	DE	428	11%	Abouton SCOT. North	Auborg - Harnstal
SI	HR	273	7 %	y Edinards Sea Newcassi specifyria	Denmark Maine
DE	FR	198	5%	United Kingdom	Hariburg Silvecin
LV	LT	190	5%	Ireland Notington WASS ENG. Notington	Premen Hanover Berlin
FR	ES	158	4%	London Dissolve Ulle B(m m	Dresden Wh
Others		955	11%	Paris	Frankfurt Crecks Stuttgart Munich Vienes
Total	trade	3,723	100%	The state of the s	The second of th

Figure 70 Biocrude trade among countries in the EU-27+UK from HTL (ds) to upgrading plants. Base scenario, 2030. Arrows point trade at country level and not the exact location of supply or demand.

Exporting country	Importing country	Flow (ktoe biocr.)	Share (% total trade)
SE	NL	799	20%
CZ	DE	505	13%
ES	FR	427	11%
FR	DE	253	6%
PL	DE	253	6%
LT	NL	253	6%
SK	DE	253	6 %
BG	PT	233	6%
PT	NL	207	5%
Others		1,489	20%
Total	l trade	3,979	100%



Figure 71 Drop-in biofuel trade among countries in the EU-27+UK from biofuel plants to blending terminals in refineries. Base scenario, 2030. Arrows point trade at country level and not the exact location of supply or demand.

Exporting country	Importing country	Flow (ktoe biofuel)	Share (% total trade)
FI	UK	980	14%
DE	UK	719	10%
PT	FR	523	8%
FR	UK	421	6%
DE	BE	387	6%
PT	IT	352	5%
PL	DE	351	5%
PT	ES	312	4%
DE	DK	280	4%
Others		3,578	38%
Total	l trade	6,960	100%

Intra-EU trade flows in 2050 (base scenarios):

For 2050, the Low-demand and High-demand Base scenarios are analysed for solid biomass trade (Figure 72, Figure 73), biocrude trade (Figure 74, Figure 75) and dropin biofuel trade (Figure 76, Figure 77). For both cases, the same trade pattern observed in 2030 is maintained in terms of the type of energy carriers traded. Specifically, solid biomass is traded in significantly smaller quantities compared to liquid intermediates (biocrude) and drop-in biofuels. This is primarily due to the low energy density of solid biomass, which makes it costly to transport over long distances. As a result, most countries continue to rely on domestic biomass resources or short-range regional trade for solid feedstocks, while cross-border trade becomes more important for biocrude and drop-in biofuels.

As demand increases from the Low to High-demand scenario, the volume and spatial distribution of trade flows across the EU also expand. Compared to 2030, there is a clear rise in the quantity of liquid intermediates transported between countries, and these flows become more geographically dispersed, reflecting the need to balance increasingly stretched supply and demand. As previously noted in the geographical distribution analysis, countries in Scandinavia and Iberian Peninsula, maintain a consistent role as key biocrude exporters across all demand scenarios. Their combination of large biomass resources and geographical placement enables efficient export capacity. An interesting shift in the trade network is the emergence of Greece and Romania as significant biocrude exporters for the High-demand case. In particular, Greece begins to mobilise its previously underutilised biomass potential to produce and export biocrude to Mediterranean countries with high biofuel demand which are under supply stress, such as France and Italy.



In 2050, the trade patterns for drop-in biofuels reveal some notable differences compared to 2030, reflecting both increased demand and a reshuffling of supply routes. A key example is Germany, which in 2030 acts as a significant exporter of biofuels. However, due to its increased internal biofuel requirement in 2050, Germany shifts its strategy to prioritise internal use, and supplement its demand through imports from other EU countries. Another significant observation is the broadening of cross-border engagement. As demand rises, more countries become actively involved in inter-country trading such as Eastern European countries like Lithuania (LT) and Latvia (LV), and Central European countries like Austria (AT) and Czechia (CZ). While these regions have a limited trading role under the lower demand in 2030, they become key contributors to the biofuel trading network under high demand conditions, helping to bridge the gap between biomass-rich areas and high-consumption centres.

Figure 72 Biomass trade flows among countries in the EU-27+UK of biomass used for biofuels (in ktoe biomass). Low-demand base scenario, 2050. Arrows point trade at country level and not the exact location of supply and demand.



Figure 73

Biomass trade flows among countries in the EU-27+UK of biomass used for biofuels (in ktoe biomass). High-demand base scenario, 2050. Arrows point trade at country level and not the exact location of supply and demand.

Exporting country	Importing country	Flow (ktoe biomass)	Share (% total trade)
SI	HR	738	8%
SK	PL	673	7 %
FR	DE	658	7 %
HU	AT	623	7 %
EL	IT	620	7 %
AT	DE	597	6%
DE	NL	565	6 %
HU	RO	401	4%
PL	DE	399	4%
Others		5,572	44%
Total	trade	9,481	100%

Figure 74

Biocrude trade among countries in the EU-27+UK from HTL (ds) to upgrading plants. Low-demand base scenario, 2050. Arrows point trade at country level and not the exact location of supply and demand.

xporting country		Flow (ktoe biocr.)	Share (% total trade)
SE	UK	1,462	23%
PT	NL	1,117	18%
FR	ES	508	8%
ES	FR	504	8%
FI	BE	504	8%
FR	DE	345	5%
ES	NL	345	5%
FI	LT	345	5%
PL	BE	345	5%
Others	5	1,902	14%
Total	otal trade	6,342	100%



Figure 75

Biocrude trade among countries in the EU-27+UK from HTL (ds) to upgrading plants. High-demand base scenario, 2050. Arrows point trade at country level and not the exact location of supply and demand.

Exporting country	Importing country	Flow (ktoe biocr.)	Share (% total trade)
SE	UK	2,174	9%
FI	UK	2,109	9%
FI	NL	1,799	7%
AT	DE	1,308	5%
EL	FR	1,263	5%
EL	IT	1,201	5%
RO	SK	1,106	4%
SE	NL	1,049	4%
SE	BE	965	4%
Others		14,955	48%
Total	trade	24,809	100%

Figure 76 Drop-in biofuel trade among countries in the EU-27+UK from biofuel plants to blending terminals in refineries. Low-demand base scenario, 2050. Arrows point trade at country level and not the exact location of supply and demand.

Exporting country		Share (% total trade)
ES	UK 1,550	16%
LT	UK 863	9%
LV	DE 589	6%
AT	DE 565	6%
LV	UK 549	6%
ES	PT 467	5%
BG	IT 455	5%
SK	DE 398	4%
FI	UK 378	4%
Others	s 5,114	40%
Total	otal trade 9,697	100%



Figure 77 Drop-in biofuel trade among countries in the EU-27+UK from biofuel plants to blending terminals in refineries. High-demand base scenario, 2050. Arrows point trade at country level and not the exact location of supply and demand.

Exporting country	Importing country	Flow (ktoe biofuel)	Share (% total trade)
RO	EL	1,005	8%
FR	IT	950	7%
CZ	DE	933	7 %
PL	DE	727	6 %
SE	UK	719	5%
BG	IT	692	5%
SK	CZ	668	5%
DE	NL	637	5%
FI	UK	608	5%
Others		8,073	47%
Total	trade	13,099	100%



10. CONCLUSIONS

This study assessed the economically optimal supply chain configurations for advanced biofuel production from lignocellulosic biomass across the EU-27 + UK, under varying future scenarios for advanced transport biofuels demand and biomass availability. Using a dedicated mixed-integer linear programming (MILP) model, the analysis incorporated spatially explicit estimates of biomass availability and costs, and accounted for inland and maritime transport networks, conversion efficiencies of biorefining technologies (Gasification and Fischer-Tropsch (GFT) and Hydrothermal Liquefaction (HTL)), and economies of scale.

The model enabled an in-depth exploration of biomass-to-biofuel supply chain strategies, highlighting key trade-offs between economies of scale and decentralised processing facilities, the role of different technology pathways, and the geographic and infrastructural factors shaping the optimal system layout. The findings offer strategic insights into the future development of EU biofuel infrastructure, the role of existing oil refineries in this transition, and the investment needs of the energy sector in adapting to bio-based feedstocks.

1) Small greenfield biorefineries vs. large-scale biorefineries integrated with existing industrial facilities:

While early biofuel projects have often prioritised siting plants close to biomass sources, a strategy that secures feedstock and suits small-scale operations, this study reveals a more nuanced picture when designing a mature, EU-wide biomass supply system capable of meeting elevated future biofuel demand.

The results clearly show that integrating future biorefineries with existing industrial assets, such as oil refineries, biofuel plants, and pulp mills, offers significant capital cost savings due to infrastructure synergies. Even when full retrofitting is not feasible, these integrated scenarios consistently outperform greenfield developments. For GFT pathways in particular, refinery integration enables both economies of scale and the reuse of existing processing units, making it the most cost-effective configuration where conditions allow.

However, a centralised approach is not always viable. In cases where industrial sites are far from biomass-rich regions, decentralised HTL plants co-located with existing pulp mills or biofuel sites become the more efficient option. These plants produce biocrude, which is then shipped via maritime routes to upgrading units at refineries with port access.

Ultimately, the choice between centralised integration and decentralised supply chain configurations is determined by several interlinked factors:

- the scale of the biorefinery, linked to each country's biofuel demand,
- the location of feedstock resources,
- and geographical aspects, such as inland positioning versus port accessibility.

2) Supply chain costs and key cost drivers across supply chains:

Across all technology configurations, conversion costs are the most significant component: CAPEX for GFT and OPEX for HTL. However, feedstock costs and upstream logistics play a pivotal role in the balance between centralised and decentralised options.



For 2030, the cost differences between technologies in each scenario are below 10%. This suggests that short-term technology selection will largely be shaped by commercial readiness and availability rather than intrinsic cost advantages.

Looking ahead to 2050, the costs picture changes considerably as a result of technological learning. GFT gains an edge thanks to greater cost reductions from technological learning, making it particularly favourable in scenarios where biomass availability is high relative to demand and centralised systems are efficient. However, when this ratio declines, decentralised HTL systems become necessary, driving variability in costs as these systems are more widely dispersed to tap into remote biomass resources.

3) The influence of domestic biomass availability and demand:

Biomass availability is a key determinant of the optimal supply chain structure. While the moderate advanced biofuel demand in 2030 does not stress the EU supply chain, in 2050, the balance between biomass availability and bioenergy demand becomes a decisive parameter.

For example, a high biomass availability-to-demand ratio of 1.9, observed under the Low biofuel demand/ High biomass availability scenario in 2050, provides greater flexibility in sourcing and enables the system to favour centralised Gasification and Fischer-Tropsch (GFT) deployment, the lowest-cost pathway when sufficient feedstock is accessible relatively close to the plant.

Conversely, a low availability-to-biomass demand ratio of ~ 1.0 (Low biofuel demand/ Low biomass availability) leads to a supply system that is highly decentralised. The system must increasingly mobilise fragmented or remote feedstocks, reinforcing the role of flexible decentralised configurations within the broader EU biofuel network.

For intermediate ratios (e.g., 1.4), a balanced mix of centralised and decentralised systems is identified as the most cost-effective configuration.

<u>4) Spatial distribution of biorefineries across Europe - the importance of geography:</u>

As advanced biofuel demand rises from 2030 to 2050, the biomass supply chain network expands in both scale and geographic complexity, becoming increasingly dispersed across the EU-27 + UK. The analysis reveals distinct geographic patterns that determine the role of different countries in the supply chain, influenced by both biomass availability and logistical infrastructure.

For instance, highly industrialised coastal countries in Western Europe, such as the United Kingdom, Belgium, and the Netherlands, possess limited domestic biomass resources but offer well-developed port and refinery infrastructure. These conditions make them ideal hubs for upgrading imported biocrude, rather than hosting centralised biomass conversion facilities.

In contrast, countries in the Iberian Peninsula and especially Scandinavia exhibit high biomass availability combined with favourable export logistics, positioning them as key locations for decentralised HTL deployment. These regions are expected to play a pivotal role in biocrude production, supplying intermediate fuels to upgrading facilities in Western Europe via maritime routes.



These trends underscore that investment decisions in biofuel technologies should not be based solely on process performance or maturity, but rather on an integrated assessment that includes geographic factors, and supply chain logistics. In other words, "where" a technology is deployed can be as important as "what" technology is deployed.

5) Intra-EU Biomass and Biofuel Trade:

Trade dynamics also evolve based on demand and availability. As biomass availability tightens relative to demand, the EU supply chain stretches, requiring intensified cross-border trade. The results consistently show that transporting liquids (biocrude, drop-in biofuels) is more cost-effective than moving solid biomass due to their higher energy density and better logistical efficiency.

Solid biomass trade remains mostly limited to landlocked or centrally located countries, where proximity to neighbouring regions makes short-haul biomass exchange viable. In contrast, biocrude exports from biomass-rich countries such as Finland, Sweden, and Spain, and imports into industrial hubs like the Netherlands, UK, and Belgium, form the backbone of long-range EU trade flows.

6) Need for ramping up biorefining infrastructure:

At present, no large-scale biorefineries are operational in Europe for producing advanced biofuels from Annex IX-A feedstocks, highlighting a critical gap between current capacity and future demand requirements. According to the model results, by 2030 a near-term milestone, for the Medium availability scenario, approximately 72 biocrude and biofuel plants will need to be built (including the biocrude upgrading plants), with several operating at large scale to achieve efficient economic performance. This represents a substantial leap from the current deployment status.

Looking ahead to 2050, the infrastructure challenge becomes even more pronounced. For example, depending on the scenario, between 92 and 265 biocrude and biofuel plants are required. Although the timeline is longer, the number of plants required, along with the urgency of initiating large-scale investments, means that delays in infrastructure development will pose a serious risk to meeting decarbonisation targets.

The model assumes a maximum biorefinery output of 400 ktoe per plant, already well above current demonstration capacities. If larger-scale facilities become technically feasible in the future, the required number of plants may decrease, but even under optimistic scaling assumptions, the combined requirements for capacity, number, and geographic dispersion of facilities make the rollout of advanced biofuel production challenging. Coordinated action is essential to close the gap and build the foundation for a sustainable, EU-wide biofuel supply network.



11. ABBREVIATIONS

CAPEX Capital Expenditure
CS Centralised System
DS Decentralised System
E/H Electricity and Heat

ESRI Environmental Systems Research Institute

FT Fischer Tropsch

GFT Gasification and Fischer Tropsch

GHG Greenhouse gas

GIS Geographic Information System

HD High Demand

HDV Heavy-Duty Vehicle

HICP Harmonised Index of Consumer Prices

HTL Hydrothermal Liquefaction
IEA International Energy Agency

JRC Joint Research Centre

LD Low Demand

LDV Light - Duty Vehicle
LHV Low Heating Value
LP Linear Programming

LR Learning rate
LUC Land Use Change

MILP Mixed Integer Linear Programming

MSW Mixed Solid Waste

NUTS Nomenclature of Territorial Units for Statistics

OPEX Operational Expenditure PCW Post-consumer Wood

RCP Representative Concentration Pathway

RCG Reed Canary Grass

RED Renewable Energy Directive

RP Repurpose

SAF Sustainable Aviation Fuel
SMR Steam Methane Reforming

S&P Standard & Poor's

TCI Total Capital Investment
TRL Technology Readiness Level

VAT Value Added Tax

Wb Wet basis



12. REFERENCES

Baranzelli, C., Jacobs-Crisioni, C., Batista e Silva, F., Perpiña Castillo, C., Barbosa, A., Arevalo Torres, J., & Lavalle, C. (2014). The Reference scenario in the LUISA platform-Updated configuration 2014. *Towards a Common Baseline Scenario for EC Impact Assessment Procedures*. *EUR*, 27019.

Bardon, P., & Massol, O. (2025). Decarbonizing aviation with sustainable aviation fuels: Myths and realities of the roadmaps to net zero by 2050. *Renewable and Sustainable Energy Reviews*, 211, 115279. https://doi.org/10.1016/J.RSER.2024.115279

Bridgwater, T. (2018). Challenges and opportunities in fast pyrolysis of biomass: Part I. *Johnson Matthey Technology Review*, 62(1), 118-130. https://doi.org/10.1595/205651318X696693

Brown, A., Waldheim, L., Landälv, I., Saddler, J., Ebadian, M., McMillan, J. D., Bonomi, A., & Klein, B. (2020). Advanced biofuels-potential for cost reduction. *IEA Bioenergy*, 88, 1-3.

Brynolf, S., Hansson, J., Anderson, J. E., Skov, I. R., Wallington, T. J., Grahn, M., Korberg, A. D., Malmgren, E., & Taljegård, M. (2022). Review of electrofuel feasibility—prospects for road, ocean, and air transport. *Progress in Energy*, 4(4), 042007. https://doi.org/10.1088/2516-1083/ac8097

Camia, A., Giuntoli, J., JONSSON, K., Robert, N., CAZZANIGA, N., Jasinevičius, G., AVITABILE, V., GRASSI, G., BARREDO, C., MUBAREKA, S., & others. (2021). The use of woody biomass for energy production in the EU.

Castello, D., Pedersen, T. H., & Rosendahl, L. A. (2018). Continuous Hydrothermal Liquefaction of Biomass: A Critical Review. *Energies 2018, Vol. 11, Page 3165, 11*(11), 3165. https://doi.org/10.3390/EN11113165

Chireshe, F., Petersen, A. M., Ravinath, A., Mnyakeni, L., Ellis, G., Viljoen, H., Vienings, E., Wessels, C., Stafford, W. H. L., Bole-Rentel, T., Reeler, J., & Görgens, J. F. (2025). Cost-effective sustainable aviation fuel: Insights from a techno-economic and logistics analysis. *Renewable and Sustainable Energy Reviews*, 210, 115157. https://doi.org/10.1016/J.RSER.2024.115157

de Jong, S., Hoefnagels, R., Faaij, A., Slade, R., Mawhood, B., & Junginger, M. (2015). The feasibility of short-term production strategies for renewable jet fuels - a comprehensive technoeconomic comparison. *Biofpr*, *9*, 778-800.

de Jong, S., Hoefnagels, R., Wetterlund, E., Pettersson, K., Faaij, A., & Junginger, M. (2017). Cost optimization of biofuel production - The impact of scale, integration, transport and supply chain configurations. *Applied Energy*, 195(Supplement C), 1055-1070.

Dees, M., Datta, P., Hohl, M., Fitzgerald, J., Verkerk, H., Zudin, S., Lindner, M., Forsell, N., Leduc, S., & Elbersen, B. S. (2017). D1. 8 Atlas with regional cost supply biomass potentials for EU 28, Western Balkan Countries, Moldavia, Turkey and Ukraine: Issue: 1.1. S2Biom.

Dees, M., Elbersen, B., Fitzgerald, J., & Et al. (2017). Atlas with regional cost supply biomass potentials for EU 28, Western Balkan Countries, Moldavia, Turkey and Ukraine.

Dyk, S. van; S. J. (2024). Progress in Commercialization of Biojet / Sustainable Aviation Fuels (SAF): Technologies and policies.

EC. (2020). COMMISSION STAFF WORKING DOCUMENT IMPACT ASSESSMENT Accompanying the document COMMUNICATION FROM THE COMMISSION TO THE EUROPEAN PARLIAMENT, THE COUNCIL, THE EUROPEAN ECONOMIC AND SOCIAL COMMITTEE AND THE COMMITTEE OF THE REGIONS Stepping up Europe's 2030 climate ambition Investing in a climate-neutral future for the benefit of our people SWD/2020/176 final.

EC. (2021). EU reference scenario 2020 - Energy, transport and GHG emissions - Trends to 2050. Publications Office. https://doi.org/doi/10.2833/35750



EC. (2024). Development of outlook for the necessary means to build industrial capacity for drop-in advanced biofuels - Final report (M. Georgiadou, T. Goumas, & D. Chiaramonti, Eds.). Publications Office of the European Union. https://doi.org/doi/10.2777/679307

Edwards, R., O'Connell, A., Padella, M., Mulligan, D., Giuntoli, J., Agostini, A., Koeble, R., Moro, A., & Marelli, L. (2017). Definition of input data to assess GHG default emissions from biofuels in EU legislation - Version 1c - July 2017. In *JRC Science for Policy Report EUR* (Vol. 28349). https://doi.org/10.2790/38802

ESRI. (2024). What is the ArcGIS Network Analyst extension? https://pro.arcgis.com/en/pro-app/latest/help/analysis/networks/what-is-network-analyst-.htm

ETISPLUS. (2013). D6 ETIS plus Database - Content and Methodology.

EU. (2023). DIRECTIVE OF THE EUROPEAN PARLIAMENT AND OF THE COUNCIL amending Directive (EU) 2018/2001, Regulation (EU) 2018/1999 and Directive 98/70/EC as regards the promotion of energy from renewable sources, and repealing Council Directive (EU) 2015/652. European Commission.

European Commission. (2018). Directive (EU) 2018/2001 of the European Parliament and of the Council of 11 December 2018 on the promotion of the use of energy from renewable sources (recast). Official Journal of the European Union.

European Commission. (2023). *Cereals, oilseeds, protein crops and rice*. https://agriculture.ec.europa.eu/farming/crop-productions-and-plant-based-products/cereals en#:~:text=More than half of cereals, each representing about one third.

Eurostat. (2024). *Crop production in EU standard humidity*. https://ec.europa.eu/eurostat/databrowser/view/APRO_CPSH1__custom_9956092/default/table

Fortenbery, T. R., Deller, S. C., & Amiel, L. (2013). The Location Decisions of Biodiesel Refineries. *Land Economics*, 89(1), 118. https://doi.org/10.3368/le.89.1.118

Fritsche, U., Hennig, C., Hess, J. R., Hoefnagels, R., Lamers, P., Li, C., Olsson, O., Schipfer, F., Thrän, D., Tumuluru, J. S., & others. (2019). *Margin potential for a long-term sustainable wood pellet supply chain*.

García-Condado, S., López-Lozano, R., Panarello, L., Cerrani, I., Nisini, L., Zucchini, A., Van der Velde, M., & Baruth, B. (2019). Assessing lignocellulosic biomass production from crop residues in the European Union: Modelling, analysis of the current scenario and drivers of interannual variability. *GCB Bioenergy*, 11(6), 809-831.

Gauthier, G. (2024). Industrial pellet market update - Working Group Pellets - Bioenergy Europe.

Haddad, M. A., Taylor, G., & Owusu, F. (2009). Locational Choices of the Ethanol Industry in the Midwest Corn Belt. *Economic Development Quarterly*, 24(1), 74-86. https://doi.org/10.1177/0891242409347722

Hoefnagels, R., & Germer, S. (2018). Supply potential, suitability and status of lignocellulosic feedstocks for advanced biofuels.

Hoefnagels, R., Resch, G., Junginger, M., & Faaij, A. (2014). International and domestic uses of solid biofuels under different renewable energy support scenarios in the European Union. *Applied Energy*, 131, 139-157. https://doi.org/10.1016/j.apenergy.2014.05.065

Hoefnagels, R., Searcy, E., Cafferty, K., Cornelissen, T., Junginger, M., Jacobson, J., & Faaij, A. (2014). Lignocellulosic feedstock supply systems with intermodal and overseas transportation. *Biofuels, Bioproducts and Biorefining*, 8(6), 794-818. https://doi.org/10.1002/bbb.1497

Huang, E., Zhang, X., Rodriguez, L., Khanna, M., de Jong, S., Ting, K. C., Ying, Y., & Lin, T. (2019). Multi-objective optimization for sustainable renewable jet fuel production: A case study



of corn stover based supply chain system in Midwestern U.S. *Renewable and Sustainable Energy Reviews*, 115, 109403. https://doi.org/10.1016/J.RSER.2019.109403

Hurtig, O., Buffi, M., Scarlat, N., Motola, V., Georgakaki, A., Letout, S., Mountraki, A., Joanny, O. G., & others. (2022). Clean Energy Technology Observatory: Advanced Biofuels in the European Union-2022 Status Report on Technology Development, Trends, Value Chains and Markets. https://doi.org/doi:10.2760/938743

IEA. (2021). Net Zero by 2050 A Roadmap for the. 222.

JRC. (2009). TRANS-TOOLS ("TOOLS for Transport Forecasting and Scenario testing"). Joint Research Centre (JRC) - Institute for Prospective Technological Studies (IPTS).

Junginger, M., & Louwen, A. (2019). Technological learning in the transition to a low-carbon energy system: Conceptual issues, empirical findings, and use, in energy modeling. Academic Press.

Karimi, M., Simsek, H., & Kheiralipour, K. (2025). Advanced biofuel production: A comprehensive techno-economic review of pathways and costs. *Energy Conversion and Management: X*, 25, 100863. https://doi.org/10.1016/J.ECMX.2024.100863

Korpinen, O. J., Aalto, M., KC, R., Tokola, T., & Ranta, T. (2023). Utilisation of Spatial Data in Energy Biomass Supply Chain Research—A Review. *Energies*, 16(2), 893. https://doi.org/10.3390/EN16020893/S1

Lamers, P., Hoefnagels, R., Junginger, M., Hamelinck, C., & Faaij, A. (2015). Global solid biomass trade for energy by 2020: an assessment of potential import streams and supply costs to North-West Europe under different sustainability constraints. *Gcb Bioenergy*, 7(4), 618-634.

Lammens, T., Vis, M., Berg, D. van den, Groot, H. de, Meulenbroek, B. van, Startisky, I., Annevelink, B., Elbersen, W., & Elbersen, B. (2016). *Bio2Match: a Tool for Matching Biomass and Conversion Technologies - S2Biom Deliverable D4.5*.

Lavalle, C., e Silva, F. B., Baranzelli, C., Jacobs-Crisioni, C., Vandecasteele, I., Barbosa, A. L., Maes, J., Zulian, G., Castillo, C. P., & Barranco, R. (2016). Land use and scenario modelling for integrated sustainability assessment. In *European landscape dynamics* (pp. 267-292). CRC Press.

Material Economics. (2021). EU Biomass Use in a Net-Zero Economy—A Course Correction for EU Biomass. Material Economics Sverige.

Motola, V., Rejtharova, J., Scarlat, N., Hurtig, O., Buffi, M., Georgakaki, A., Letout, S., Mountraki, A., Salvucci, R., Rózsai, M., & Schade, B. (2024). *Clean Energy Technology Observatory: Advanced Biofuels in the European Union - 2024 Status Report on Technology Development, Trends, Value Chains and Markets* (Issue KJ-01-24-063-EN-N (online)). Publications Office of the European Union. https://doi.org/10.2760/6538066 (online)

OSMF. (2023). OpenStreetmap (OSM). https://www.openstreetmap.org/

Panoutsou, C., & Maniatis, K. (2021). Sustainable Biomass Availability in the EU, to 2050. In Concawe Report RED II Annex IX A/B.

Pari, L., Suardi, A., Santangelo, E., García-Galindo, D., Scarfone, A., & Alfano, V. (2017). Current and innovative technologies for pruning harvesting: A review. *Biomass and Bioenergy*, 107, 398-410. https://doi.org/10.1016/J.BIOMBIOE.2017.09.014

Perpiña Castillo, C., Lavalle, C., Baranzelli, C., & Mubareka, S. (2015). Modelling the spatial allocation of second-generation feedstock (lignocellulosic crops) in Europe. *International Journal of Geographical Information Science*, 29(10), 1807-1825.

PWC. (2017). Sustainable and optimal use of biomass for energy in the EU beyond 2020 - BioSustain (Issue May). https://ec.europa.eu/energy/en/studies/sustainable-and-optimal-use-biomass-energy-eu-beyond-2020



Ramirez-Almeyda, J., Elbersen, B., Monti, A., Staritsky, I., Panoutsou, C., Alexopoulou, E., Schrijver, R., & Elbersen, W. (2017). Assessing the potentials for nonfood crops. In *Modeling and optimization of biomass supply chains* (pp. 219-251). Elsevier.

Rodrigue, J.-P. (2020). *The geography of transport systems - SIXTH EDITION*. Routledge. https://transportgeography.org/

Rothenburger, K. (2023). Location specific factors that shape the future rollout of advanced biofuel production in the European Union - Master's thesis. https://studenttheses.uu.nl/handle/20.500.12932/45536

RRG. (2008). Short Sea Shipping Routes in Europe. RRG Spatial Planning and Geoinformation.

Ruiz, P., Sgobbi, A., Nijs, W., Thiel, C., Dalla Longa, F., Kober, T., Elbersen, B., & Hengeveld, G. (2015). The JRC-EU-TIMES model. Bioenergy potentials for EU and neighbouring countries. *JRC Science for Policy Report, European Commission*.

Schils, R., Olesen, J. E., Kersebaum, K.-C., Rijk, B., Oberforster, M., Kalyada, V., Khitrykau, M., Gobin, A., Kirchev, H., & Manolova, V. (2018). Cereal yield gaps across Europe. *European Journal of Agronomy*, 101, 109-120.

Searcy, E., Lamers, P., & Deutmeyer, M. (2016). Commodity-Scale Biomass Trade and Integration with Other Supply Chains. In P. Lamers, E. Searcy, J. R. Hess, & H. Stichnothe (Eds.), *Developing the Global Bioeconomy* (pp. 116-136). Elsevier Academic Press.

Sonnleitner, A., & Bacovsky, D. (2024). *Development and Deployment of advanced biofuel demonstration* facilities. https://task39.ieabioenergy.com/wp-content/uploads/sites/37/2024/12/IEA-Report-T39-T4-Development-and-Deployment-of-advanced-biofuel-demonstration-facilities-2024.pdf

S&P. (2025). Study on the potential evolution of Refining and Liquid Fuels production in Europe.

Tagomori, I., Daioglou, V., Rochedo, P., Angelkorte, G., Schaeffer, R., van Vuuren, D., & Szklo, A. (2023). BLOEM: A spatially explicit model of bioenergy and carbon capture and storage, applied to Brazil. *GCB Bioenergy*, *15*(2), 116-127. https://doi.org/10.1111/GCBB.13008

Tian, X., Engel, B. A., Qian, H., Hua, E., Sun, S., & Wang, Y. (2021). Will reaching the maximum achievable yield potential meet future global food demand? *Journal of Cleaner Production*, 294, 126285.

Vera, I., Hoefnagels, R., Junginger, M., & van der Hilst, F. (2021). Supply potential of lignocellulosic energy crops grown on marginal land and greenhouse gas footprint of advanced biofuels—A spatially explicit assessment under the sustainability criteria of the Renewable Energy Directive Recast. *GCB Bioenergy*, 13(9), 1425-1447.

Verkerk, P. J., Fitzgerald, J. B., Datta, P., Dees, M., Hengeveld, G. M., Lindner, M., & Zudin, S. (2019). Spatial distribution of the potential forest biomass availability in Europe. *Forest Ecosystems*, 6(1), 1-11.

Vogt, E. T. C., & Weckhuysen, B. M. (2024). The refinery of the future. *Nature 2024 629:8011*, 629(8011), 295-306. https://doi.org/10.1038/s41586-024-07322-2

WBA. (2015). WBA factsheet THERMOCHEMICAL GASIFICATION OF BIOMASS.

Witcover, J., & Williams, R. B. (2020). Comparison of "Advanced" biofuel cost estimates: Trends during rollout of low carbon fuel policies. *Transportation Research Part D: Transport and Environment*, 79, 102211.

Witzel, C.-P., & Finger, R. (2016). Economic evaluation of Miscanthus production-A review. *Renewable and Sustainable Energy Reviews*, 53, 681-696.

Yáñez, É., Meerman, H., Ramírez, A., Castillo, É., & Faaij, A. (2021). Assessing bio-oil coprocessing routes as CO2 mitigation strategies in oil refineries. *Biofuels, Bioproducts and Biorefining*, 15(1), 305-333.



https://doi.org/10.1002/BBB.2163;JOURNAL:JOURNAL:19321031;PAGEGROUP:STRING:PUBLICA TION

Zhu, Y., Rahardjo, S. T., & Valkenburt, C. (2011). *Techno-economic analysis for the thermochemical conversion of biomass to liquid fuels*. https://www.osti.gov/biblio/1128665



Concawe

Boulevard du Souverain 165 B-1160 Brussels Belgium

Tel: +32-2-566 91 60 Fax: +32-2-566 91 81 e-mail: info@concawe.org http://www.concawe.eu

